IPPJ-AM-46

ATOMIC DATA INVOLVING HYDROGENS RELEVANT TO EDGE PLASMAS

H. TAWARA, Y. ITIKAWA, Y. ITOH
T. KATO, H. NISHIMURA, S. OHTANI
H. TAKAGI, K. TAKAYANAGI AND M. YOSHINO

INSTITUTE OF PLASMA PHYSICS
NAGOYA UNIVERSITY

NAGOYA, JAPAN

IPPJ-AM-46

ATOMIC DATA INVOLVING HYDROGENS RELEVANT TO EDGE PLASMAS

Hiroyuki Tawara, Yukikazu Itikawa[1], Yoh Itoh[2], Takako Kato, Hiroyuki Nishimura[3], Shunsuke Ohtani, Hidekazu Takagi[4], Kazuo Takayanagi[1] and Masahiro Yoshino[5]

Institute of Plasma Physics, Nagoya University, Chikusa-ku, Nagoya 464, Japan

July 1986

Permanent Address:

1) Institute of Space and Astronautical Science, Komaba, Tokyo 153
2) Faculty of Science, Josai University, Sakado 350-02
3) Department of Physics, Niigata University, Niigata 950-21
4) Medical School, Kitazato University, Sagamihara 226
5) Department of General Education, Shibaura Institute of Technology, Ohmiya 330

Abstract

The atomic and molecular data involving atomic hydrogens, molecular hydrogens and positive and negative hydrogen ions under electron, photon and ion/atom/molecule collisions, which are relevant to the study of cold edge plasmas, are surveyed and compiled.

Contents

Introduction

Up to now, much attention has been paid to the understanding of characteristics and behaviour of high temperature plasmas in order to realize thermonuclear fusions. Therefore a series of atomic and molecular (A/M) data surveyed in the past have been relevant to mainly those at high temperature plasmas, such as those of highly ionized (impurity) ions and their atomic structures.

On the other hand, it has now been realized that, in order to achieve high temperature plasmas, we have to understand the plasma behaviour near the edge or near the wall of plasma chambers. The properties of these cold plasmas are quite dependent upon the design of plasma apparatus. Some characteristics of such cold plasmas in a typical apparatus are shown in the following table.[1)]

	edge plasmas		
	scrape-off plasma	peripheral plasma	core plasma
n_e	10^{10} - 10^{13} /cm^3	10^{12} - 10^{13} /cm^3	10^{13} - 10^{14} / cm^3
T_e	1 - 100 eV	50 - 1000 eV	1 - 20 KeV

General characteristics of such cold edge plasmas are 1) low temperature (1 - 100 eV) and 2) relatively high density (10^{10} - 10^{13} /cm^3). Even at such low temperatures, therefore, the ionization rates are still high (90%). Then, there are a large number of ions (mainly protons). Therefore, the collisions involving molecular hydrogens in the ground and excited states, atomic hydrogens, positive and negative hydrogen ions, electrons and photons seem to play an important role in such low temperature plasmas. In order to understand and simulate the behaviour of such plasmas near the edge, A/M data at low energies are necessary. Few compilations of such A/M data at low energies are available presently[2]. In as early as 1975 - 1976[3,4], compilations of A/M data have been reported by the Study Group at Institute of Plasma Physics, Nagoya University. Since then some new and improved results have been reported.

In this Report, we compile A/M collision data involving hydrogen atoms and molecules and their ions in collisions with electrons, photons and ion/atom/molecule themselves which seem to be relevant to understanding of such cold edge plasmas. After compiling the relevant A/M data, we try to evaluate them and, instead of plotting all the data available, show smooth curves for different but similar processes to make a comparison easy and to show which processes are dominant.

In this compilation, the sections are divided into 1) electron collisions, 2) photon collisions and 3) ion/atom/molecule collisions, each section being further divided into a number of sub-sections. The relevant references are given at the end of each sub-section.

For the convenience, we show the potential energy curves of hydrogen molecule taken from a paper by Sharp[5] in Fig.1.

References

1) J. Nucl. Materials 128/129 (1984) (Proc. Sixth International Conference on Plasma Surface Interactions in Controlled Fusion Devices (ed. A. Miyahara, H. Tawara, N. Itoh, K. Kamada and G.M. McCracken)

2) R. K. Janev, W. D. Langer, K. Evans, Jr. and D. E. Post, PPPL-TM-368 (1985, Princeton Plasma Physics Laboratory)

3) IPPJ-DT-48 (1975, Institute of Plasma Physics, Nagoya University, ed. K. Takayanagi and H. Suzuki)

4) IPPJ-AM-50 (1976, Institute of Plasma Physics, Nagoya University, ed. K. Takayanagi, H. Suzuki and S. Ohtani)

5) T.E. Sharp, Atomic Data Tables 2 (1971) 119

Acknowledgements

The authors would like to acknowledge M. Itonaga and M. Udaka for their typing of the manuscript.

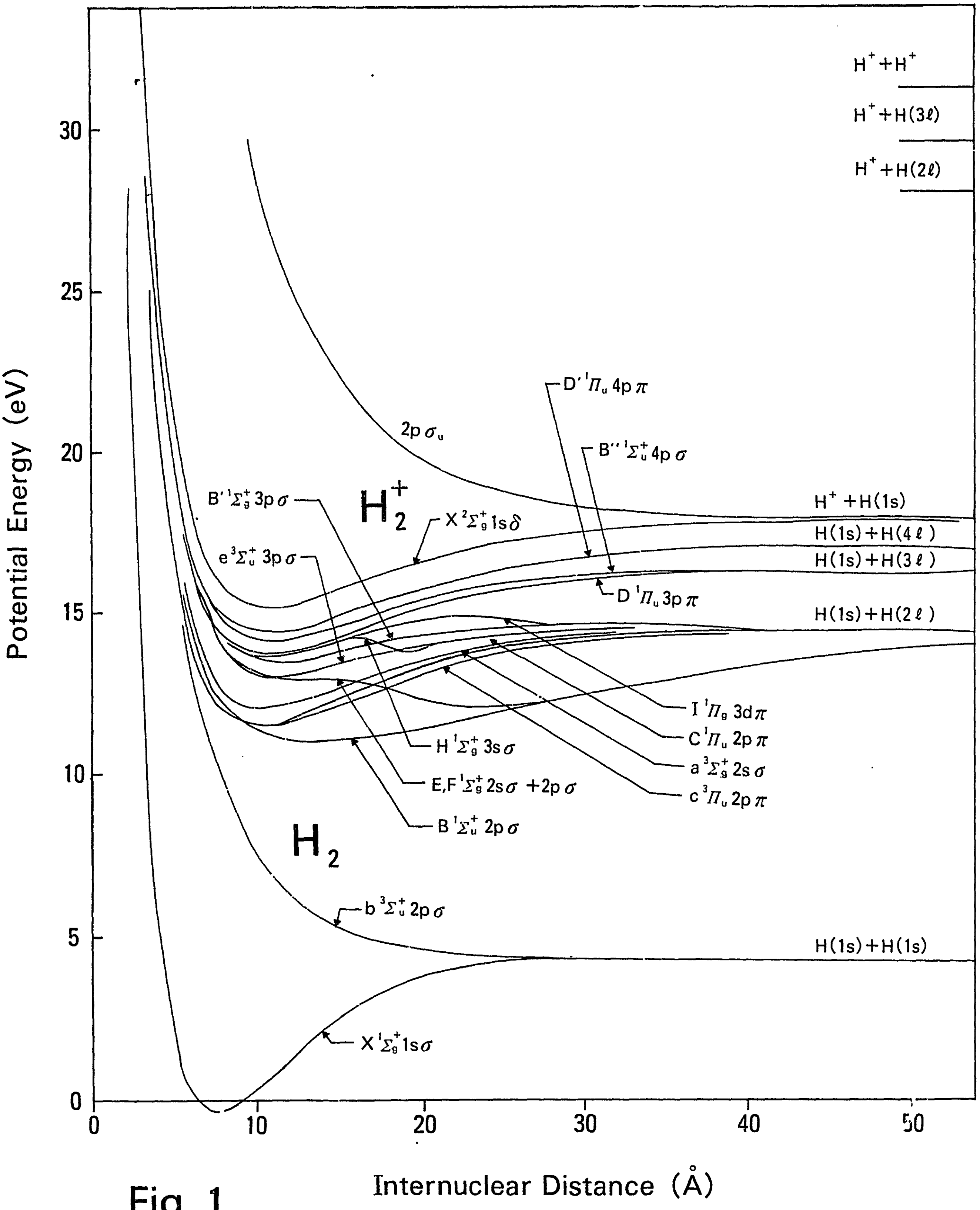
Potential Energy (eV)
Internuclear Distance (Å)
0
5
10
15
20
25
30
0
10
20
30
40
50
H⁺+H⁺
H⁺+H(3ℓ)
H⁺+H(2ℓ)
2p σᵤ
D' ¹Πᵤ 4p π
B'' ¹Σᵤ⁺ 4p σ
H₂⁺
B' ¹Σg⁺ 3p σ
X ²Σg⁺ 1s δ
e ³Σᵤ⁺ 3p σ
H⁺ +H(1s)
H(1s)+H(4 ℓ)
H(1s)+H(3 ℓ)
D ¹Πᵤ 3p π
H(1s)+H(2 ℓ)
I ¹Πg 3d π
C ¹Πᵤ 2p π
a ³Σg⁺ 2s σ
c ³Πᵤ 2p π
H ¹Σg⁺ 3s σ
E,F ¹Σg⁺ 2s σ +2p σ
B ¹Σᵤ⁺ 2p σ
H₂
b ³Σᵤ⁺ 2p σ
H(1s)+H(1s)
X ¹Σg⁺ 1s σ

Fig. 1

Figure Index

I Electron collisions

I-1 Rotational, vibrational and electronic excitation cross sections of H_2 and D_2 by electron impact

1.Experiment

The selected values of the experimental cross sections for the rotational, vibrational and electronic excitations of H_2 and D_2 by electron impact are shown in Figs. 2-13, together with typical theoretical results. The excited states considered and the sources of the cross sections are listed in Table 1. Recent experimental and theoretical situations in electron-molecule collisions were discussed extensively by Trajmar et al.[1], Csanak et al.[2] and Trajmar and Cartwright.[3]

As an illustration, the cross sections are summarized in Fig.2 with the total cross sections recommended by Hayashi(E1).

Measurement of rotational excitation cross sections were reported by Crompton et al.(J=0-2, swarm, E2), Gibson(J=1-3, swarm, E3) and Linder and Schmidt(J=1-3, beam, E4). Their cross sections are shown in Fig.3.

There are many measurements for the vibrational excitation. Almost all of the measurements were carried out without rotational states resolved. The measurement with rotational states resolved was carried out by Linder and Schmidt(v=0-1, J=0 and J=1-3, Beam, E4). The excitation cross sections for higher vibrational states were reported by Ehrhardt et al.(v=1,2,3, beam, E6) and Allan(v=1,2,3,4,5,6, beam, E8). Allan measured relative cross sections for various vibrational states and normalized them to the results(v=1) of Ehrhardt et al.(E6). The vibrational excitation cross sections are shown in Fig.4 with the theoretical results of Klonover and Kaldor[4].

Electronic excitation cross sections are determined usually by optical spectroscopy and/or electron energy loss spectroscopy. Reliability of the cross sections determined by the optical measurement depends on the calibration methods employed. In the excitation processes of H_2 accompanied by VUV photon radiation, the cross sections are usually determined by normalizing the relative photon intensity to an established Lyman-α emission cross section at a certain electron energy or to cross sections calculated by the first Born approximation at high electron energies. Recently, Shemansky et al.(E10) re-established the Lyman-α emission cross section ($\sigma = 8.18 \times 10^{-18} cm^2$ at 100eV) as a standard. The cross sections determined by Ajello et al.(optical, E9) are re-normalized to this new Lyman-α emission cross section by the present authors. de Heer and Carriere(optical, E12) normalized the measured relative intensities to the absolute values calculated by the first Born approximation at 1500eV. Khakoo and Trajmar(beam, E11) measured the excitation cross sections by the electron energy loss spectroscopy. Those and some other excitation cross sections are shown in Figs.5-13.

References

1. S.Trajmar, D.F.Register and A.Chutjian, Phys.Rept. 97 (1983) 219 "Electron Scattering by Molecules II. Experimental Methods and Data"
2. G.Csanak, D.C. Cartwright, S.K.Srivastava and S.Trajmar, Electron-Molecule Interactions and Their Applications vol.1 (ed. by L.G.Christophorou, Academic Press, 1984) p.1
3. S.Trajmar and D.C.Cartwright, ibid. p.155
4. A.Klonover and U.Kaldor, J. Phys. B 12 (1979)3797

Table 1. Experimentally determined cross sections for rotational, vibrational and electronic excitations of H_2 by electron impact.

Excited states	References
Total	E1
$X\ ^1\Sigma_g^+$, v=0, J=0→2	E2
J=1→3	E3, E4
$X\ ^1\Sigma_g^+$, v=0→1 (J:unresolved)	E2, E5, E6, E7, E8
(ΔJ=0 and J=1→3)	E4
$B\ ^1\Sigma_u^+$	E9, E10, E11
$B'\ ^1\Sigma_u^+$, $B''\ ^1\Sigma_u^+$	E9, E10
$C\ ^1\Pi_u$	E9, E10, E11, E12
$D\ ^1\Pi_u$, $D'\ ^1\Pi_u$	E9, E10
$a\ ^3\Sigma_g^+$	E11
$b\ ^3\Sigma_u^+$	E13, E14, E15
$c\ ^3\Pi_u$	E11

References to Table 1.

E1 M. Hayashi, IPPJ-AM-19 (Inst. Plasma Phys., Nagoya Univ., 1981)

E2 R. W. Crompton, D. K. Gibson and A. I. McIntosh, Aust. J. Phys. 22 (1969) 715 swarm

E3 D. K. Gibson, Aust. J. Phys. 23 (1970) 683 swarm

E4 F. Linder and H. Schmidt, Z. Naturforsch. 269 (1971) 1603 beam

E5 S. J. Schulz, Phys.Rev. 135 (1964) A988 beam

E6 H. Ehrhardt, L. Langhouse, F. Linder and H. S. Taylor, Phys. Rev. 173 (1969) 222 beam

E7 H.Nishimura, A. Danjo and H. Sugahara, J. Phys.Soc.Jpn. 54 (1985) 1757 beam

E8 M. Allan, J. Phys. B. 18 (1985) L451 beam

E9 J. M. Ajello, D. Shemansky, T. L. Kwok and Y. L. Yung, Phys.Rev. A291 (1984) 636 optical

E10 D. E. Shemansky, J.M. Ajello and D. T. Hall, Astrophys. J. 296 (1985) 765 optical

E11 M. A. Khakoo and S. Trajmar (1986, to be published) beam

E12 F.J.de Heer and J. D. Carriere, J.Chem. Phys. 55 (1971) 3829 beam

E13 S. J. B. Corrigan, J. Chem. Phys. 43 (1965) 4381 beam

E14 R. I. Hall and L. Andric, J.Phys.B. 17 (1984) 3815 beam

E15 H. Nishimura and A. Danjo (1986, to be published) beam

2. Theory

2-1: vibrational excitation

There are many calculations reported for the vibrational excitation of hydrogen molecules in lower energy region (below 10 eV). In his review, Lane discussed extensively those calculations published before 1980.[1] Further, he has given an additional remark in his recent review talk at the XIII ICPEAC.[2]

The most complete calculation reported so far is that made by Klonover and Kaldor.[3] They treated ab initio the static, electron-exchange and polarization interactions, but resort to the adiabatic nuclei approximation. Their result for the excitation $v=0 \rightarrow 1$ is compared with the experimental data in Fig. 4. The adiabatic nuclei approximation has been examined recently by Morrison et al. and found to be satisfactory except in the near-threshold region(below 2 eV).[4]

For the energies higher than about 10 eV, relatively few calculations have been reported. Lee and Freitas[5] applied their incoherent renormalized multicenter potential model to the vibrational excitation of H_2, in which they took into account approximately the electron-exchange and polarization effects. They gave only differential cross sections. There is a large discrepancy depending on the scattering angles, though a good overall agreement is seen with the measured data.

Truhlar and his colleague[6,7] made the Born and modified Born calculations up to 912 eV. Their values, however, are much dependent on the effective potential adopted in their calculation.

References

1. N. F. Lane, Rev. Mod. Phys. 52 (1980) 29

2. N. F. Lane, in Electronic and Atomic Collisions, (ed. by J. Eichler, I. V. Hertel and N. Stolterfoht, Elsevier Sci. Pub, 1984) p.127

3. A. Klonover and U. Kaldor, J. Phys. B 12 (1979) 3797

4. M. A. Morrison, A. N. Feldt and B. C. Saha, Phys. Rev. A 30 (1984) 2811

5. N.-T. Lee and L. C. G. Freitas, J. Phys. B 14 (1981) 4691

6. D. G. Truhlar and J. K. Rice, J. Chem. Phys. 52 (1970) 4480

7. D. G. Truhlar, Phys. Rev. A 7 (1973) 2217

2-2: electronic excitation

In Table 2, a list is given of the calculations reported since 1970 for the excitation of the electronic states of H_2. A similar list and rather extensive discussion on the theory (and also the experiment) are presented in a recent review by Trajmar and Cartwright.[1] Some elaborate calculations (i.e., by either a distorted-wave method or a close-coupling approximation) are shown and, where possible, compared with experimental data in Figs.5-7 and 9-13. In some cases the agreement with experiments is good, but in others there is a large discrepancy. This reflects the difficulty in the calculation of electronic excitation cross sections of molecules. Much work remains to be done to provide accurate theoretical data on this process.

The Born calculation, in principal, should be reliable at higher energies (say, above a few hundreds of electron volts). Their reliability, however, is to be confirmed experimentally.

1. S. Trajmar and D. C. Cartwright, in Electron-Molecule Interactions and Their Applications vol.1 (ed. by L. G. Christophorou, Academic Press, 1984) p.155

Table 2. Theoretical calculations for electron-impact excitation of the electronic states of H_2 published since 1970.

Excited states	References
B $^1\Sigma^+_u$	1, 2, 5, 7, 8, 10, 16
B' $^1\Sigma^+_u$	1, 2, 11, 16
B'' $^1\Sigma^+_u$	1, 2
C $^1\Pi_u$	1, 2, 11
D $^1\Pi_u$	1, 2
D' $^1\Pi_u$	1, 2
E,F $^1\Sigma^+_g$	1, 2, 10, 11
H $^1\Sigma^+_g$	1, 2
I $^1\Pi_g$	1, 2
a $^3\Sigma^+_g$	3, 5, 13
b $^3\Sigma^+_u$	3,4,5,7,9,12,13,14,15,17,18,19
c $^3\Pi_u$	3, 5, 11
e $^3\Sigma^+_u$	3, 5

References to Table 2 - method of calculation -

1 G. P. Arrighini, F. Biondi and C. Guidotti, Mol.Phys. 41 (1980) 1501
Born+Ochkur

2 G. P. Arrighini, F. Biondi and C. Guidotti, A. Biagi and F. Marinelli, Chem. Phys. 52 (1980) 133 Born

3 M. Cacciatore and M. Capitelli, Chem. Phys. 55 (1981) 67 Gryzinski

4 S. Chung, C.C. Lin and E. T. P. Lee, Phys. Rev. A 12 (1975) 1340
Born-Ochkur-Rudge

5 S. Chung and C. C. Lin, Phys. Rev. A 17 (1978) 1874 2CC

6 A. G. Domenicucci and K. J. Miller, J. Chem. Phys. 66 (1977) 3927 Born

7 A. W. Fliflet and V. McKoy, Phys, Rev. A 21 (1980) 1863 DW

8 A. U. Hazi, Phys, Rev. A 23 (1981) 2232 Semiclassical IPM

9 T. K. Holley, S. Chung, C. C. Lin and E. T. P. Lee, Phys. Rev. A 26 (1982) 1852 CC

10 W. Kołos, H. J. Monkhorst and K. Szalewicz, J. Chem. Phys. 77 (1982) 1335
Born

11 M.-T. Lee, R. R. Lucchese and V. McKoy, Phys. Rev. A 26 (1982) 3240 DW

12 T. N. Rescigno, C.W. McCurdy, Jr. and V. McKoy, J. Phys. B 8 (1975) L433
DW

13 T. N. Rescigno, C. W. McCurdy, Jr., V. McKoy and C.F.Bender, Phys. Rev. A 13 (1976) 216 DW

14 J. C. Steelhammer and S. Lipsky, J. Chem. Phys. 53 (1970) 1445
Born+Ochkur

15 C. A. Weatnerford, Phys. Rev. A 22 (1980) 2519 2CC

16 M. J. Redmon, B. C. Garrett, L. T. Redmon and C. W. McCurdy, Phys. Rev. A 32 (1985) 3354 Semiclassical IMP

17 K. L. Baluja, C. J. Noble and J. Tennyson, J. Phys. B 18 (1985) L851
R-matrix

18 B. I. Schneider and L. A. Collins, J. Phys. B 18 (1985) L857
2CC with optical potential and short-range correlation

19 M. A. P. Lima, T. L. Gibson, W. M. Huo and V McKoy, J. Phys. B 18 (1985) L865 Schwinger variational

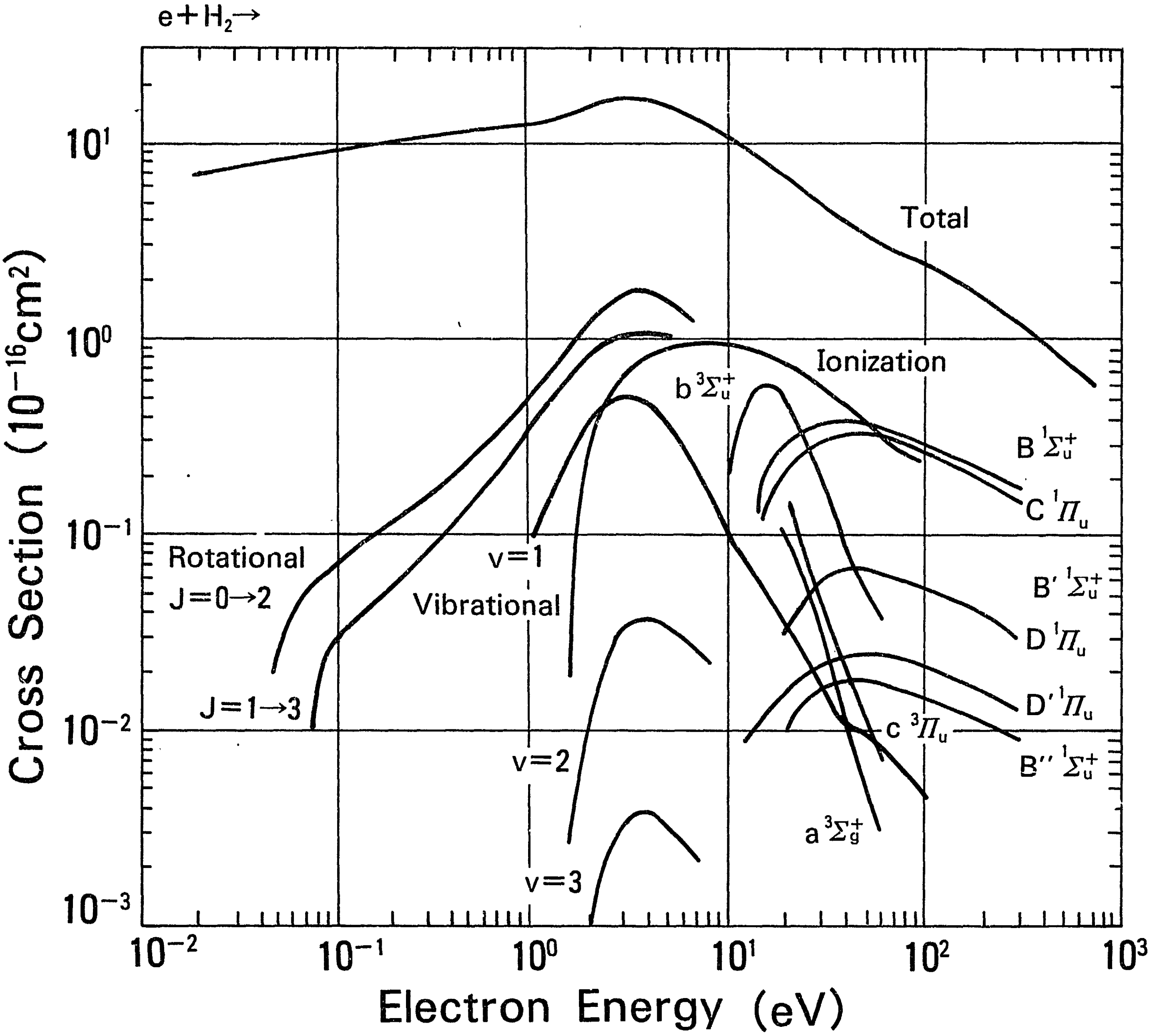
e+H₂→
Total
Ionization
Rotational
J=0→2
J=1→3
v=1
Vibrational
v=2
v=3
b ³Σu⁺
B ¹Σu⁺
C ¹Πu
B' ¹Σu⁺
D ¹Πu
D' ¹Πu
c ³Πu
B'' ¹Σu⁺
a ³Σg⁺
Cross Section (10⁻¹⁶cm²)
Electron Energy (eV)
10¹
10⁰
10⁻¹
10⁻²
10⁻³
10²
10³

Fig. 2

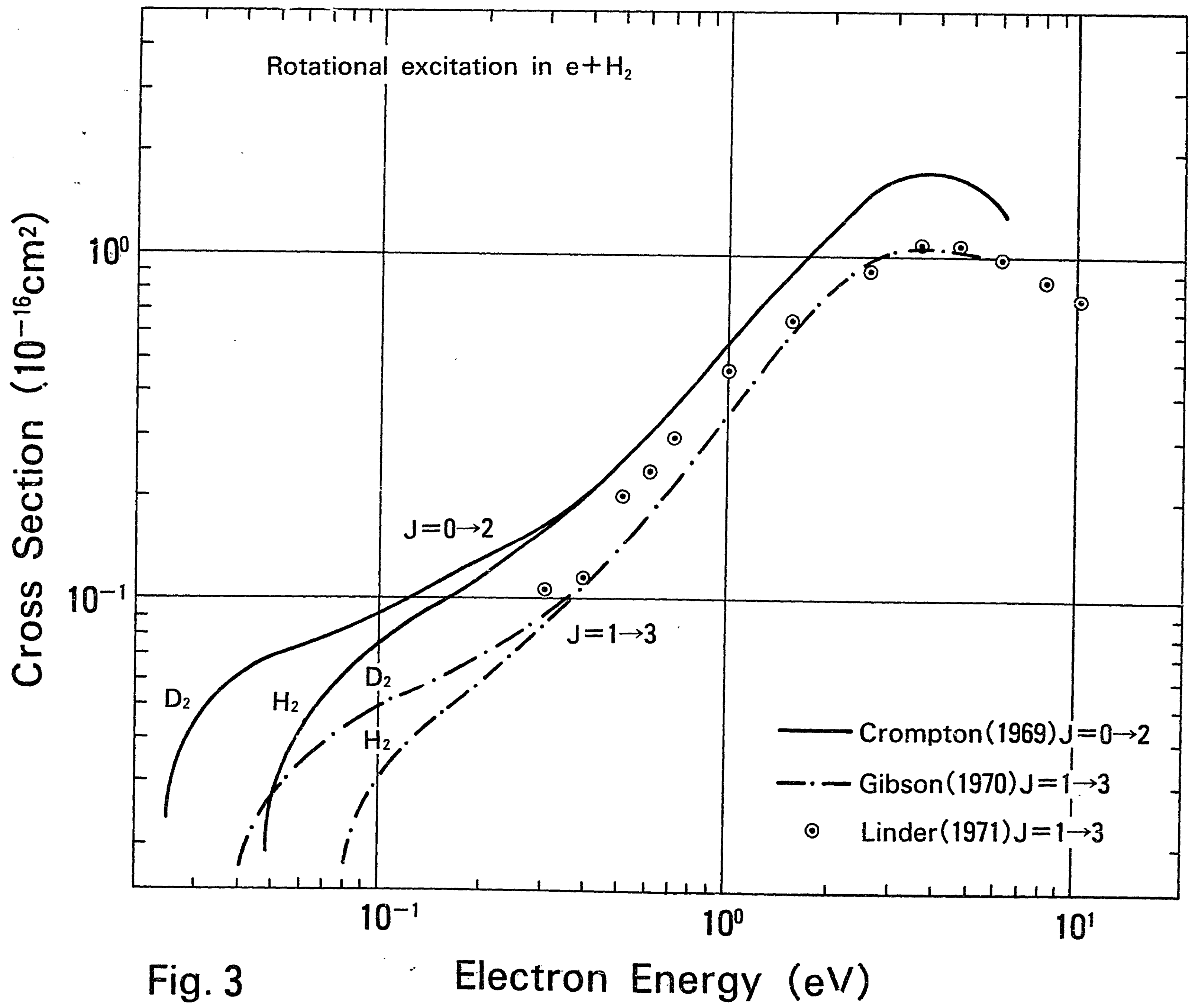
Rotational excitation in e+H₂
Cross Section (10⁻¹⁶cm²)
10⁰
10⁻¹
J=0→2
J=1→3
D₂
H₂
D₂
H₂
Crompton(1969)J=0→2
Gibson(1970)J=1→3
Linder(1971)J=1→3
10⁻¹
10⁰
10¹
Electron Energy (eV)

Fig. 3

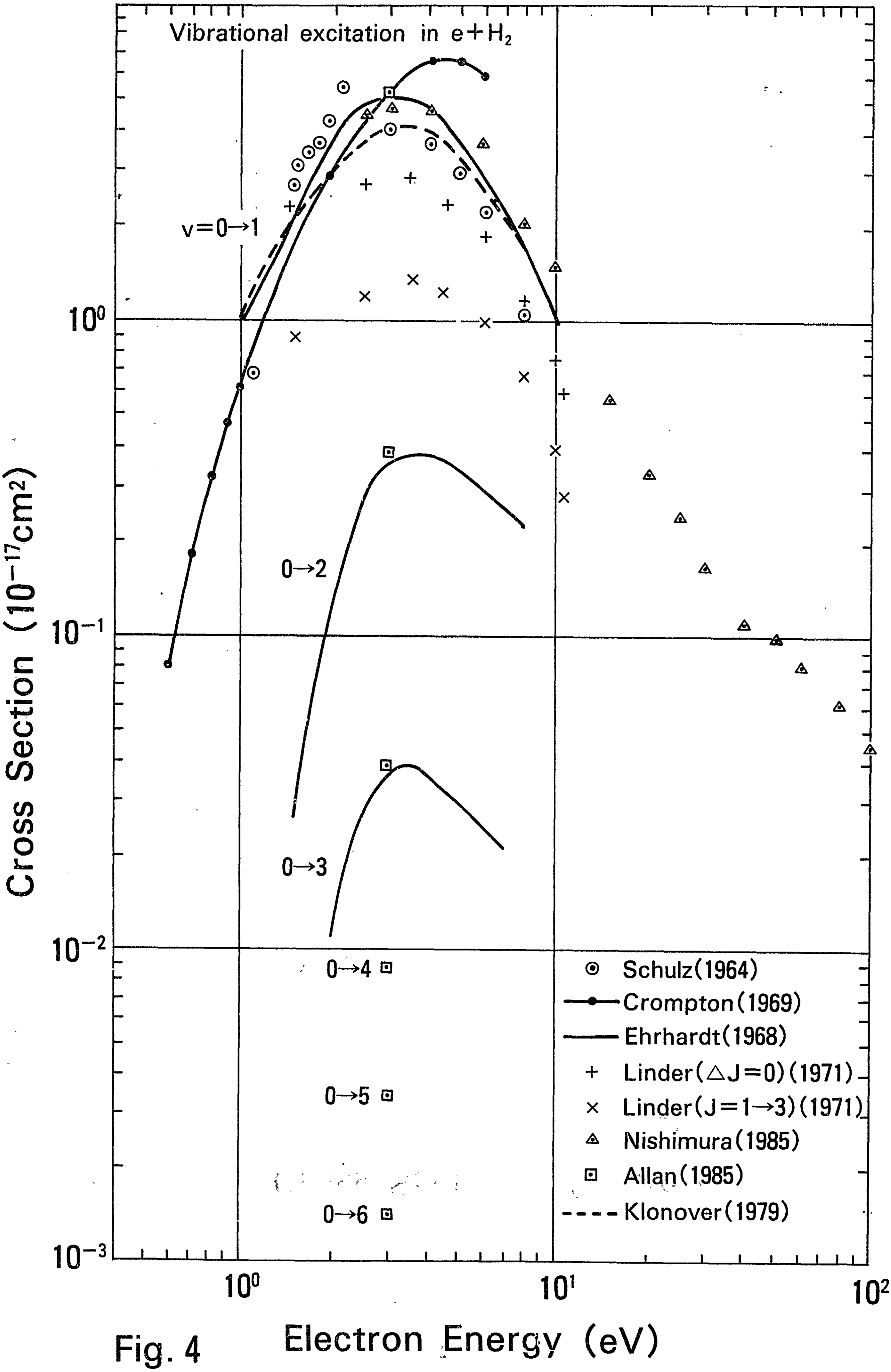
Vibrational excitation in e+H_2
v=0→1
0→2
0→3
0→4
0→5
0→6
Schulz(1964)
Crompton(1969)
Ehrhardt(1968)
Linder(△J=0)(1971)
Linder(J=1→3)(1971)
Nishimura(1985)
Allan(1985)
Klonover(1979)
Cross Section ($10^{-17}cm^2$)
10^0
10^{-1}
10^{-2}
10^{-3}
10^0
10^1
10^2
Electron Energy (eV)

Fig. 4

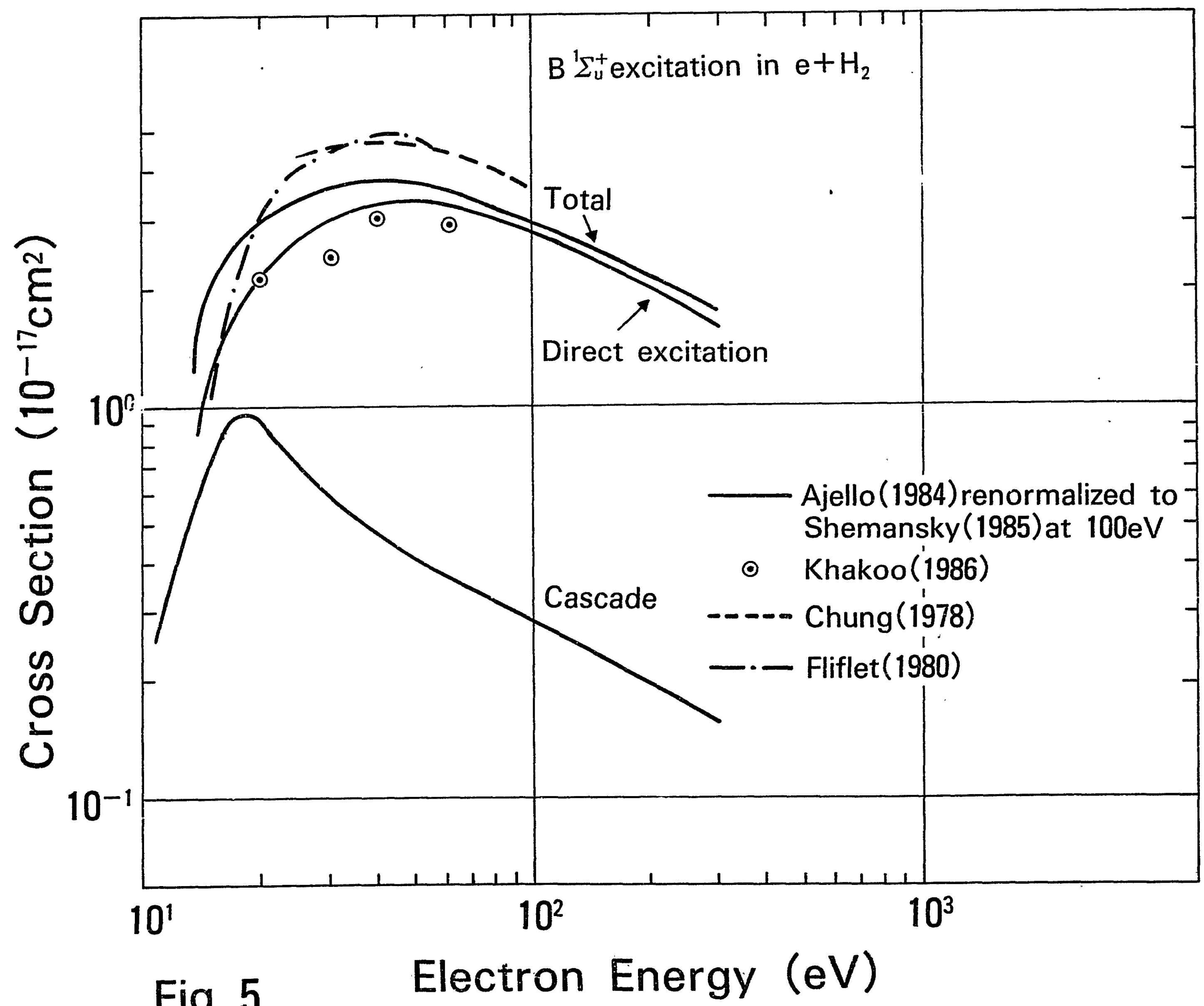

B ¹Σu⁺ excitation in e+H2
Total
Direct excitation
Cascade
Ajello(1984)renormalized to Shemansky(1985)at 100eV
Khakoo(1986)
Chung(1978)
Fliflet(1980)
Cross Section (10⁻¹⁷cm²)
10⁰
10⁻¹
10¹
10²
10³
Electron Energy (eV)

Fig. 5

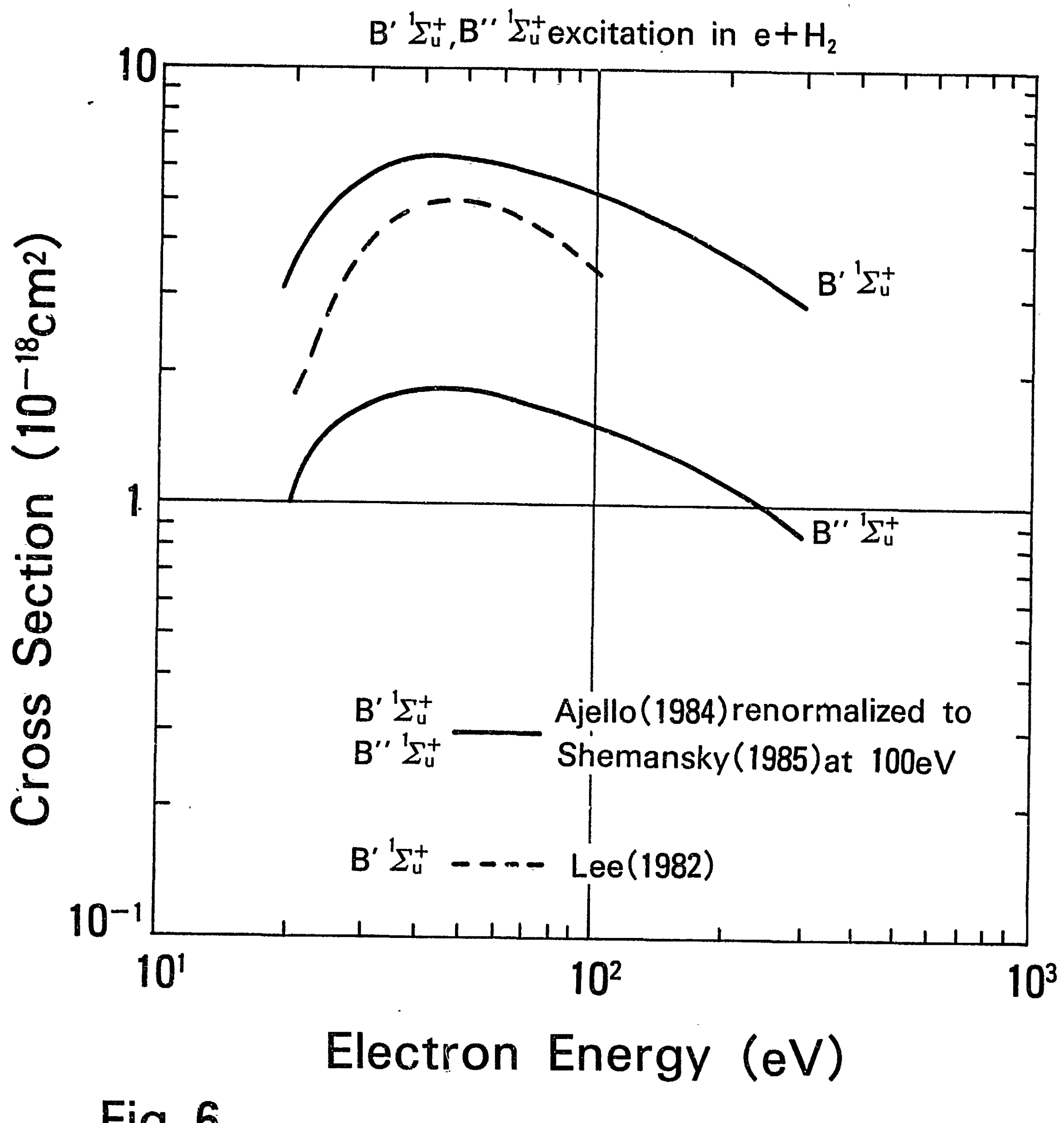

B′ $^1\Sigma_u^+$, B″ $^1\Sigma_u^+$ excitation in e+H_2
10
1
10^{-1}
10^1
10^2
10^3
Cross Section ($10^{-18}cm^2$)
Electron Energy (eV)
B′ $^1\Sigma_u^+$
B″ $^1\Sigma_u^+$
B′ $^1\Sigma_u^+$
B″ $^1\Sigma_u^+$
Ajello(1984)renormalized to
Shemansky(1985)at 100eV
B′ $^1\Sigma_u^+$
Lee(1982)

Fig. 6

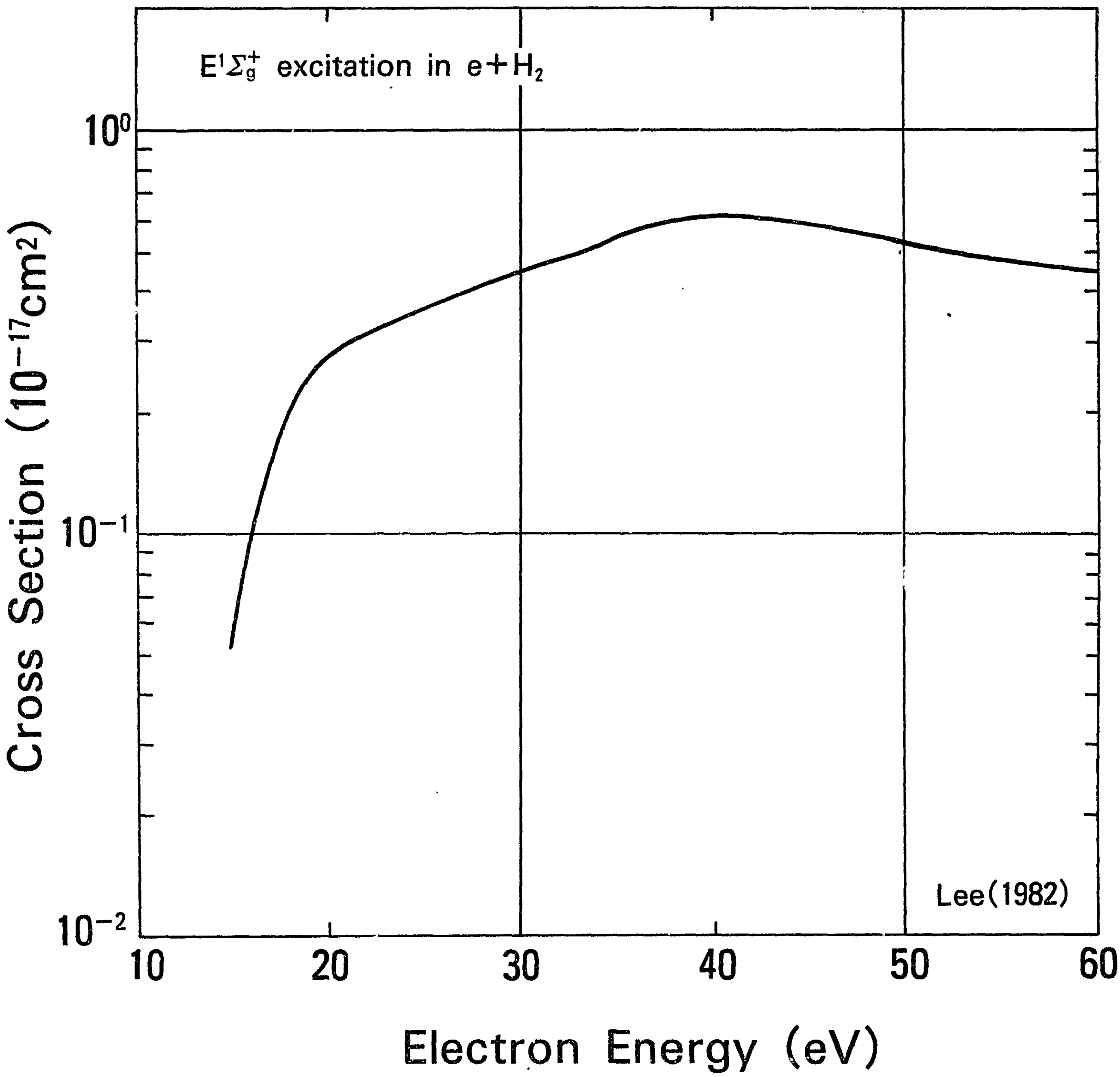

$E^1\Sigma_g^+$ excitation in $e+H_2$
Cross Section ($10^{-17}cm^2$)
10^0
10^{-1}
10^{-2}
10
20
30
40
50
60
Electron Energy (eV)
Lee(1982)

Fig. 7

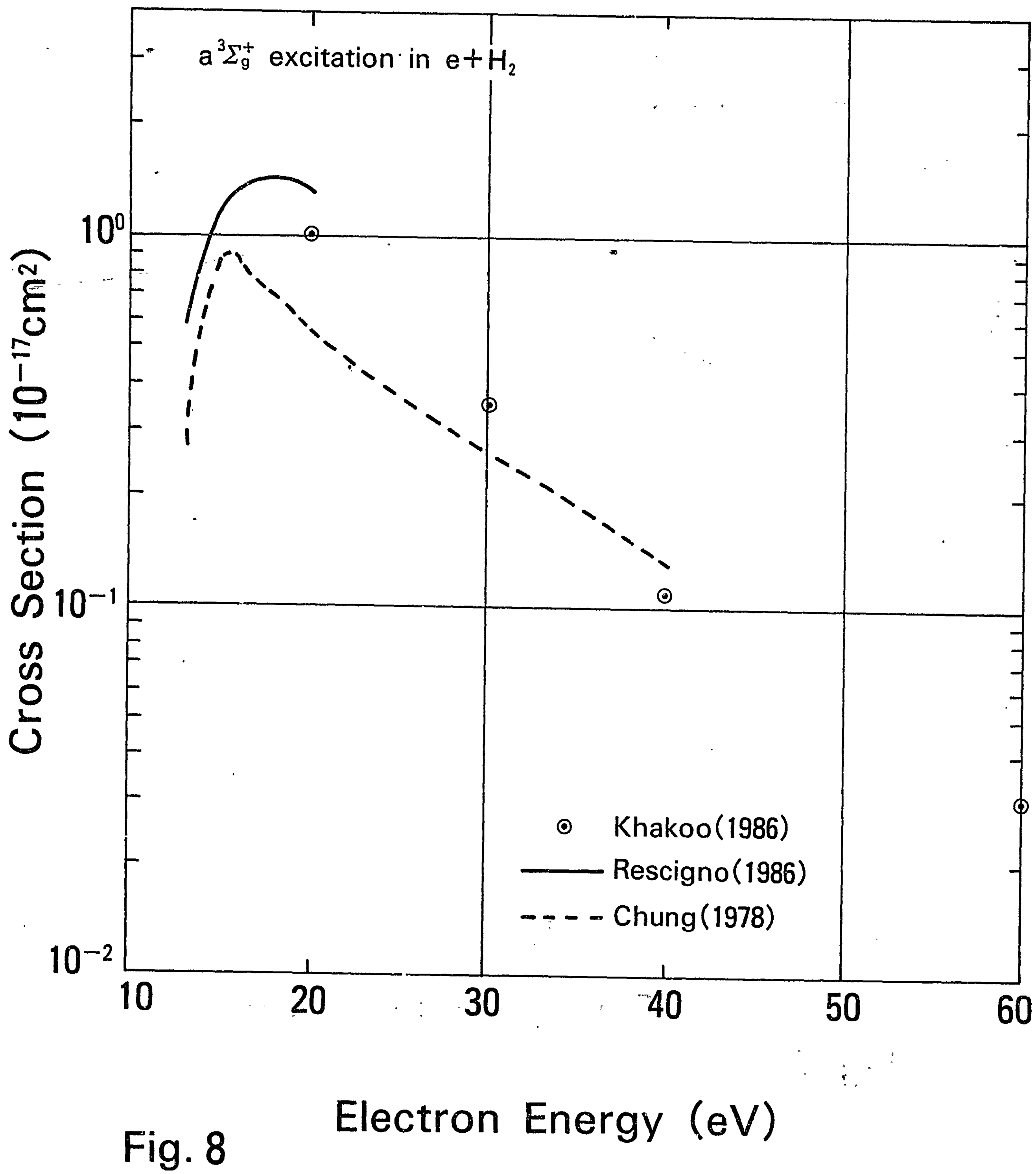
a ${}^3\Sigma_g^+$ excitation in e+H_2
Cross Section (10^{-17}cm^2)
10^0
10^{-1}
10^{-2}
10
20
30
40
50
60
Khakoo(1986)
Rescigno(1986)
Chung(1978)
Electron Energy (eV)

Fig. 8

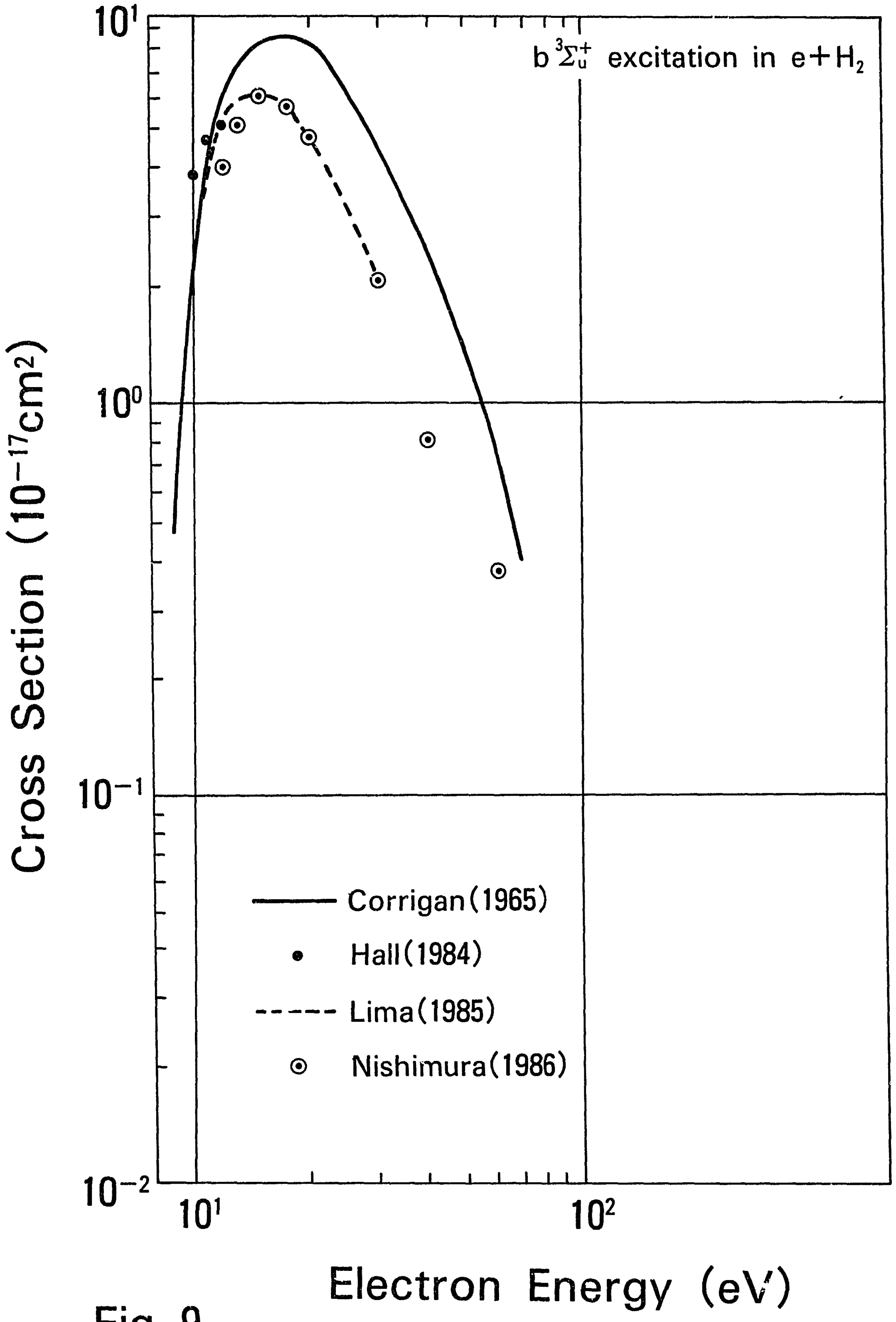

10^1
10^0
10^{-1}
10^{-2}
10^1
10^2
Cross Section ($10^{-17}cm^2$)
Electron Energy (eV)
$b\,^3\Sigma_u^+$ excitation in $e+H_2$
Corrigan(1965)
Hall(1984)
Lima(1985)
Nishimura(1986)

Fig. 9

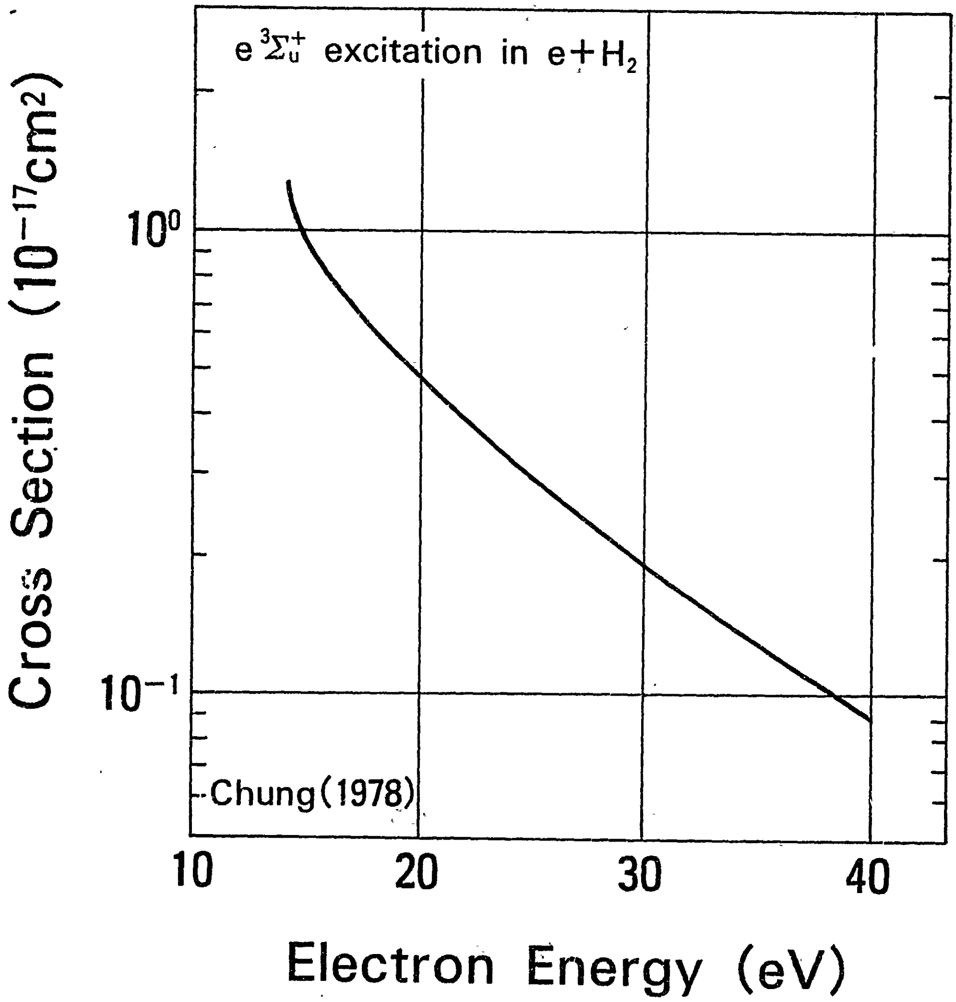

e ³Σu+ excitation in e+H2
Cross Section (10⁻¹⁷cm²)
10⁰
10⁻¹
Chung(1978)
10
20
30
40
Electron Energy (eV)

Fig. 10

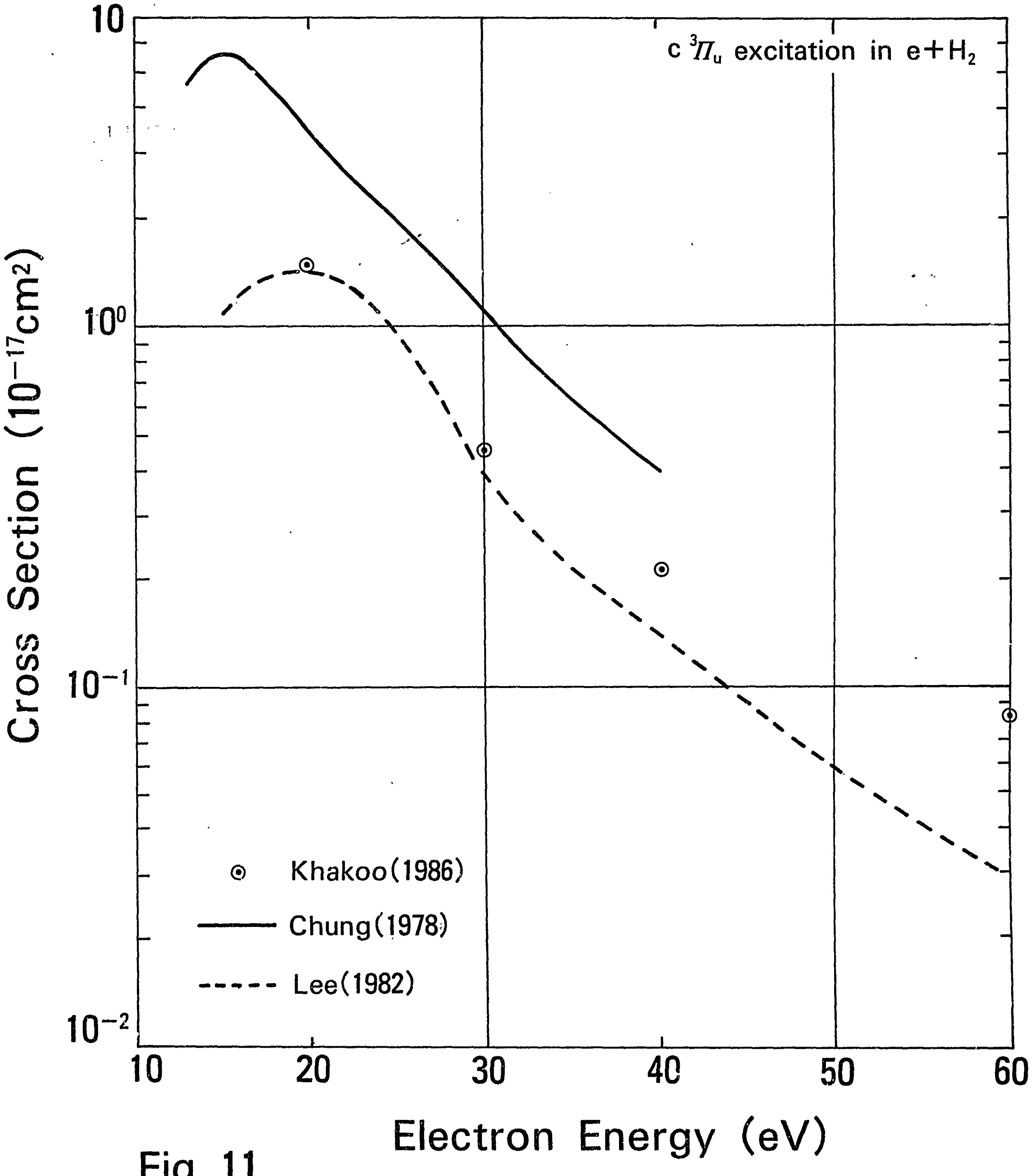
c $^3\Pi_u$ excitation in e+H_2
Cross Section ($10^{-17}cm^2$)
10
10^0
10^{-1}
10^{-2}
10
20
30
40
50
60
Electron Energy (eV)
Khakoo(1986)
Chung(1978)
Lee(1982)

Fig. 11

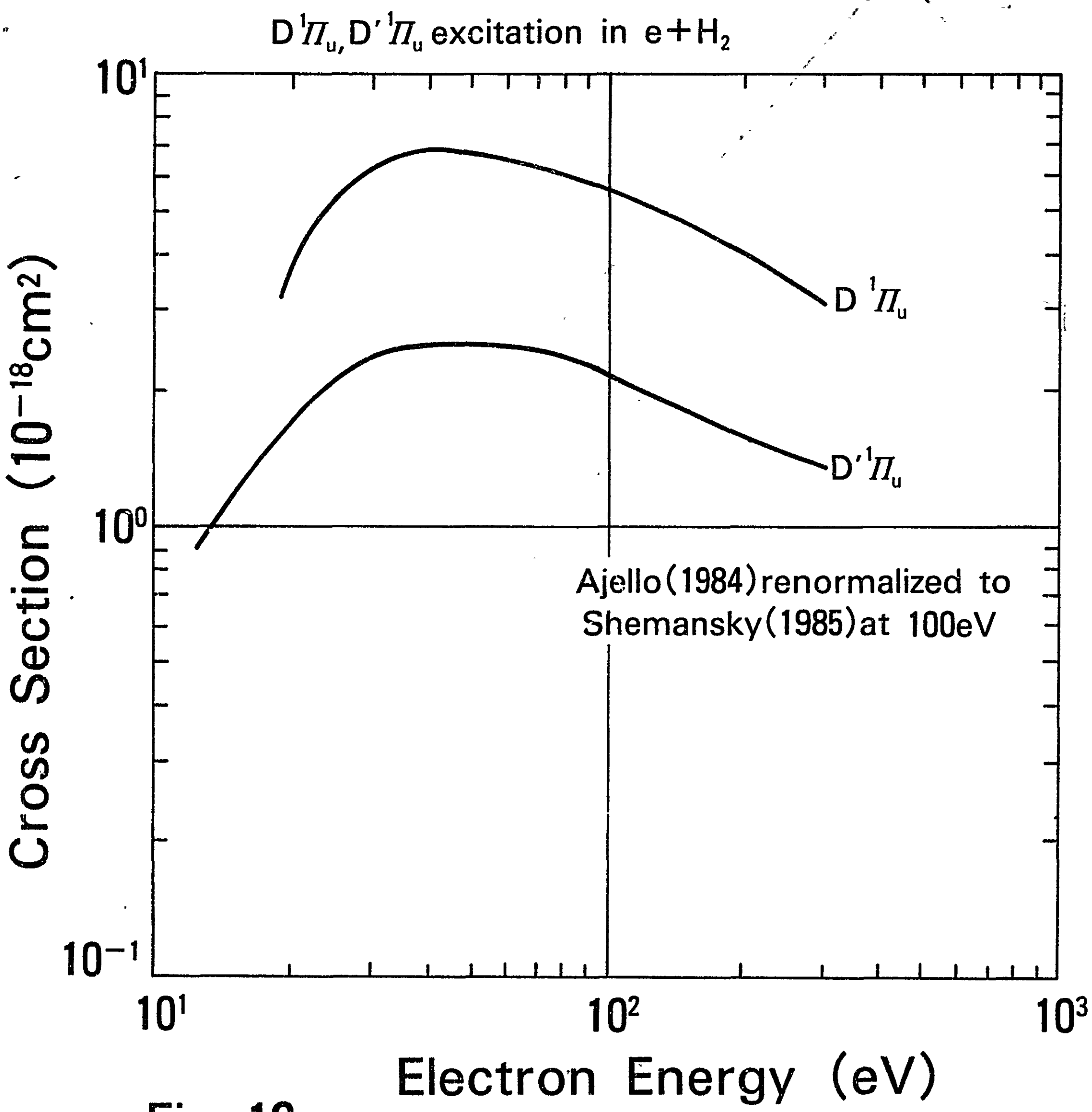

D ¹Πu, D′ ¹Πu excitation in e+H2
Cross Section (10⁻¹⁸cm²)
10¹
10⁰
10⁻¹
D ¹Πu
D′ ¹Πu
Ajello(1984)renormalized to
Shemansky(1985)at 100eV
10¹
10²
10³
Electron Energy (eV)

Fig. 12

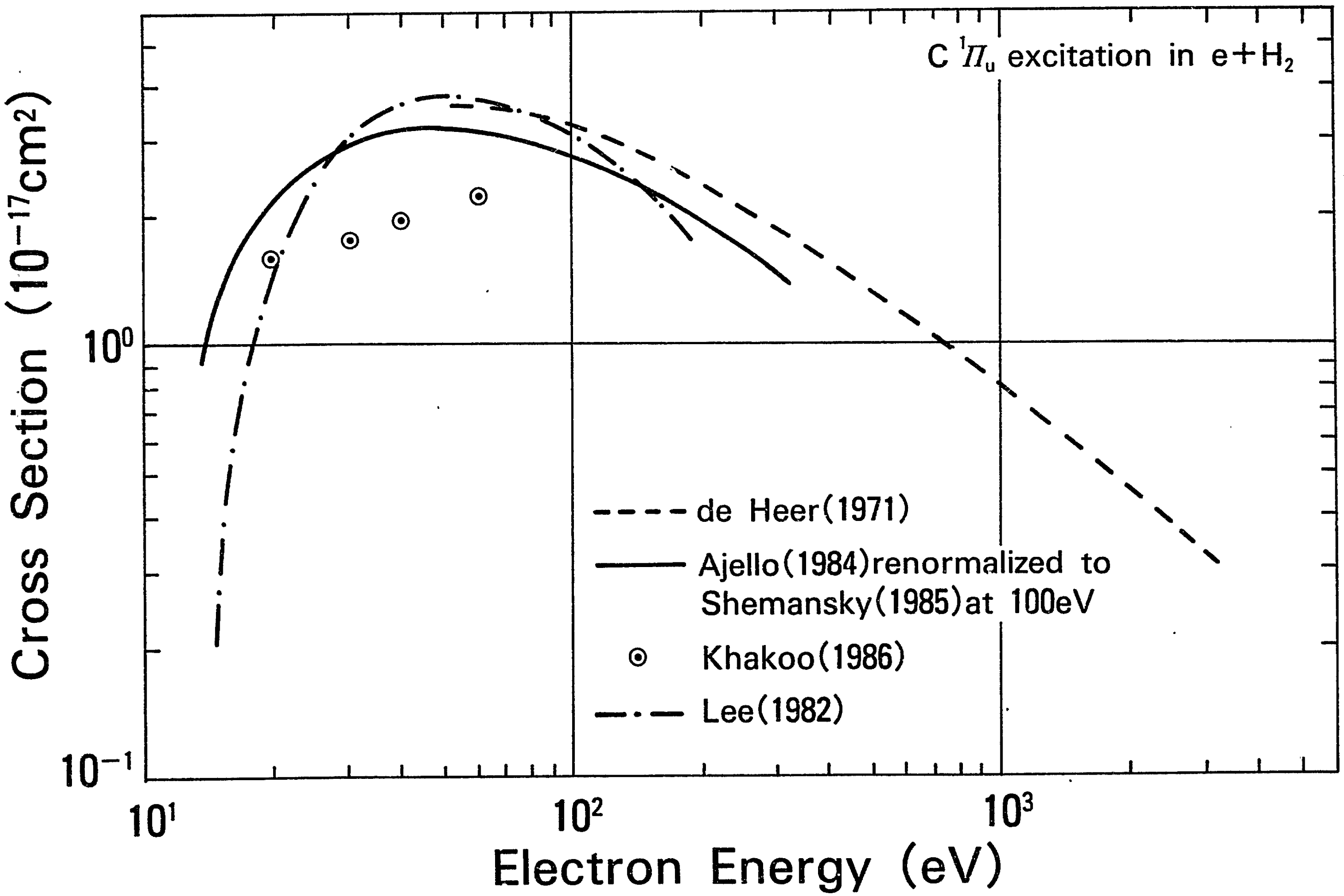

C ¹Πu excitation in e+H₂
Cross Section (10⁻¹⁷cm²)
10⁰
10⁻¹
10¹
10²
10³
Electron Energy (eV)
de Heer(1971)
Ajello(1984)renormalized to
Shemansky(1985)at 100eV
Khakoo(1986)
Lee(1982)

Fig. 13

I-2 Dissociative excitation of H_2 by electron impact

$e + H_2 \rightarrow$ photons

The cross sections on dissociative excitation by electron impact are often measured through photon detections (see Fig. 14).

(1) Emission cross sections of Balmer-α, β, γ and δ lines.

$$e + H_2 \rightarrow e + H + H + h\nu \ (n=3\rightarrow2) \quad \text{Balmer-}\alpha \quad (1)$$
$$(n=4\rightarrow2) \quad \text{Balmer-}\beta \quad (2)$$
$$(n=5\rightarrow2) \quad \text{Balmer-}\gamma \quad (3)$$
$$(n=6\rightarrow2) \quad \text{Balmer-}\delta \quad (4)$$

A number of the absolute emission cross sections of Balmer-α, β, γ and δ lines from H_2 have been reported. The agreement among different measurements seems to be fairly good except for those by Vroom and de Heer whose data at lower energies (below 150 eV) show slightly different behavior. Also these emission cross sections for D_2 have been determined. The cross section ratios $\sigma(H_2)/\sigma(D_2)$ for H_2 and D_2 are varied with the election energy. For example, those for Balmer-α line change from 1.4 at low energies to 1.1 at high energies (above 100 eV) and those for Balmer-β line change from 1.7 at low energies to 1.1 at high energies(above 60 eV).

(2) Emission cross sections of Lyman-α and -β lines

$$e + H_2 \rightarrow e + H + H + h\nu \ (n=2\rightarrow1) \quad \text{Lyman-}\alpha \quad (5)$$
$$(n=3\rightarrow1) \quad \text{Lyman-}\beta \quad (6)$$

Mumma and Zipf[5] determined their absolute cross sections from ratios of the cross section for production of the countable ultra-violet (CUV) radiations to the cross sections for excitation of Lyman-α radiations[6] which absolute value is taken from that at 100 eV by Long et al.[7], taking into account the contribution of molecular radiations transmitted through a LiF-O_2 filter[8].

This value (1.2×10^{-17} cm^2 $\pm 11\%$ at 100 eV) was often used as a standard for determing the cross sections for other collision processes for more than 10 years.[9,10] However, very recently Shemansky et al.[11] have reexamined carefully and redetermined the cross section which should be $(8.18 \pm 1.20) \times 10^{-18}$ cm^2 at 100 eV, based upon the Born approximation calculation for H_2 Rydberg system cross sections using the measured excitation function. Thus, all the measured cross sections which are used this standard should be reduced by a factor of 0.69. Data in Fig.14 taken from the original values by Mumma and Zip[5], Ajello et at.[5] and Vroom and de Heer,[2] have been corrected in this way.

3) Production cross sections of metastable H(2s) state

$$e + H_2 \rightarrow e + H \rightarrow H(2s) \qquad (7)$$

Vroom and de Heer[2] and later Möhlmann et al.[9] measured the production cross sections of H(2s) metastable state by electron impact in the energy range from 50 eV up to several thousands of eV by means of the electrostatic field quenching method. The independent determination of the production cross sections of D(2s) metastable state was also reported by Cox and Smith.[12] In their experiment, the absolute scale was established on a purely experimental basis in contrast to Möhlmann et al.[9] whose measured relative values were normalized to the Mumma and Zipf cross section value at the electron energy of 100 eV. The method Cox and Smith utilized depended on the application of an rf field at the Lamb-shift frequency to quench the metastables at the point of excitation. The Cox and Smith results are in good agreement with the recent work by Möhlmann et al.[9] in the high energy region. However, a considerable discrepancy is seen between both results in the lower electron energy region. The cross sections for production of H(2s) state, shown in Fig.14, are deduced from the data by Cox and Smith for

D_2 under the assumption that the ratios of H(2s) from H_2 to D(2s) from D_2 are the same as observed by Vroom and de Heer[2] (1.20) over the energy range investigated.

4) Cross section for dissociative excitation to high-Rydberg atoms

Schiavone et al.[13] determined absolute excitation cross section for production of high-Rydberg(HR) atomic fragments to be 2.2 x 10^{-20} cm^2 at the electron energy of 100 eV from measurements of total HR signal and other experimental parameters. This cross section value was compared with that obtained by Carnahan and Zipf[14] after correcting the radiative decay effect and other apparatus-dependent factors. The agreement within the experimental uncertainties was obtained.

5) Emission of the Werner-and Lyman-band systems

$$e + H_2 \rightarrow e + H_2^{*}\ (C^1\Pi_u \rightarrow X^1\Sigma_g^+)\quad \text{Werner-band} \quad (8)$$

$$(B^1\Sigma_u^+ \rightarrow X^1\Sigma_g^+)\quad \text{Lyman-band.} \quad (9)$$

The cross sections for the emissions of these bands were reported.[15,16] Though these processes are not dissociative, they seem to be relevant to comparing with other dissociative processes which result in photon emission.

Other types of experimental work which clarifies the nature of dissociative products are summarized briefly:

i) Many time-of-flight studies of H(2s) metastable fragments produced in the dissociative excitation of molecular hydrogen by electron impact were reported.[14,17,18] Further, the dissociation into two 2p state atoms was investigated.[19]

ii) The kinetic energy distributions of fragment atoms were also studied for the states with short life times by means of analyzing the Doppler profiles of the Balmer emission spectra[20,21].

iii) The angular distributions of the dissociative products were reported by Misakian and Zorn[22] for H(2s), by Takahashi et al.[23] for H(n=3), and by Kurawaki and Ogawa [24] for H(n=4).

References

1. G.R. Möhlmann and F.J. de Heer, Chem. Phys. 40 (1979)157; 25 (1977) 103
2. D.A. Vroom and F.J.de Heer, J. Chem. Phys. 150(1969) 580
3. G.A. Khayrallah, Phys. Rev. A 13 (1976) 1983
4. C. Karolis and E. Harting, J. Phys. B 11 (1978) 357
5. M.J. Mumma and E.C.Zipf, J.Chem. Phys. 55 (1971) 1661
6. W.E. Kauppila, P.J.O. Tuebner, W. L. Fite and H.I Girnius, J.E.Giemius, J.Chem.Phys. 54 (1971) 1670
7. R.L.Long, D.M. Cox and S.J. Smith, J. Res. NBS 72A (1968) 521
8. J.D. Carriere and F.J. de Heer, J. Chem. Phys. 56(1972) 2993
9. G.R. Möhlmann, K.H.Shima and F.J. de Heer, Chem. Phys. 28 (1978) 331
10. J.M. Ajello, D.Shemansky, T.L.Kwok and Y.L. Yung, Phys.Rev. A 29 (1984) 636
11. D.E. Shemansky, J.M.Ajello and D.T.Hall, Astrophys.J. 296 (1985) 765
12. D.M. Cox and S.J. Smith, Phys. Rev. A 5 (1972) 2428
13. J.A. Schiavone, S.M. Tarr and R.S Freund, J. Chem. Phys. 70 (1979) 4468
14. B.L. Carnahan and E.C. Zipf, Phys. Rev. A 16 (1977) 991
15. E.J. Stone and E.C. Zipf, J. Chem. Phys. 56 (1972) 4646
16. J.M. Ajello, S.K. Srivastava and Y.K. Yung, Phys. Rev. A 25 (1982) 2485
17. S.R. Ryan, J.J. Spezeski, O.F. Kolman, O.F. Lamb and H.H. Wing, Phys. Rev. A 19 (1979) 2192
18. J.J. Spezeski, O.F. Kalman and L.C. McIntyre, Phys. Rev. A 22 (1980) 1906
19. N. Böse, J. Phys. B 11 (1978) L309

20. M. Higo, S. Kamata and T. Ogawa, Chem. Phys. 66 (1982) 243

21. G. Glass-Maujean, J. Phys. B 11 (1978) 431

22. M. Misakian and J.C. Zorn, Phys. Rev. A 6 (1972) 2180

23. N. Takahashi, S. Arai, N. Kouchi, N. Oda and Y. Hatano, J. Phys. B 16 (1983) L547

24. J. Kurawaki and T. Ogawa, Chem. Phys. 86 (1984) 295

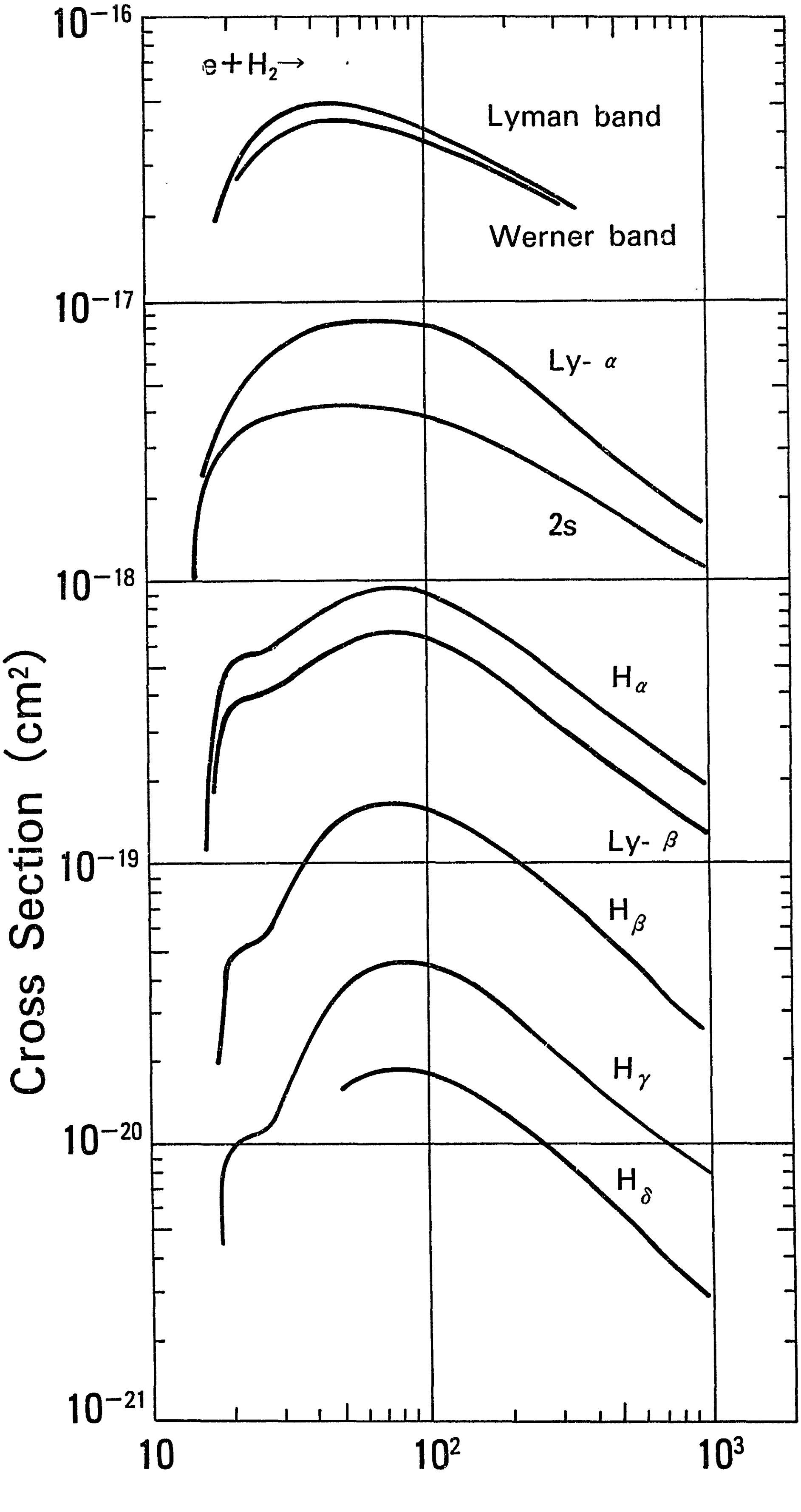

$e+H_2\rightarrow$
Lyman band
Werner band
Ly- α
2s
Hα
Ly- β
Hβ
Hγ
Hδ
Cross Section (cm²)
Electron Energy (eV)
10⁻¹⁶
10⁻¹⁷
10⁻¹⁸
10⁻¹⁹
10⁻²⁰
10⁻²¹
10
10²
10³

Fig. 14

I-3 Simple ionization and dissociative ionization of H_2 by electrons

The following ionization processes are probable in electron impact on H_2 (see Fig.15):

$$e + H_2 \rightarrow H_2^+ + 2e \quad (1)$$
$$\rightarrow H + H^+ + 2e \quad (2)$$
$$\rightarrow H + H^+ + 3e \quad (3)$$
$$\rightarrow \text{Sum } (1)+(2)+(3) \quad (4).$$

These cross sections are given in our previous compilations[1, 2]. It should be noted that the contribution of process(3) to production of protons may not be negligible and the differentiation of these processes (2) and (3) should be important. For a reference, the cross sections for ionization of atomic hydrogens in ground and metastable states are shown:

$$e + H \rightarrow H^+ + 2e \quad (5)$$
$$e + H(2s) \rightarrow H^+ + 2e \quad (6)$$

References

1. H. Tawara, T. Kato and M. Ohnishi, IPPJ-AM-37 (1985)
2. K. Takayanagi and H. Suzuki(ed.), IPPJ-DT-48(1975)

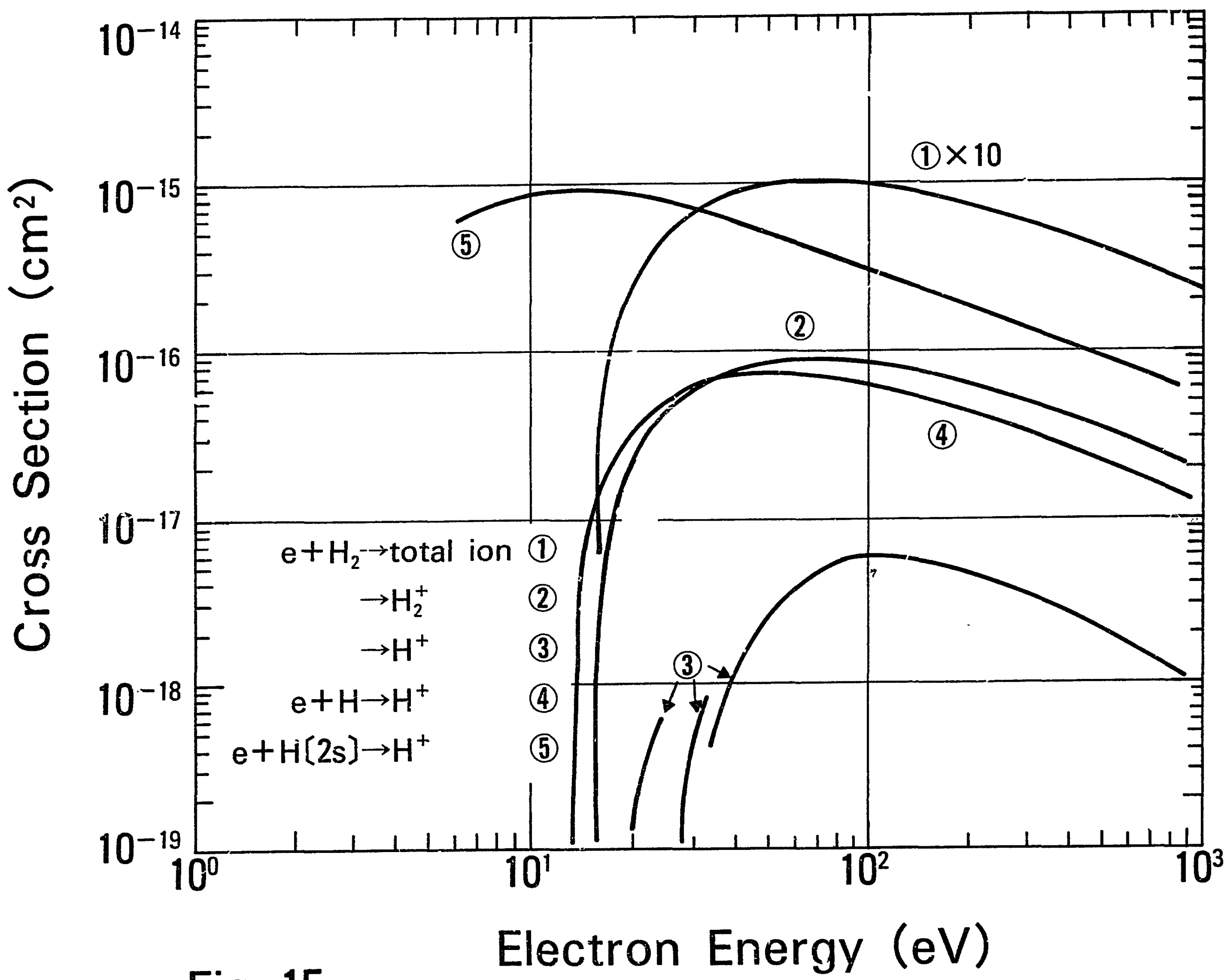

Cross Section (cm²)
10⁻¹⁴
10⁻¹⁵
10⁻¹⁶
10⁻¹⁷
10⁻¹⁸
10⁻¹⁹
10⁰
10¹
10²
10³
Electron Energy (eV)
①×10
②
③
④
⑤
e+H₂→total ion ①
→H₂⁺ ②
→H⁺ ③
e+H→H⁺ ④
e+H(2s)→H⁺ ⑤

Fig. 15

I-4 Dissociative attachment to H_2 and D_2 by electron impact

$e + H_2 \rightarrow H + H^-$

The cross sections for dissociative electron attachment are shown in Fig.16 which is taken from our previous compilation[1-3]. Practically no significant change of these data is necessary except for one point. Recently it has been confirmed experimentally and theoretically that a small peak near the impact energy of 4 eV is strongly enhanced if H_2 targets are in the excited states (either rotationally or vibrationally)[4-6]. For example, the cross sections for D_2^* at the vibrationally excited states (v=4) are four to five orders of magnitude larger than those for the ground state (v=0). This finding is now contributing to production of intense negative hydrogen beams for application to fusion research.

References

1. K. Takayanagi and H. Suzuki, IPPJ-DT-48 (1975) M-D-Fig.5.
2. G.J. Schulz and R.K. Asundi, Phys. Rev. 158(1967) 25
3. D. Rapp, J.E. Sharp and D.D. Briglia, Phys. Rev. Letters 14(1965) 533
4. M. Allan and S.F. Wong, Phys. Rev. Letters 41(1978) 1791.
5. J.N. Bardsley and J. M. Wadehra, Phys. Rev. A 20(1979) 1398
6. J.P. Gauyacq, J. Phys. B 18(1985) 1859

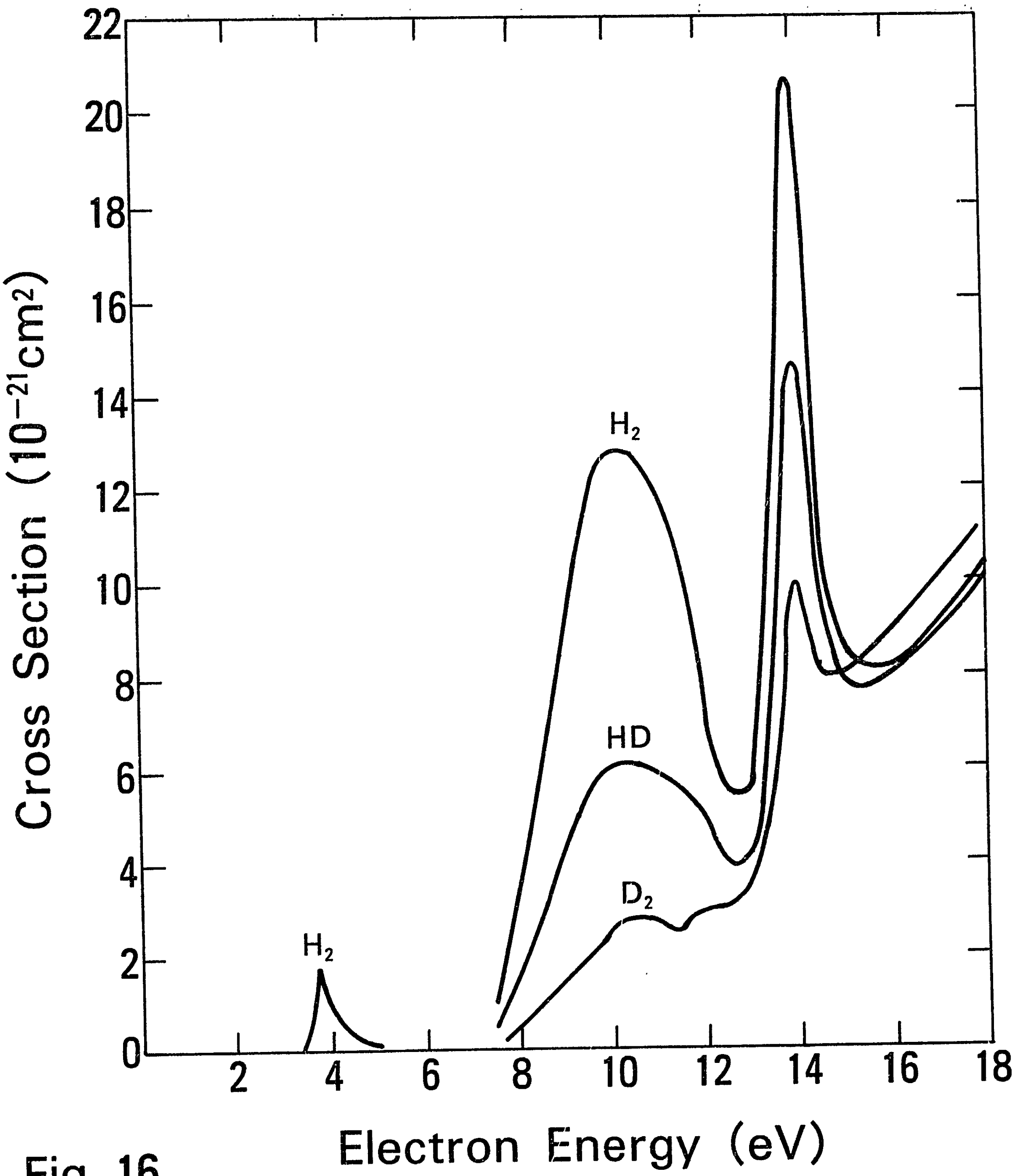

Fig. 16

Taken from M-D-Fig.5 Dissociative Attachment[19)20)]
IPPJ-DT-48 (1975)

I-5 e + H collisions

The cross sections for the following processes were measured (see Fig. 17):

$$e + H \rightarrow e + H(2s) \quad (1)$$

$$\rightarrow e + H(2p) \quad (2)$$

$$\rightarrow e + H(n=3) \quad (3)$$

$$\rightarrow 2e + H^{+} \quad (4)$$

Long et al.[1] measured the cross sections for Lyman-α radiation emission observed at 90°. Based upon their data, together with the correction for the cascading and polarization effects, the cross sections for 1s2p excitation process(2) were established by van Wyngaarden and Walters[2] who calculated them using the pseudo state method and found their values are in good agreement with the experimental data over the energy range of 12.2-54.4 eV. The cascade effect is estimated to be relatively small.[3] The cross sections for 1s→2s excitation process(1) were determined by normalizing to those of Long et al.[1] for Lyman α radiation.[4] The calculated values by Callaway[5] using the pseudo state method are slightly smaller than the experimental data.

Mahan et al.[6] investigated the Balmer-α line emission process corresponding to process(3) and determined the cross sections by normalizing to the Born approximation at 500 eV. The ionization cross sections for process(4) are taken from our previous compilation[7].

References

1. R.L. Long, D.M. Cox and S.J. Smith, J.Res. NBS 72A (1968) 521; W.L. Fite, R.F. Stebbings and R.T. Brackmann, Phys.Rev. 116 (1959) 356; W.L. Fite and R.T. Brackmann, Phys.Rev 112 (1958) 1151

2. W.L. van Wyngaarden and H.R.J. Walters, J. Phys. B 19 (1986) L53

3. D.J.T. Morrison and M.R.H. Rudge, Proc. Phys. Soc. 89 (1966) 45

4. W.E. Kauppila, W.R. Ott and W.L. Fite, Phys. Rev. A 1 (1970) 1099

5. J. Callaway, Phys. Rev. A 2 (1985) 775

6 A.H.Mahan, A. Gallagher and S.J. Smith, Phys. Rev. A 13 (1976) 156

7. H. Tawara, T.Kato and M. Ohnishi, IPPJ-AM-37 (1985)

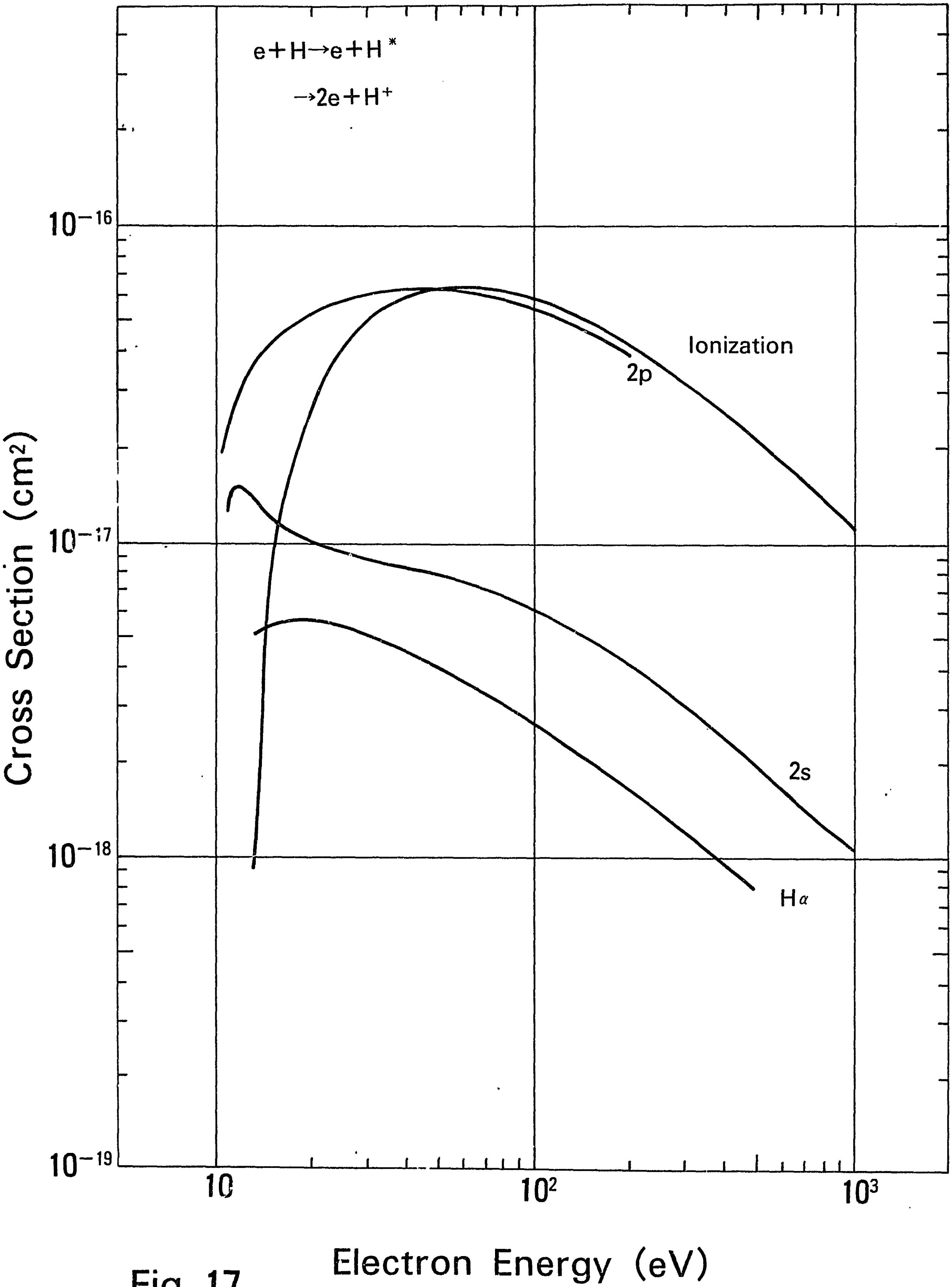

e+H→e+H*
→2e+H+
Ionization
2p
2s
Hα
Cross Section (cm²)
10⁻¹⁶
10⁻¹⁷
10⁻¹⁸
10⁻¹⁹
10
10²
10³
Electron Energy (eV)

Fig. 17

I-6 Electron + H_2^+ collisions

In electron + H_2^+ collisions, the cross sections for the following processes have been measured:

$e + H_2^+$	$\rightarrow$ $H^+ + H + e$	:	dissociative excitation	(1)
	$\rightarrow$ $H^+ + H^+ + 2e$	:	dissociative ionization	(2)
	$\rightarrow$ $H^+ + H^-$	:	dissociative recombination	(3)
	$\rightarrow$ $H + H^*$	:	dissociative recombination	(4)
	$\rightarrow$ total proton production.			(5)

In this type of experiments, the crossed-beams or merged-beams technique is used. The measured cross sections for these processes are summarized in Fig. 18. It is important to note that H_2^+ beams used in the experiments include various vibrational states which may follow approximately the Frank-Condon principle and, therefore, the observed cross sections depend on the actual distribution of these states. If all H_2^+ ions are in the vibrationally ground state, the cross sections should decrease significantly, for example by one order of magnitude. The measured cross sections for proton production are the sum of those for processes (1), (2) and (3)[1-3]. However, those for processes(2)[4] and (3)[5]are more than one order of magnitude smaller than those for process (1)[6].

The dissociative recombination process(4) resulting in two neutral atoms, either in the excited state or ground state, has been investigated extensively by means of the merging-beams technique. Auerbach et al.[7] have shown rich structures in the cross section curve plotted as a function of the collision energy under high energy resolution experiment. In Fig. 18, these structures are not shown, except for a few pronounced structures observed in H_2^+ ions in relatively low vibrational states (v=0,1,2). Instead, the smoothed lines are drawn, both having the $E^{-0.87}$-dependence over the energy range of 0.01 - 4 eV. These data are roughly in agreement with those of Peart and Dolder[8]. Also those measured using the ion-trapping technique[9] are in agreement with other data over 0.1 -1.0 eV. Recently an analysis of this process based on the multichannel quantum defect theory has been reported by Takagi and Nakamura[10] who reproduced the observed data[7] well. The dissociative recombination resulting in deuterium atoms in higher excited states

$$e + D_2^+ \rightarrow D + D^* \ (n\ell=2p)^{11)} \qquad (6)$$

$$\rightarrow D + D^* \ (n=4)^{12)} \qquad (7)$$

was investigated by observing the emitted photons. These cross sections are one order of magnitude smaller than total dissociative recombination cross sections measured by Peart and Dolder[13]:

$$e + D_2^+ \rightarrow D + D^*. \qquad (8)$$

It should be noted that the dominant final state resulting from the dissociative recombination process is expected to be n=3 from the Landau-Zener model[11].

References

1. G.H. Dunn and B. van Zyl, Phys. Rev. 154(1967) 40
2. B. Peart and K.T. Dolder, J. Phys. B 4 (1971) 1496
3. B. Peart and K.T. Dolder, J. Phys. B 5 (1972) 1554
4. B. Peart and K.T. Dolder, J. Phys. B 6 (1973) 2409
5. B. Peart and K.T. Dolder, J. Phys. B 8 (1975) 1570
6. B. Peart and K.T. Dolder, J. Phys. B 5 (1972) 860
7. D. Auerbach, R. Casak, R. Caudano, T.D. Gaily, C.J. Keyser, J.Wm. McGowan, J.B.A. Mitchell and S.F.G. Wilk, J. Phys. B 10 (1977) 3797
8. B. Peart and K.T. Dolder, J. Phys. B 7 (1974) 236

9. D. Mathur, S.U. Khan and J.B. Hasted, J. Phys. B 11 (1978) 3615

10. H. Takagi and H. Nakamura, J. Chem. Phys. 84 (1986) 2431

11. M. Voyler and G.H. Dunn, Phys. Rev. A 11 (1975) 1983

12. R.A. Phaneuf, D.H. Crandall and G.H. Dunn, Phys. Rev. A 11 (1975) 528.

13. B. Peart and K.T. Dolder, J. Phys. B 6 (1973) L359.

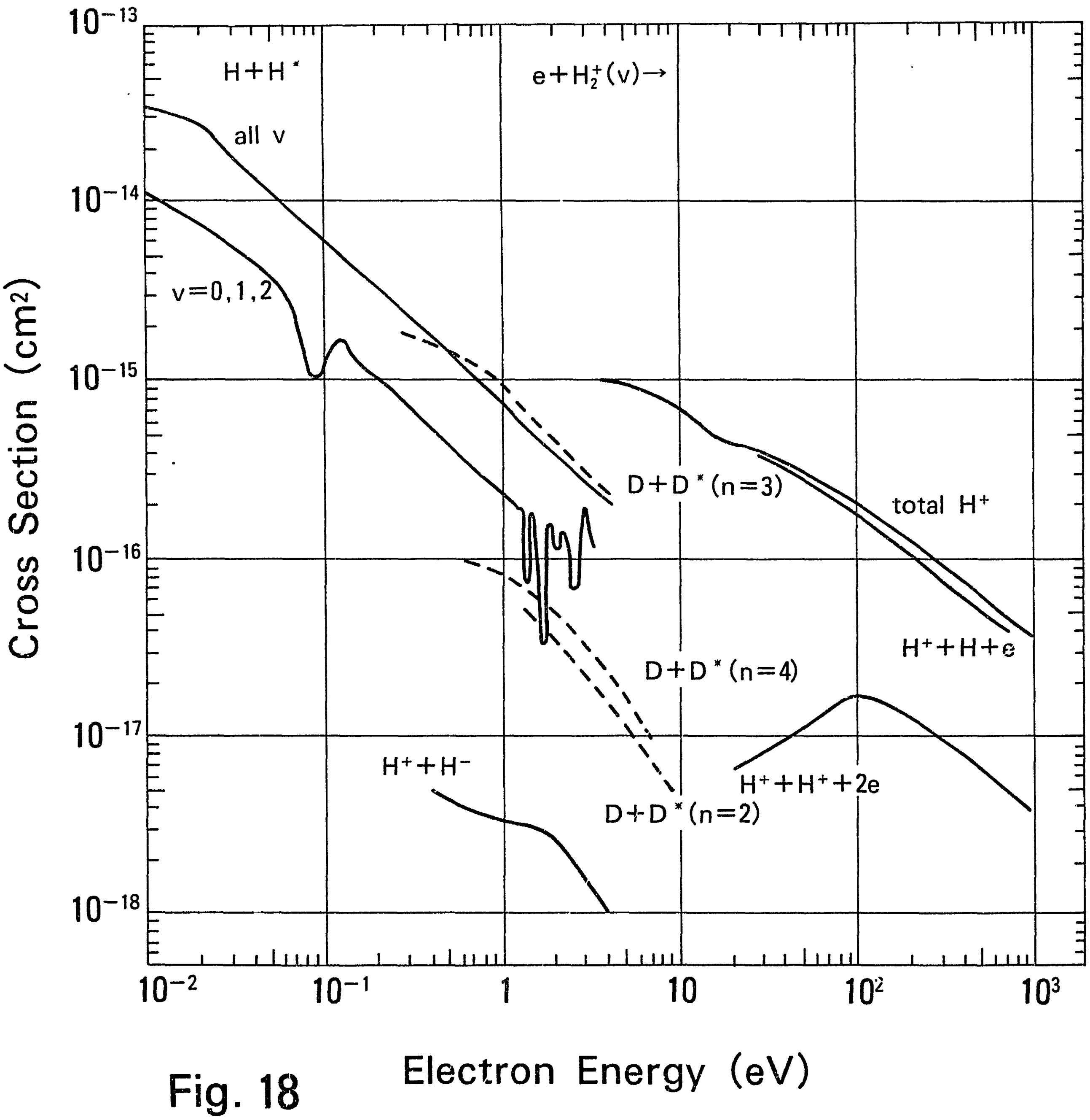
H+H*
e+H₂⁺(v)→
all v
v=0,1,2
D+D*(n=3)
total H⁺
H⁺+H+e
D+D*(n=4)
H⁺+H⁻
H⁺+H⁺+2e
D+D*(n=2)
Cross Section (cm²)
Electron Energy (eV)

Fig. 18

I-7 Electron + H_3^+ collisions

The cross sections for the following processes have been measured:

$$e + H_3^+ \rightarrow H + H + H \quad : \text{dissociative recombination} \quad (1)$$

$$\rightarrow H_2 + H \quad : \text{dissociative recombination} \quad (2)$$

$$\rightarrow H_2^+ + H^- \quad : \text{dissociative recombination} \quad (3)$$

$$\rightarrow H^+ + 2H^* + e \quad : \text{dissociative excitation.} \quad (4)$$

In Fig. 19 are shown these cross sections. The sum of the cross sections for processes (1) and (2) was measured by the crossed-beam, merged-beam, ion trapping or after-glow technique[1-6]. Comparing these cross sections, it should be borne in mind that the cross sections are strongly dependent on the internal energy of H_3^+ ions. Particularly the distribution of the vibrational states of H_3^+ ions influences significantly the observed cross sections. This is clearly shown in Fig. 19 where the observed cross sections are in significant disagreement among different authors who used H_3^+ ions produced in different type of ion sources. For example, the cross sections obtained using the after-glow/Langmuir probe method were found to be fairly small, compared with those shown in Fig. 19. This probably indicates that H_3^+ ions in their beam are almost relaxed to the vibrational ground state through collisions in swarms.

Similar results have been reported by Mitchell et al.[7] who observed significant isotope effect of the cross sections (those for H_3^+ ions are about three times those for D_3^+ ions) at low energies and explained this effect can be due to the lower vibrational frequency of D_3^+ ions. But this difference almost disappears at high energies (> 0.5 eV). It should also be noted that there are rich structures in the cross sections at higher energies when high energy resolution measurements were made[2]. Only significant oscillations at $E \sim 3$ eV are indicated in Fig. 19.

Recently, Mitchell et al.[8] differentiated two channels in dissociative recombination processes (1) and (2) and found that process (1) is dominant over process (2) by a factor of two to three over the energy range of 0.01 - 0.5 eV. The cross sections for process (3) resulting in production of negative hydrogen ions are small[4], shown in Fig. 19 multiplied by 10^3. The cross sections for proton production, mainly due to process(4), show a clear threshold around 15 eV [10,11]. Some theoretical aspects on dissociative recombination in e + H_3^+ collisions are given by Michels and Hobbs.[12]

References

1. B. Peart and K.J. Dolder, J. Phys. B 7 (1974) 1948
2. D. Auerbach, R. Casak, R. Caudano, T.D. Gaily, C.J. Keyser, J. Wm. McGowan, J.B.A. Mitchell and S.F.J. Wilk, J. Phys. B 10 (1977) 3797
3. D. Mathur, S.U. Khan and J.B. Hasted, J. Phys. B 11 (1978) 3615
4. J. A. Macdonald, M.A. Biondi and R. Johnsen, Planet. Space Sci. 32(1984)651
5. M.T. Leu, M.A. Biondi and R. Johnsen, Phys. Rev. A 8(1973) 413
6. N.G. Adams, D. Smith and E. Alge, J. Chem. Phys. 81 (1984) 1778
7. J.B.A. Mitchell, C.T. Ng, L.Forand, R.Janssen and J. Wm. McGowan, J. Phys. B 17 (1984) L909.
8. J.B.A. Mitchell, J.L. Forand, C.T. Ng, D.P. Levac, R.E. Mitchell, P.M. Mul, W. Claeys, A. Sen and J. Wm. McGowan, Phys. Rev. Letters 51 (1983) 885
9. B. Peart, R.A. Forrest and K. Dolder, J. Phys. B 12 (1979) 3441
10. B. Peart and K.T. Dolder, J. Phys. B 7 (1974) 1567
11. B. Peart and K.T. Dolder, J. Phys. B 8 (1974) L143
12. H.H. Michels and R.H.Hobbs, AIP Conf. Proc. No.111 (1984) p.118

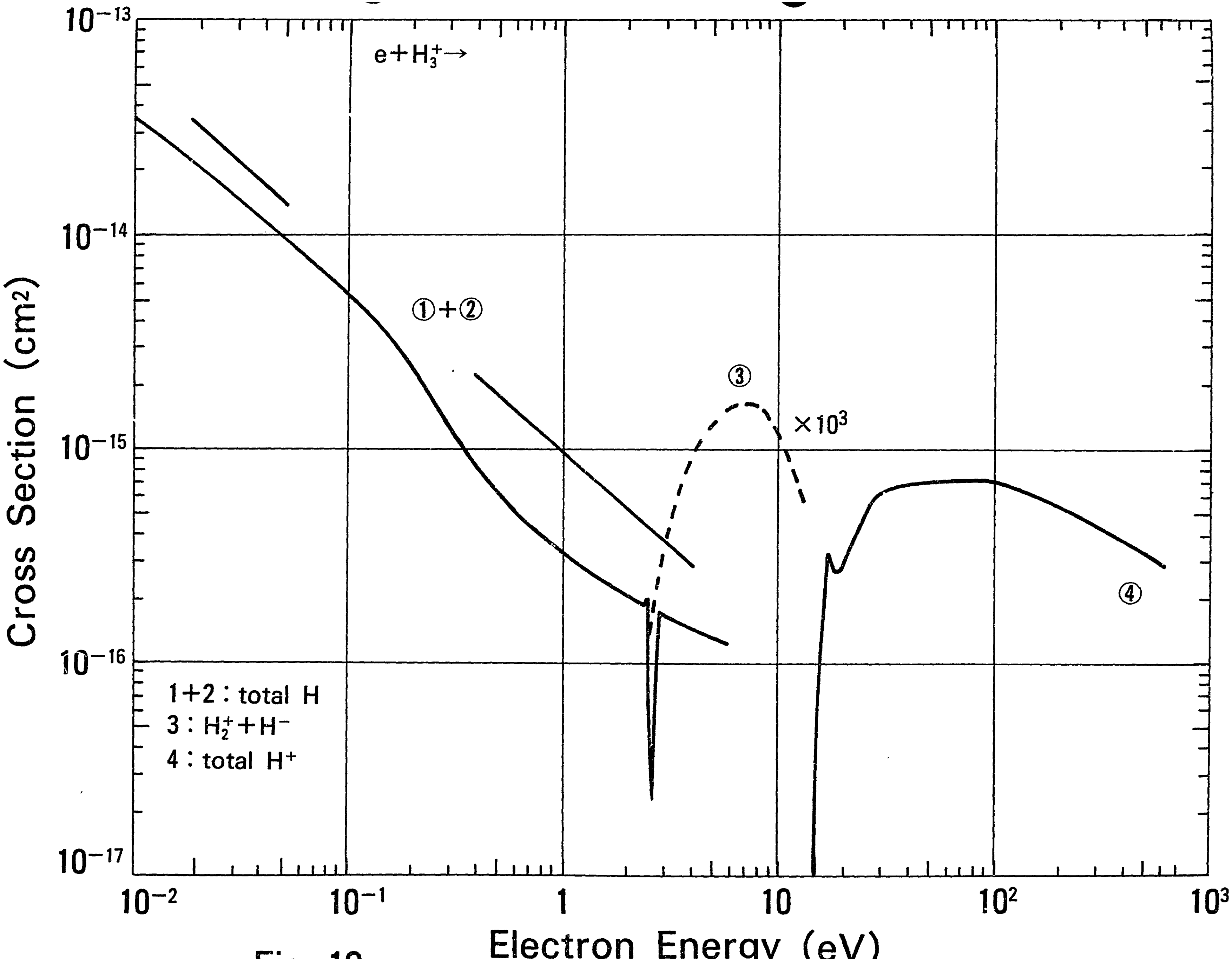

e+H$_3^+$→
①+②
③
×10^3
④
1+2 : total H
3 : H$_2^+$+H$^-$
4 : total H$^+$
Cross Section (cm²)
10^{-13}
10^{-14}
10^{-15}
10^{-16}
10^{-17}
10^{-2}
10^{-1}
1
10
10^2
10^3
Electron Energy (eV)

Fig. 19

I-8. $e + H^-$ collisions

The cross sections for single and double electron detachment (ionizaion) have been measured and shown in Fig.20.

$$e + H^- \rightarrow H + 2e \qquad (1)$$
$$\rightarrow H^+ + 3e. \qquad (2)$$

The observed cross sections for process (1) are in general agreement among different groups,[1-3] except for those by Tisone and Branscomb[4] whose data show behaviour different from others and Born approximation at high energies. The cross sections for process(2) have been determined by Defrance et al.[5] who found that data by Peart et al.[6] seem to be apparently too large by almost one order of magnitude due to the charge transfer of H^- ions with slow positive ions trapped in the space potential well of the electron beam.

References

1. D.F. Dance, M.F.A. Harrison and R.D. Rundel, Proc.Phys. Soc. A299 (1967) 525
2. B. Peart, D.S. Walton and K.T. Dolder, J. Phys. B 3 (1970) 1346
3. D.S Walton, B. Peart and K.T. Dolder, J. Phys. B 4 (1971) 1343 : D.S. Walton, P. Beart and K. Dolder, J. Phys. B 3 (1970) L148
4. G.C. Tisone and L.M. Branscomb, Phys. Rev. 170 (1968) 169 : Phys. Rev. Letters 17 (1966) 236
5. P.Defrance, W. Claeys and F. Brouillard, J. Phys. B 15 (1982) 3509
6. B. Peart, D.S. Walton and K.T. Dolder, J.Phys. B 4 (1971) 88

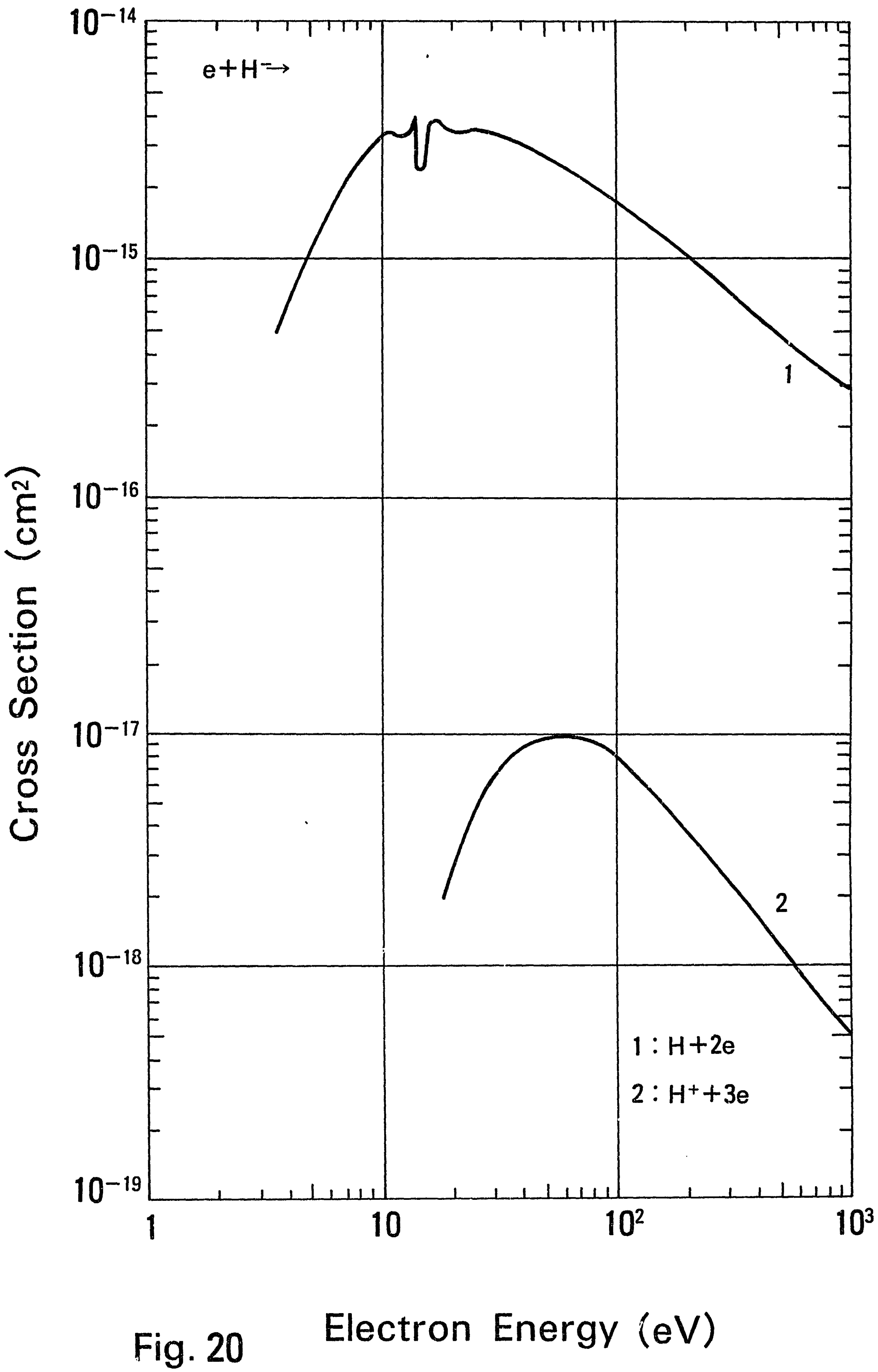
e+H⁻→
1
2
1 : H+2e
2 : H⁺+3e
Cross Section (cm²)
10⁻¹⁴
10⁻¹⁵
10⁻¹⁶
10⁻¹⁷
10⁻¹⁸
10⁻¹⁹
1
10
10²
10³
Electron Energy (eV)

Fig. 20

II Photon collisions

II-1 Photo-dissociation of H_2

$$H_2 + h\nu \rightarrow H(1s) + H^*(n) \qquad (1)$$

No photo-dissociation resulting in both atoms in the ground state is expected to occur. Instead, at least one of them is always in excited states. Dalgarno and Allison[1)] calculated the transition moments from the ground state to the continua of the excited states of H_2 ($B\ ^1\Sigma_u^+\ 2p\sigma$, $C^1\Pi_u\ 2p\pi$) and evaluated the photo-dissociation cross sections over the photon energy range (14.8 - 17.5 eV). Recently Glass-Maujean[2)] calculated these cross sections for n=2 using the accurate ab initio potential energy and dipole moment values. Glass-Maujean et al.[3)] measured the cross sections by observing Lyman-α photons which are shown in Fig.21 together with his theoretical results. The results of Dalgarno and Allison are fairly large. The major contribution ($\sim$ 70%) seems to come from the predissociation of more highly excited states like $D^1\Pi_u 3p\pi$ and $B''^1\Sigma_u 4p\sigma$. However, it is rather curious that the experimental data are in good agreement with theoretical values where the predissociation is totally neglected. In Fig.21 are also shown the experimental data for n=3-6 measured by Lee and Judge[4)]. Fig.22 shows total photo-dissociation cross sections measured by Mentall and Gentieu[5)] which are compared with total absorption cross sections. (taken from IPPJ-D-48 (1975) M-A-Fig.5).

The average kinetic energy of H(1s) + H(1s) system resulting from the $B^1\Sigma_u^+$ and $C^1\Pi_u$ states with photon emission was calculated by Stephens and Dalgarno.[6)] And the oscillator strengths and transition probabilities from the v vibrational level of $X^1\Sigma_g^+$ of H_2 to the v' vibrational level of these states were given by Allison and Dalgarno.[7)]

References

1. A. Dalgarno and A.C. Allison, J. Geophys. Res. 74 (1969) 4178
2. M. Glass-Maujean, Phys. Rev. A 33 (1986) 342
3. M. Glass-Maujean, P.M. Guyon and J. Breton, Phys. Rev. A 33 (1986) 346
4. L.C. Lee and D.L. Judge, Phys. Rev. A 14 (1976) 1094
5. J.E. Mentall and E.P. Gentieu, J. Chem. Phys. 52 (1970) 5641
6. T.L. Stephens and A. Dalgarno, Astrophys. J. 186 (1973) 165
7. A.C. Allison and A. Dalgarno, At.Data 1 (1970) 289

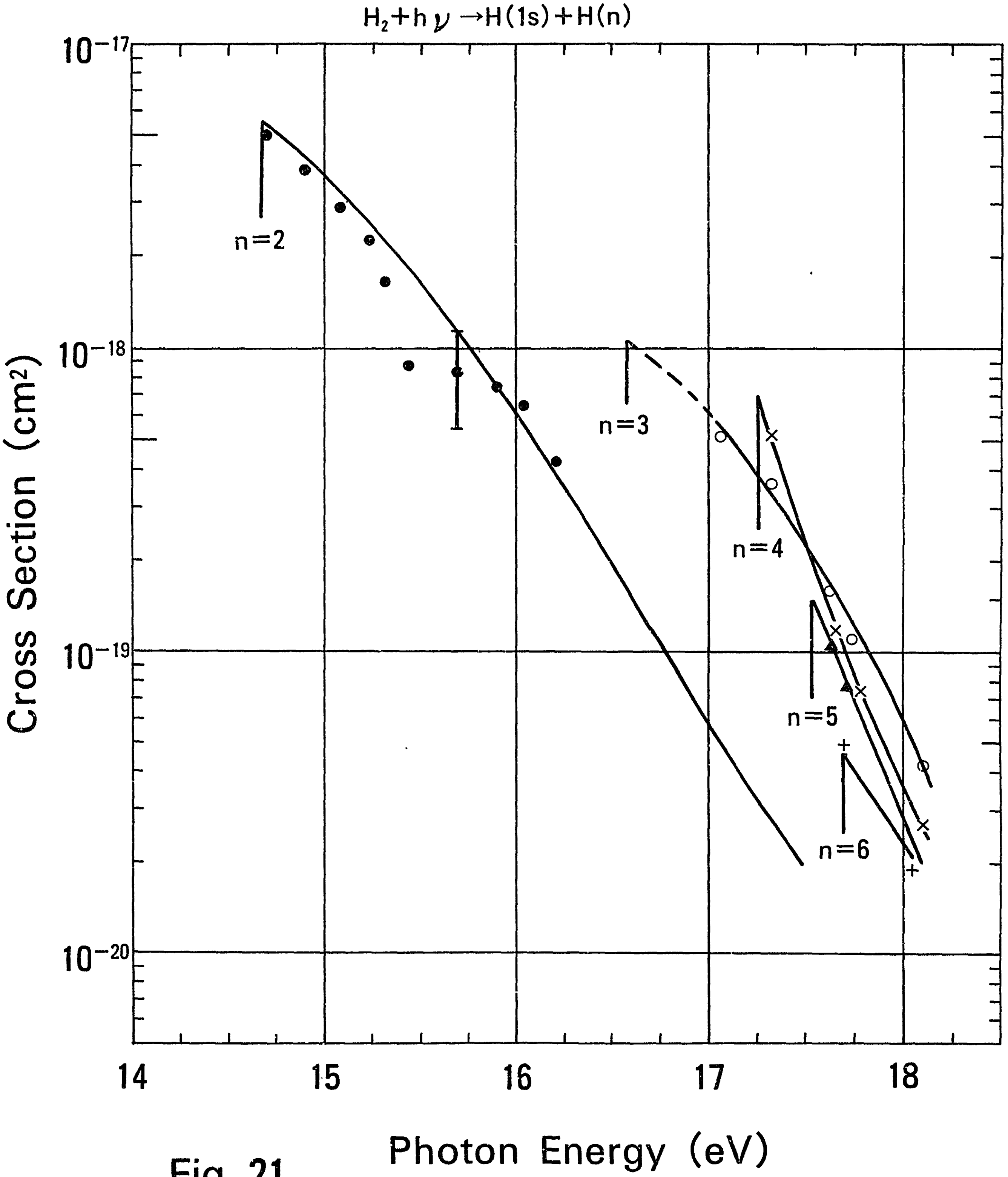
$H_2 + h\nu \rightarrow H(1s) + H(n)$
10^{-17}
10^{-18}
10^{-19}
10^{-20}
Cross Section (cm^2)
n=2
n=3
n=4
n=5
n=6
14
15
16
17
18
Photon Energy (eV)

Fig. 21

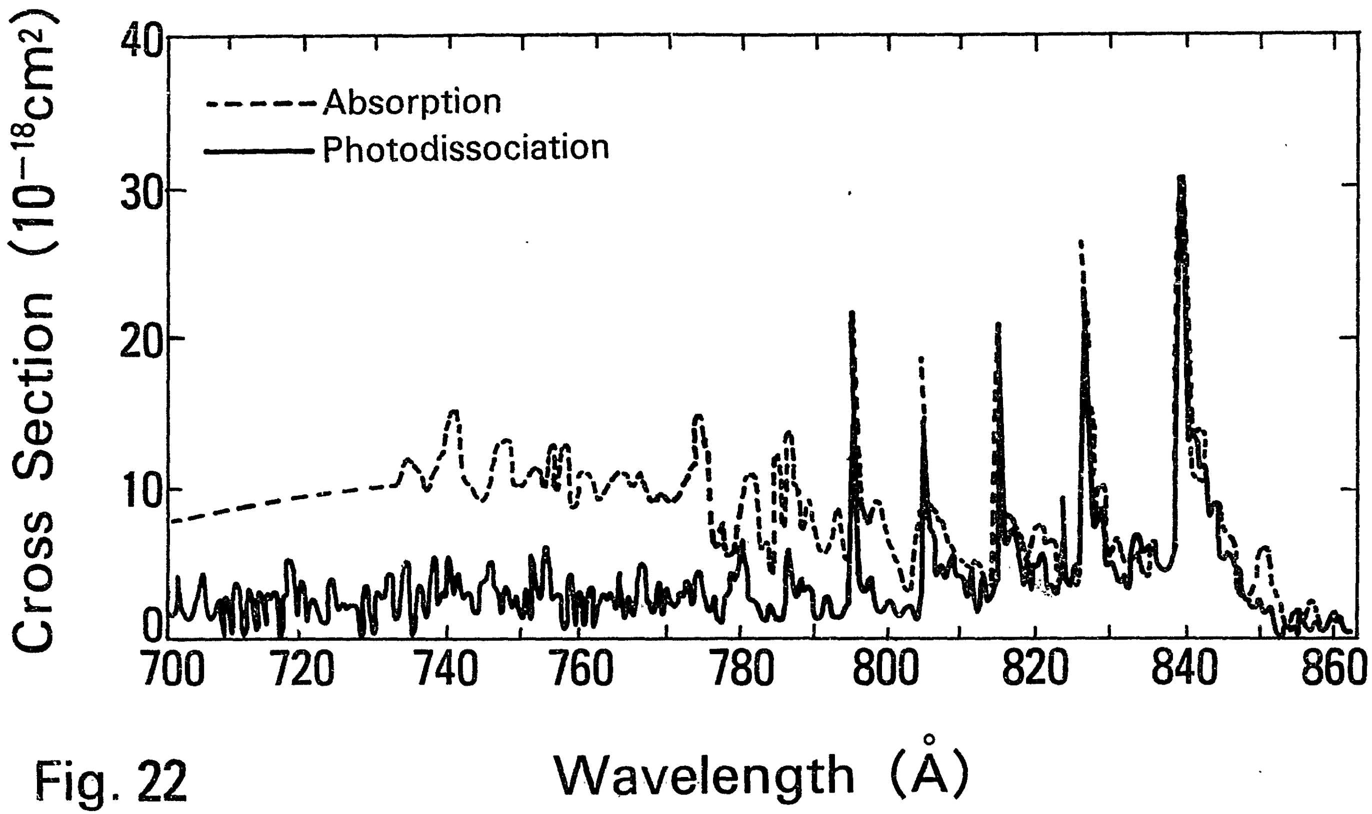

Fig. 22

Taken from M-A-Fig.5 Photodissociation and Total Absorption Cross Sections for H_2.
〔from J.E. Mentall & E.P. Gentieu, J. Chem. Phys. 52, 5641 (1970)〕
IPPJ-DT-48 (1975)

II-2 Photo-dissociative ionization of H_2

$$H_2 + h\nu \rightarrow H + H^+ + e \qquad (1)$$

Ratios of product ions H^+ to H_2^+ by photon impact on H_2, measured by Browning et al.[1] and Masuoka[2], are shown in Fig.23 together with those obtained by a fast electron impact method.[3] They begin to increase at the photon energy of around 30 eV which is due to the contribution of two-electron excited dissociative states of H_2. These ratios are used to obtain absolute cross sections for dissociative ionization by combining with total photo-ionization cross sections. Fig.24 show those results based on data by Masuoka (ratio of H^+ / H_2^+) and by Lee et al.(cross section)[4]. The kinetic energy distributions of product H^+ ions were also investigated experimentally[5-6] and theoretically.[7]

References

1. R. Browning and J. Fryar, J. Phys. B 6 (1973) 364
2. T. Masuoka, J. Chem. Phys. 81 (1984) 2652
3. C. Backx, G. R. Wight and M.J. van der Wiel, J. Phys. B 9 (1976) 315
4. L.C. Lee, R.W. Carson and D.L. Judge, J. Quant. Spectros. Radit. Transfer 16 (1976) 873
5. S. Strathdee and R. Browning, J. Phys. B 12 (1979) 1789
6. J.L. Gardner and J.A.R. Samson, Phys. Rev. A 12 (1975) 1405
7. S. Kanter and M. Shapiro, J. Phys. B 16 (1983) L655

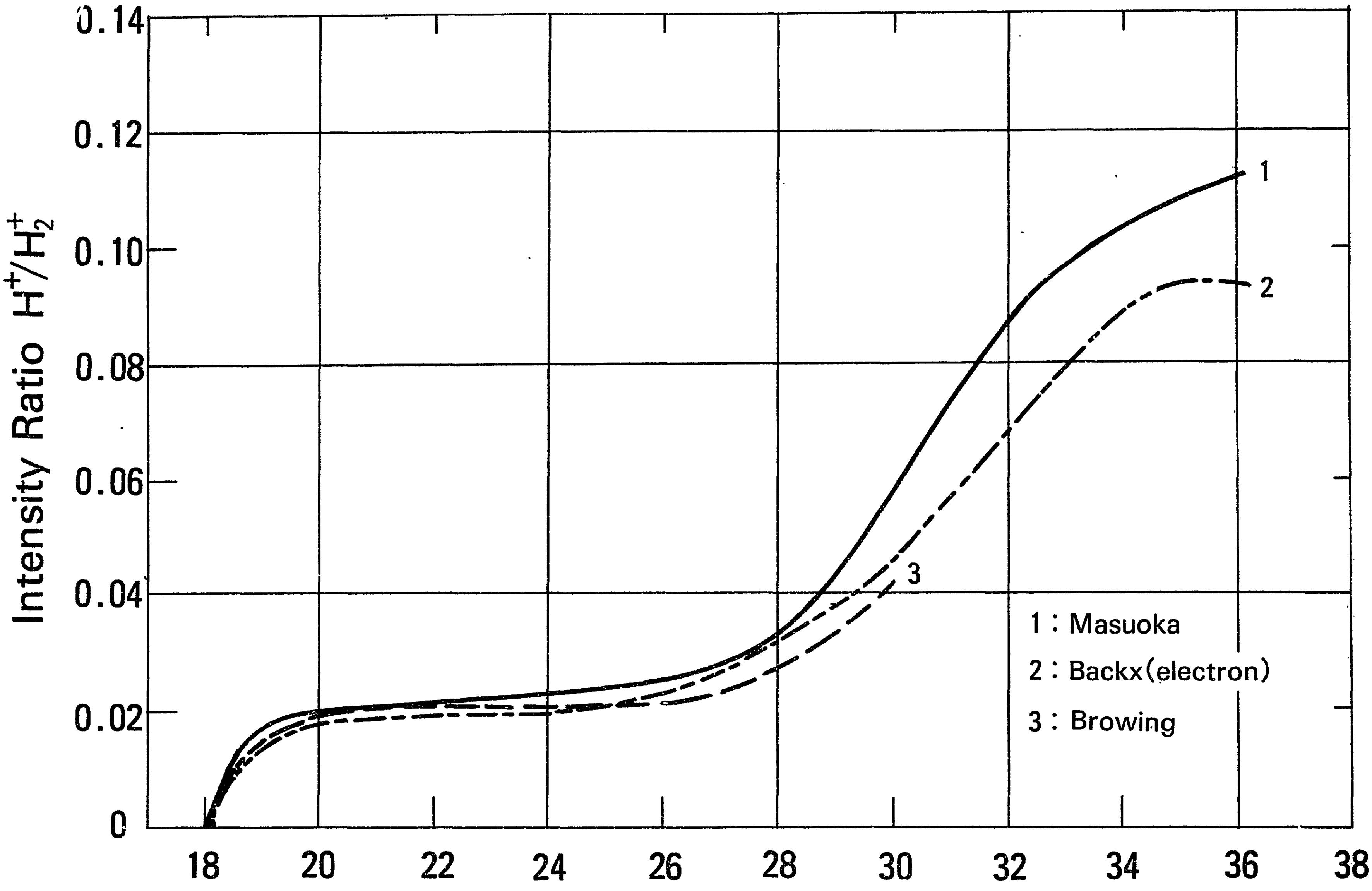

0.14
0.12
0.10
0.08
0.06
0.04
0.02
0
Intensity Ratio H^+/H_2^+
18
20
22
24
26
28
30
32
34
36
38
Photon Energy (eV)
1
2
3
1 : Masuoka
2 : Backx(electron)
3 : Browing

Fig. 23

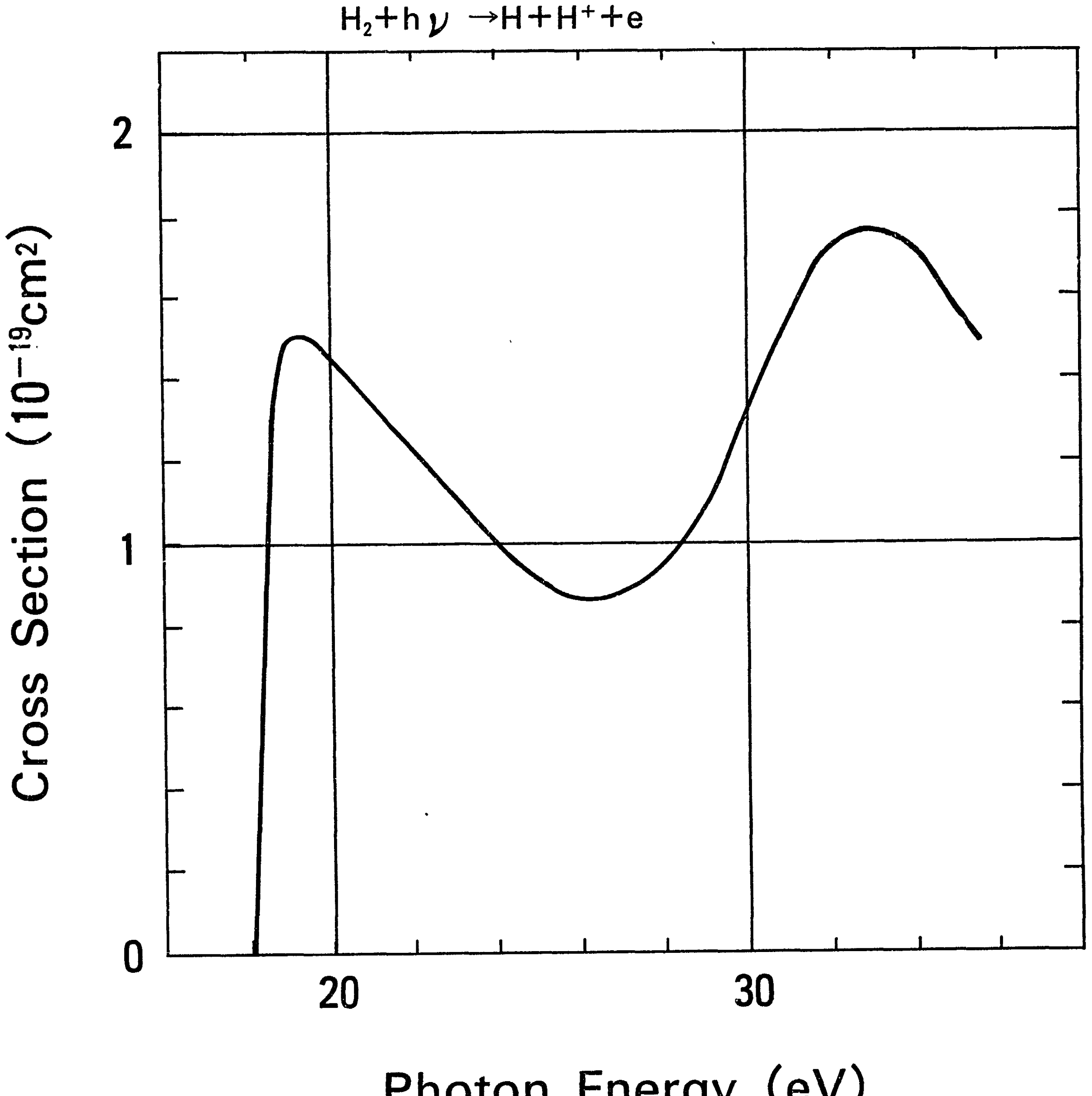
$H_2 + h\nu \rightarrow H + H^+ + e$
Cross Section ($10^{-19}cm^2$)
2
1
0
20
30
Photon Energy (eV)

Fig. 24

II-3 Photo-ionization of H_2

$$H_2\ (X^1\Sigma_g) + h\nu \rightarrow H_2^+ + e \qquad (1)$$

Total photo-ionization cross sections shown in Fig.25 seem to be well established both experimentally[1-9] and theoretically,[10-12] though some detailed structures including resonances are still obscure. Some numerical data are given in Table 3. Recently Kosarev and Podolyak[13] compiled experimental data above 20 eV and found simple functional forms for fitting them (see Fig.26). One of them has the following form:

$$\sigma = 5.35 \times 10^{-20}\ (100/E)^{3.228}\ \mathrm{cm}^2 \qquad (2)$$

where E is the photon energy in eV. More simply, the cross sections are given as

$$\sigma = 3.02\ \sigma_H \qquad (3)$$

where σ_H is the cross section for atomic hydrogen. More detailed calculations of cross sections for the vibrationally resolved photo-ionization process:

$$H_2(X^1\Sigma_g^+, v_i) + h\nu \rightarrow H_2^+ (X^2\Sigma_g^+, v_f) + e \qquad (4)$$

have been made by Ford et al.[14] (12.4 - 13.6 eV; v_i = 4 - 14 : v_f = 0 - 16) and Flannery et al.[15] (12.4 - 27.6 eV: v_i = 0 - 14 : v_f = 0 - 18). In Fig.27 are shown the calculated cross sections for different initial vibrational states v_i, summed over the final vibrational states v_f. Some vibrationally resolved cross sections[10,11] at 21.2 eV photon energy are compared with experimental data[16] in Table 4.

References

1. R.H. Messner, Z. Phys. 85 (1933) 727
2. A.H. Compton and S.K. Allison, in X-rays in Theory and Experiment (McMillan, N.Y., 1935)
3. P. Lee and G.L. Weissler, Astrophys. J. 115 (1852) 570
4. G.R. Cook and P.H. Metzer, J. Opt. Soc. Am. 54 (1964) 968
5. J.A.R. Samson and R.B. Cairns, J. Opt. Soc. Am. 55 (1965) 1035
6. B.L. Henke, D.L. Elgin, R.E. Lent and R.B. Ledingham, Norelco Rept. 14 (1967) 112
7. D.R. Denne, J. Phys. B 3 (1970) 1392
8. R.E. Rebbert and P.J. Ausloos, J. Res. NBS A 75 (1971) 481
9. S.W. Bennett, J.B. Tellinghuisen and L.F. Philips, J. Phys. Chem. 75 (1971) 719
10. S.V. O'Neil and W.P. Reinhardt, J. Chem. Phys. 69 (1978) 2126
11. Y. Itikawa, H. Takagi, H. Nakamura and H. Sato, Phys. Rev. A 27 (1983) 1319
12. G. Raseev and H. LeRouzo, Phys. Rev. A 27 (1983) 208
13. E.L. Kosarev and E.R. Dodolyak, Opt. Spektrosk. 56 (1984) 643
14. A.L. Ford, K.K. Docken and A. Dalgarno, Astrophys. J. 200 (1975) 788
15. M.R. Flannery, H. Tai and D.L. Albritton, At. Data and Nucl. Data Tables 20 (1977) 563
16. J.E. Pollard, D.J. Trevor, J.E. Reutt, Y.T. Lee and D.A. Shirley, J. Chem. Phys. 77 (1982) 34

Table 3. Total cross sections (in 10^{-18} cm^2)

H_2 (v = 0) + hν → H_2^+ + e

photon energy		Cross section	
λ(A)	eV	Lee	Samson(Å)
180	68.88	0.25	
190	65.26	0.28	
200	61.99	0.31	
210	59.04	0.33	0.266(209.3)
220	56.36	0.36	
230	53.91	0.40	0.402(234.2)
240	51.66	0.46	0.439(239.6)
250	49.59	0.53	0.494(247.2)
260	47.69	0.62	0.579(260.5)
270	45.92	0.70	0.638(266.3)
280	44.28	0.78	0.790(283.5)
290	42.75	0.85	
300	41.33	0.93	0.949(297.6)
310	40.00	1.0	1.02(303.1)
320	38.75	1.1	1.12(314.9)
330	37.57	1.3	1.22(323.6)
340	36.47	1.4	1.36(335.1)
350	35.42	1.5	1.51(345.1)
360	34.44	1.7	1.75(358.5)
370	33.51	2.0	1.84(362.9)
380	32.63	2.0	2.04(374.4)
390	31.79	2.2	2.26(387.4)
400	31.00	2.3	
410	30.24	2.5	
420	29.54	2.6	
430	28.83	2.8	2.88(428.2)
			3.02(434.3)

Photon energy		Cross Section			
λ(A)	eV	Lee	O'Neil	Itikawa(Å)	Samson
440	28.18	3.0	2.82		3.16
450	27.55	3.2			
460	26.95	3.3	3.20		3.48
470	26.38	3.5			
480	25.83	3.7	3.61		3.94
490	25.30	3.9			
500	24.80	4.1	4.05		4.43
510	24.31	4.4			
520	23.84	4.6	4.53		5.02(522.1)
530	23.39	4.9			
540	22.96	5.2	5.04		5.54(544.7)
550	22.54	5.5			
560	22.14	5.7	5.59		5.88(558.5)
570	21.75	5.9			
580	21.38	6.2	6.17	6.201(584)	
590	21.01	6.4			
600	20.66	6.6	6.80		7.00(596.7)
610	20.33	7.0			
620	20.00	7.3	7.47		7.59
630	19.68	7.5			
640	19.37	7.7	8.17		8.30(641.3)
650	19.07	8.2		8.278	
660	18.79	8.6	8.89		9.08(664.9)
670	18.51	8.8			
680	18.23	8.9	9.58		9.64
690	17.97	9.1			
700	17.71	9.3	10.04	9.809(736)	9.97

Table 4 Vibrationally resolved cross sections (in 10^{-18} cm^2) at 21.2 eV (λ=584 Å) photon energy

H_2 (v) + hν → H_2^+ (v') + e

	v = 0			v = 1	v = 2
v'	Pollard	O'Neil	Itikawa	O'Neil	O'Neil
0	0.477±0.006	0.4533	0.5051	1.1806	1.1870
1	0.907±0.008	0.8639	0.9454	0.8079	0.0155
2	1.048±0.008	1.0036	1.082	0.1968	0.2873
3	0.975±0.007	0.9313	0.9915	0.0001	0.5029
4	0.793±0.006	0.7656	0.7960	0.0912	0.3397
5	0.598±0.005	0.5866	0.6016	0.2441	0.1174
6	0.446±0.004	0.4315	0.4382	0.3484	0.0097
7	0.315±0.004	0.3105	0.3112	0.3853	0.0104
8	0.223±0.003	0.2211	0.2197	0.3724	0.0609
9	0.157±0.003	0.1568		0.3321	0.1156
10	0.1095±0.0007	0.1113		0.2811	0.1534
11	0.0773±0.0005	0.07927		0.2301	0.1698
12	0.0543±0.0005	0.05659		0.1834	0.1682
13	0.0377±0.0011	0.04038		0.1428	0.1538
14	0.0264±0.0003	0.02856		0.1082	0.1315
15	0.0179±0.0002	0.01969		0.0787	0.1044
16	0.0111±0.0002	0.01273		0.0528	0.0746
17	0.0068±0.0002	0.006933		0.0295	0.0433
18		0.002162		0.0093	0.0139
19		0.000098		0.0004	0.0006
Sum	6.280	6.083	6.201*	5.0741	3.660

* The values of O'Neil (1978) for v ≧ 9 are added.

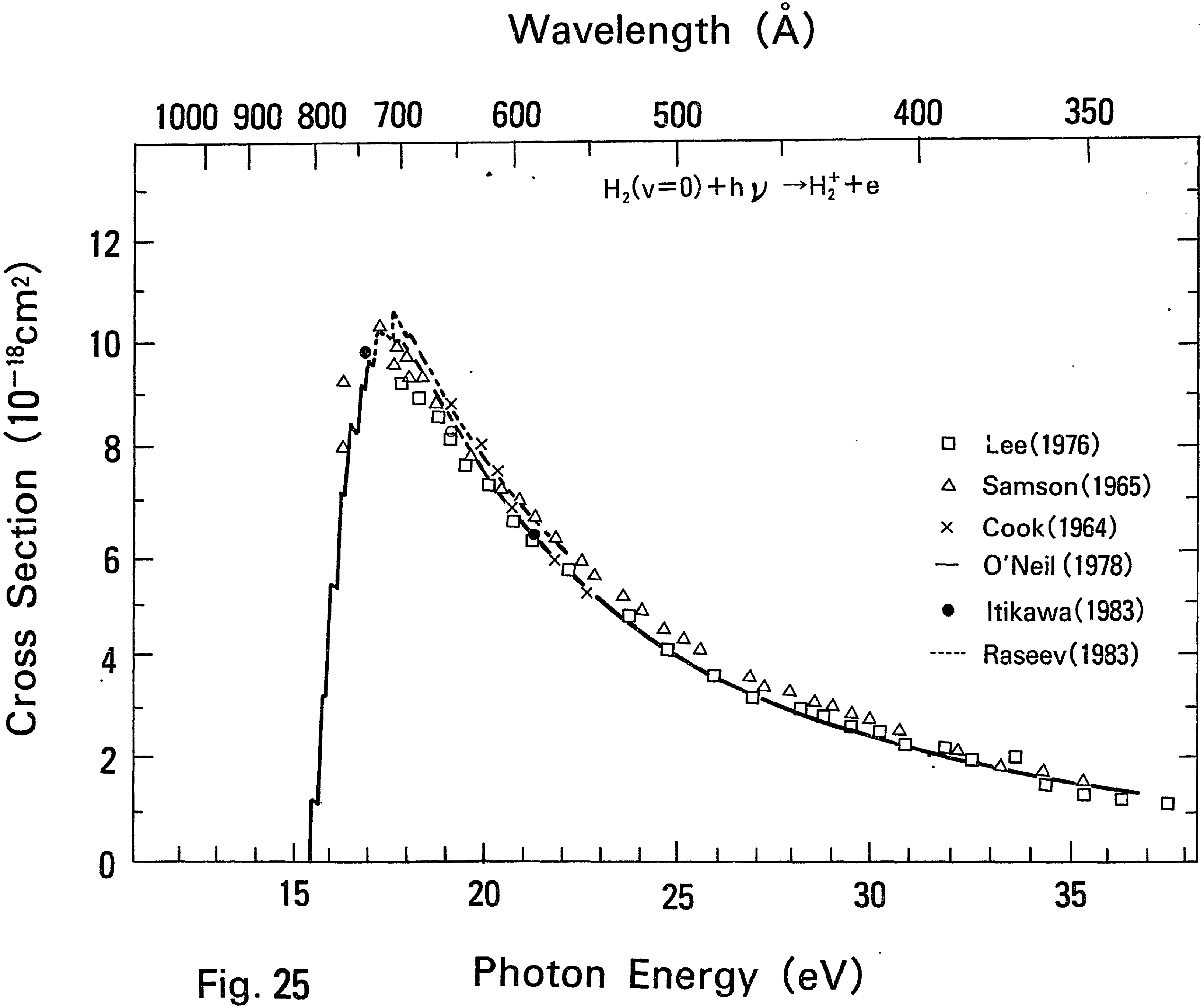

Wavelength (Å)
1000 900 800 700 600 500 400 350
$H_2(v=0) + h\nu \rightarrow H_2^+ + e$
Cross Section ($10^{-18}cm^2$)
0 2 4 6 8 10 12
Lee (1976)
Samson (1965)
Cook (1964)
O'Neil (1978)
Itikawa (1983)
Raseev (1983)
15 20 25 30 35
Photon Energy (eV)

Fig. 25

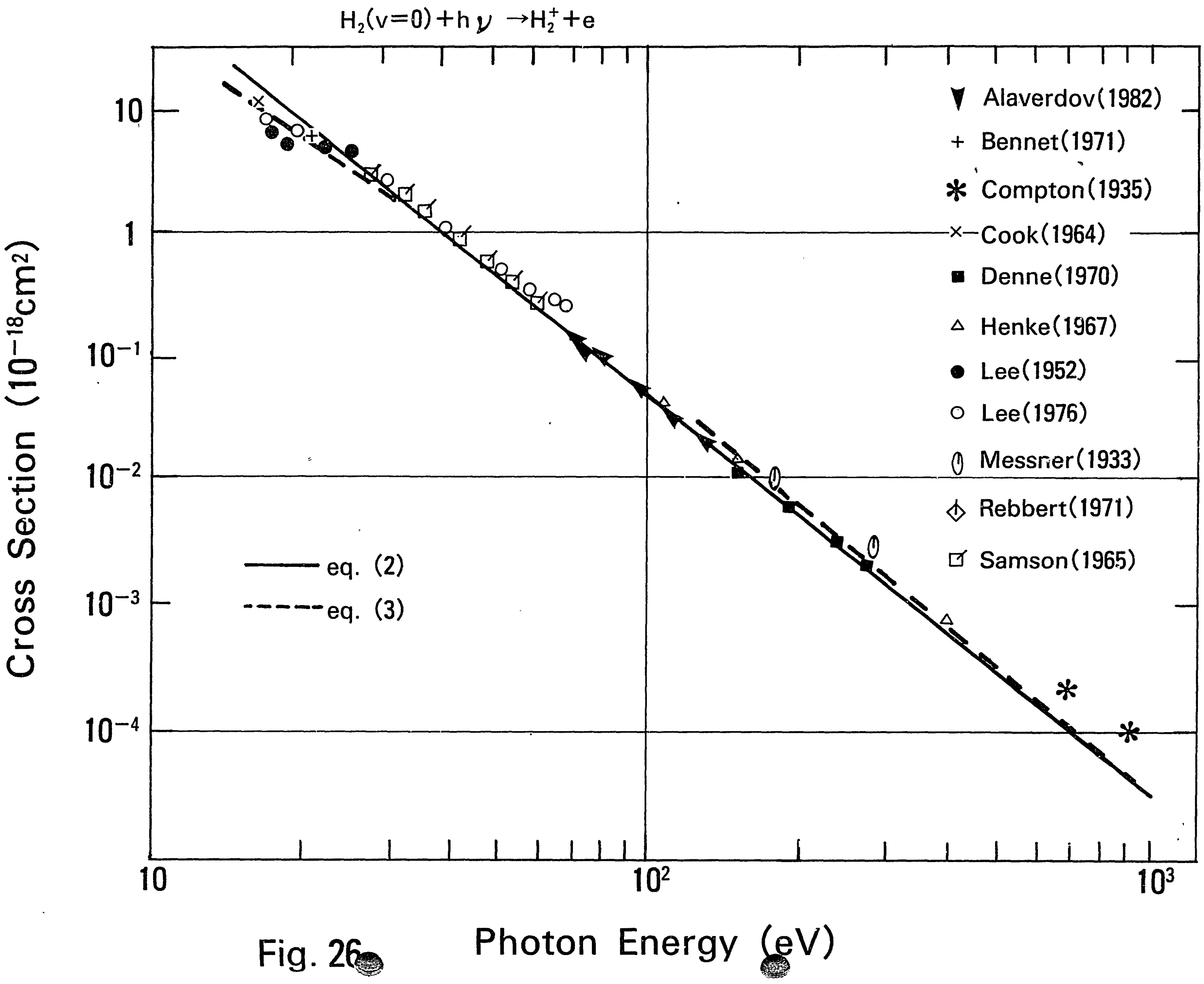

$H_2(v=0)+h\nu \rightarrow H_2^+ + e$
Cross Section ($10^{-18}cm^2$)
10
1
10^{-1}
10^{-2}
10^{-3}
10^{-4}
10
10^2
10^3
Photon Energy (eV)
Alaverdov(1982)
Bennet(1971)
Compton(1935)
Cook(1964)
Denne(1970)
Henke(1967)
Lee(1952)
Lee(1976)
Messner(1933)
Rebbert(1971)
Samson(1965)
eq. (2)
eq. (3)

Fig. 26

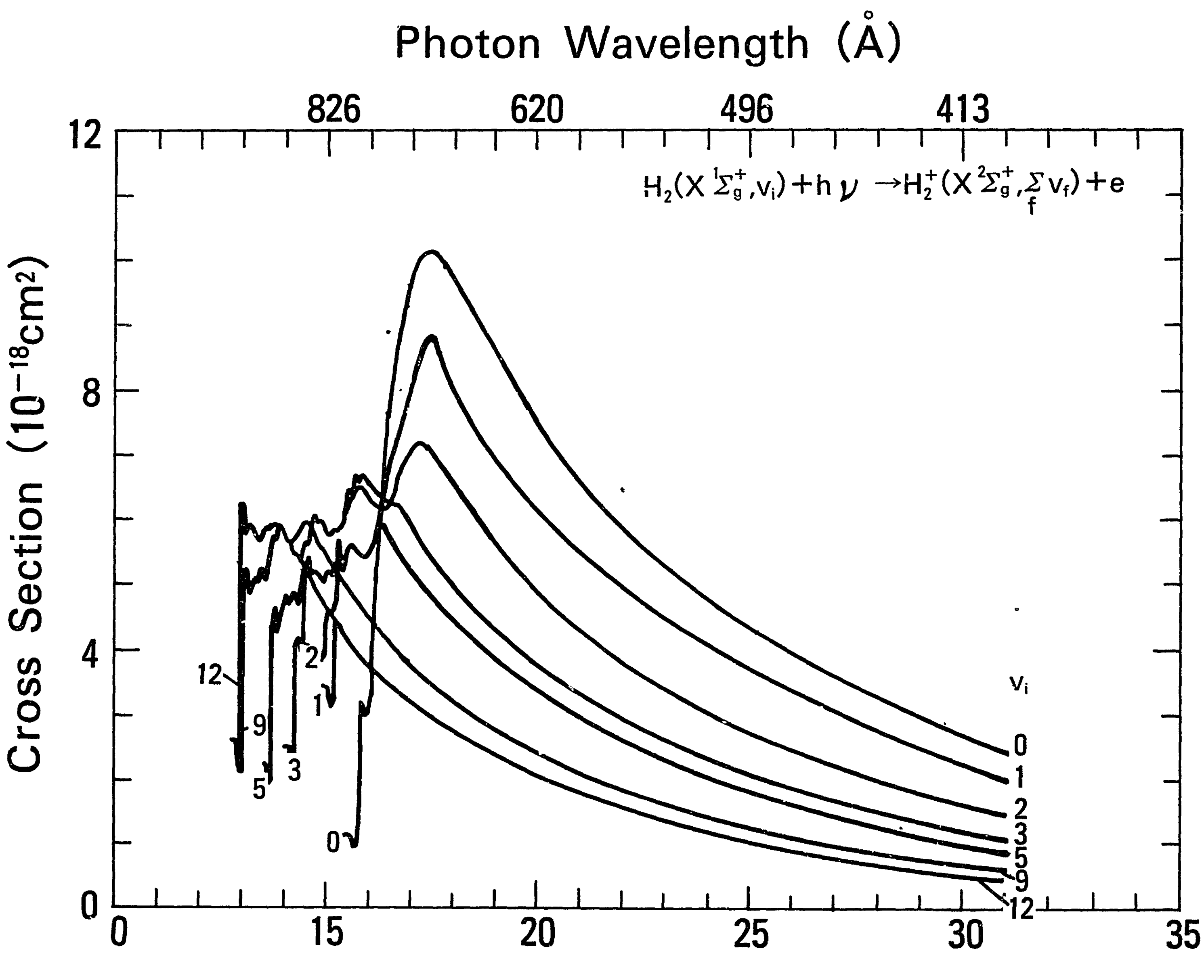
Photon Wavelength (Å)
826
620
496
413
$H_2(X\,^1\Sigma_g^+, v_i) + h\nu \rightarrow H_2^+(X\,^2\Sigma_g^+, \sum_f v_f) + e$
v_i
0
1
2
3
5
9
12
Cross Section ($10^{-18}cm^2$)
12
8
4
0
0
15
20
25
30
35
Photon Energy (eV)

Fig. 27

II-4 Photo-dissociative formation of ion pair in H_2

$$H_2 + h\nu \rightarrow H^+ + H^-$$

McCullogh and Walker[1] experimentally studied the ion pair formation for para-H_2 and for normal mixture of H_2. This reaction occurs in very narrow photon energy region (17.3-17.6 eV), even though the energy region becomes slightly wider at higher temperature. Chupka et al.[2] measured the cross sections with higher resolution and determined the ratio of H^-/H_2^+ to be 0.004 at 714.20 Å (the most intense peak position for H^+ production) the cross section being estimated to be 4 $\times 10^{-20}$ cm^2 at the peak, as shown in Figure 28.

References

1. K.E. McCullogh and J.A. Walker, Chem. Phys. Letters 25 (1974) 439
2. W.A. Chupka, P.M. Dehmer and W.T. Jivery, J. Chem. Phys. 63 (1975) 3929

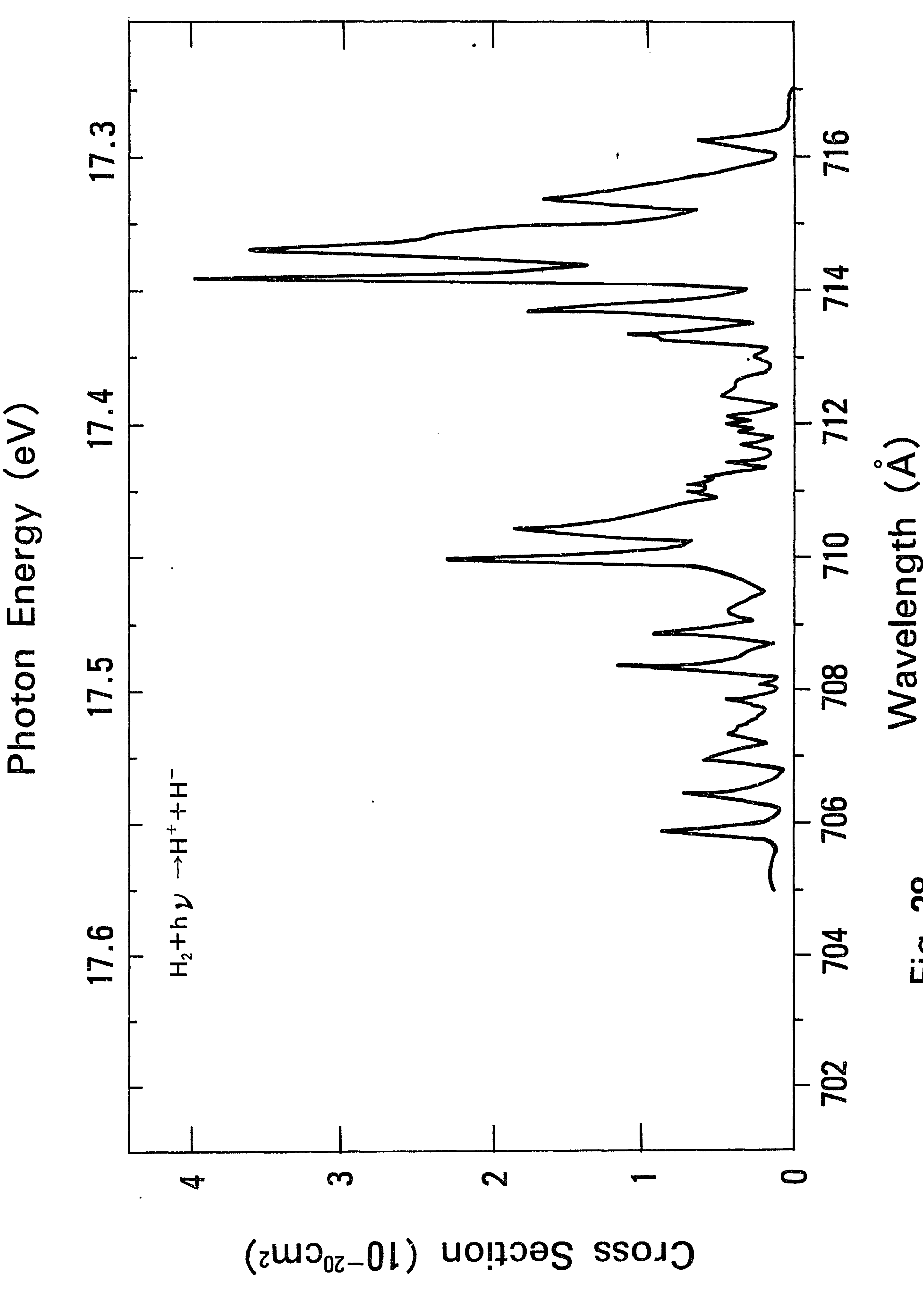

Photon Energy (eV)
17.6
17.5
17.4
17.3
$H_2+h\nu \rightarrow H^+ + H^-$
Cross Section ($10^{-20}cm^2$)
0
1
2
3
4
702
704
706
708
710
712
714
716
Wavelength (Å)

Fig. 28

II-5 Photo-dissociation of H_2^+

$$H_2^+ (v) + h\nu \rightarrow H + H^+ \qquad (1)$$

The photo-dissociation of H_2^+ ions was first treated by Bates[1] who used the semiclassical method, i.e., the nuclear motion was assumed to obey the classical mechanics, meanwhile electron was treated quantum mechanically. Busch and Dunn[2] measured the absolute cross sections for photo-dissociation over the photon energy range from 2472 to 13013 Å. Their H_2^+ ions were produced through bombardment with electrons with the average energy of 128 eV but were not in thermal equilibrium (the average temperature of H_2 gas being 100 C). The distribution of the vibrational states of ions was determined experimentally from the photon energy dependence of photo-dissociation cross section of H_2 ("observed" column in Table 5) and also culculated using the empirical electronic transition momemts of $H_2 + e \rightarrow H_2^+(v) + 2e$ ("calculated" column in Table 5). Assuming this distribution of the vibrational states, the cross sections for photo-dissociation of H_2^+ ions were calculated, as shown in Fig.29 together with experimental data. The agreement between calculation and experiment seems to be fairly good. Similar method was used by Argyros[3] to calculate the photo-dissociation cross sections for H_2^+ ions in thermal equilibrium. In his calculation, the cross sections were averaged over rotational states as well as over vibrational states, assuming the Boltzmann distribution. In Fig.30 are shown the calculated cross sections as a function of photon energy from threshold to 25000 Å with the temperature-dependent parameter. It is noted that in the photon energy range over 500-1200 Å the dissociation via the repulsive $2p\pi_u$ state is dominant. In this wavelength range, Saha et al.[4] calculated the excitation cross sections to $2p\pi u$ state from $1s\sigma_g$ (v=0-18, J=1) state resulting in a maximum value of 6.89×10^{-18} cm^2 at around 800 Å, after averaging over the vibrational states.

References

1. D.R. Bates, Mon. Not. Roy. Astr. Soc. 112 (1952) 40

2. F. von Busch and G.H. Dunn, Phys. Rev. 5 (1972) 1726

3. J.D. Argyros, J.Phys. B 7 (1974) 2025

4. S. Saha, K.K. Datta, D. Basu and A.K. Barua, J. Phys. B 13 (1980) 3755

Table 5 The distribution of the vibrational states in H_2^+ ions used in taking data in Fig.29.

v	observed	calculated
0	0.119	0.11916
1	0.190	0.18994
2	0.188	0.18791
3	0.152	0.15173
4	0.125	0.11097
5	0.075	0.07732
6	0.052	0.05270
7	0.037	0.03564
8	0.024	0.02411
9	0.016	0.01638
10	0.0117	0.01121
11	0.0082	0.00773
12	0.0057	0.00536
13	0.00374	0.00374
14	0.00258	0.00258
15	0.00175	0.00175
16	0.00109	0.00109
17	0.00056	0.00056
18	0.00012	0.00012

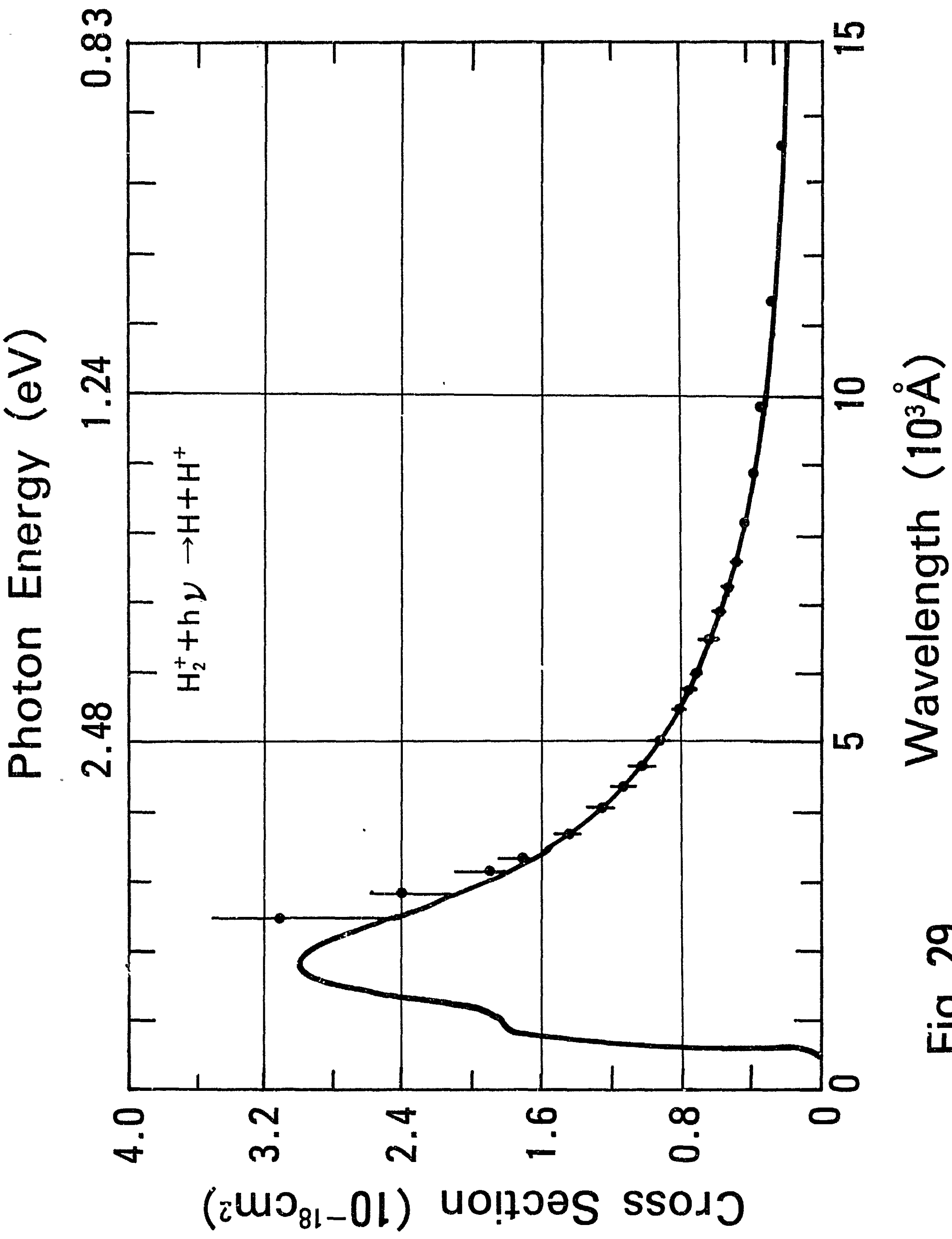
Photon Energy (eV)
0.83
1.24
2.48
$H_2^+ + h\nu \rightarrow H + H^+$
Cross Section ($10^{-18}cm^2$)
4.0
3.2
2.4
1.6
0.8
0
Wavelength (10^3Å)
0
5
10
15

Fig. 29

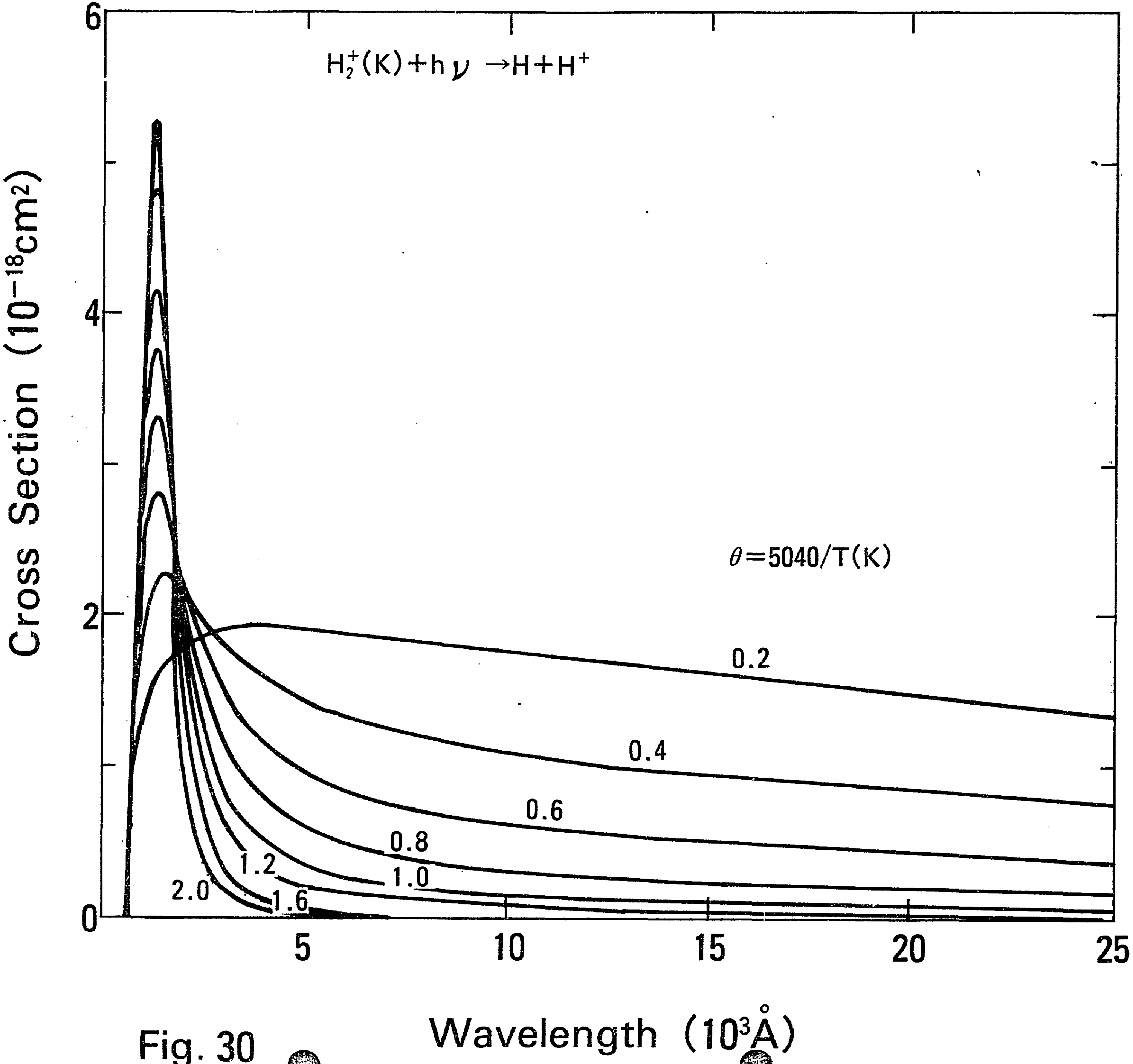
$H_2^+(K)+h\nu \rightarrow H+H^+$
Cross Section ($10^{-18}cm^2$)
Wavelength (10^3Å)
θ=5040/T(K)
0.2
0.4
0.6
0.8
1.0
1.2
1.6
2.0
0
2
4
6
5
10
15
20
25

Fig. 30

This page is intentionally left blank

II-6 Radiative association of H and H^+

$$H + H^+ \rightarrow H_2^+ + h\nu$$

This is the inverse process of photo-dissociation of H_2^+ and was studied by Bates semiclassically[1]. A quantum mechanical calculation was done by Ramaker and Peek[2]. The rate coefficients of the molecular ion formation are shown in Fig.31 for both treatments. The quantum effect turns out to be quite apparent for T < 500 K, where T is the temperature. For T > 500 K, the quantum calculation seems to be less reliable than the semiclassical, but the difference between them is within 5 %. Ramaker and Peek[3] also calculated the rates for this process due to the induced emissions under intense radiation field.

References

1. D.R. Bates, Mon. Not. Roy. Astr.Soc. 111 (1951) 303
2. D.E. Ramaker and J.M. Peek, Phys. Rev. A 13 (1976) 58
3. D.E. Ramaker and J.M. Peek, J. Chem. Phys. 71 (1979) 1844

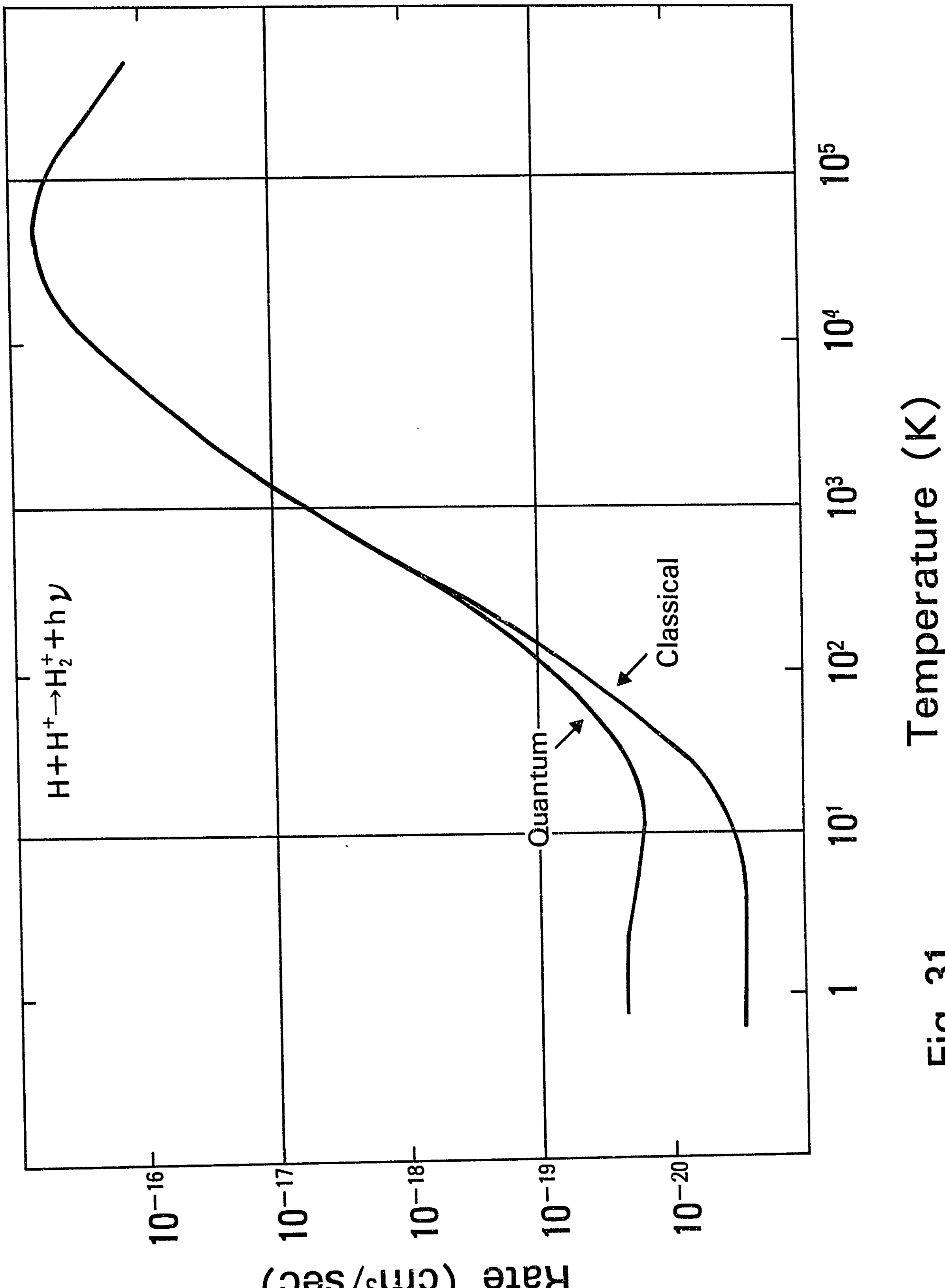

H+H⁺→H_2^++hν
Quantum
Classical
Rate (cm³/sec)
10−16
10−17
10−18
10−19
10−20
Temperature (K)
1
10¹
10²
10³
10⁴
10⁵

Fig. 31

III Ion/atom/molecule collisions

III-1 Vibrational excitation of H_2 by proton impact

$$H^+ + H_2(v=o) \rightarrow H^+ + H_2(v') - \Delta E_{v'} \qquad (1)$$

The vibrational energies $\Delta E_{v'}$ are given as follows:

v'	1	2	3	4
$\Delta E_{v'}$(eV)	0.516	1.003	1.461	1.890

Several investigations on this process were made. The absolute cross sections are reported only by Herrero and Doering[1)] who claimed, by considering the angular distribution of the inelastically scattered particles, that the measured values are interpreted as the integral (or total) cross sections at above E = 100 eV, meanwhile they are only the partial cross sections in the forward direction within the acceptance angle of ± 1.9° at lower energies (see Fig.32).

The classical trajectory calculation based on the ab initio potential surface of H_3^+ ions were made by Gentry and Giese[2)]. Kruger and Schinke[3)], using the same interaction potential, made the quantum calculations. After calculating more accurate potential surface, the cross sections have been evaluated using the infinite-order-sudden method.[4,5)] These results are found to be in good agreement with relative differential cross sections determined by Hermann et al.[6)] Though the theoretical results from different approaches agree fairly well with each other, serious discrepancy, particularly at lower energies, is clearly seen between experimental and theoretical values. This is partly due to the limited acceptance angle in the experiment, resulting in smaller cross sections.

References

1. F.A. Herrero and J.P. Doering, Phys.Rev. A 5 (1972) 702

2. W.R. Gentry and C.F. Giese, Phys.Rev. A 11 (1975) 90

3. H. Krüger and R. Schinke, J. Chem. Phys. 66 (1977) 5087

4. R. Schinke, M. Dupuis and W.A. Lester, J.Chem.Phys. 72 (1980) 3909

5. R. Schinke, J. Chem. Phys. 72 (1980) 3916

6. V. Hermann, H. Schmidt and F. Linder, J. Phys. B 11 (1978) 493

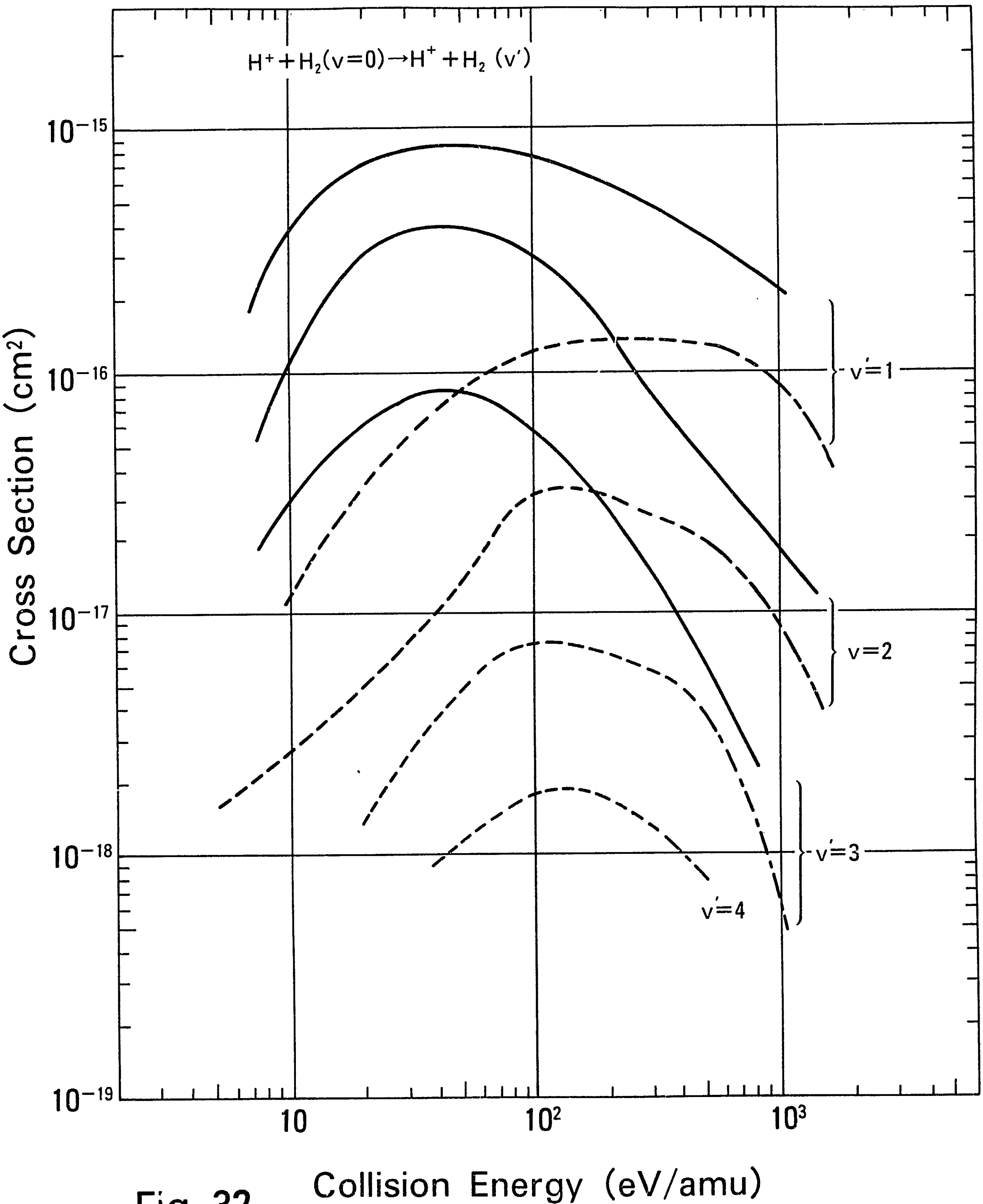

$H^+ + H_2(v=0) \rightarrow H^+ + H_2\ (v')$
10^{-15}
10^{-16}
10^{-17}
10^{-18}
10^{-19}
Cross Section (cm²)
v'=1
v=2
v'=3
v'=4
10
10^2
10^3
Collision Energy (eV/amu)

Fig. 32

III-2 Lyman-α line emissions in $H^+ + H_2$ collisions

One of the possible processes resulting in the emission of Lyman-α line in the collisions is the charge-capture into projectiles:

$$\underline{H}^+ + H_2 \rightarrow \underline{H}^*(2s,\ 2p) + [\ H_2{}^+] \qquad :\sigma_p \qquad (1)$$

and the other is the dissociative excitation of targets:

$$\underline{H}^+ + H_2 \rightarrow \underline{H}^+ + H^*(2s,\ 2p) + [H] \qquad :\sigma_p \qquad (2)$$

Here [ ] indicates the inclusion of all the possible processes including the ionization, excitation and so on.

The Total cross sections ($\sigma_p + \sigma_t$) for the line emissions for processes (1) and (2) were measured by Dunn et al.[1] and van Zyl et al.[2] In these measurements, the oxygen-filters were used to select Lyman-α emissions and the detectors were set at 90 with respect to the projectiles so as to minimize the Doppler shift. In both measurements, no electric field to quench the metastable state atoms $H^*(2s)$ was used. Therefore, their data can be assumed to correspond to total $H^*(2p)$ production cross sections. Bayfield[3] set his Lyman-α detector far from the collision region to quench the projectiles in the metastable 2s state and, then, determined the cross sections for capture into 2s projectils state $\sigma_p(2s)$(see Fig.33).

On the other hand, Birely and McNeal[4] observed photons emitted at 54.7° and 125.3° to separate the unshifted lines due to the dissociative excitation process(2) of targets and the shifted lines due to the charge capture process(1) into projectiles. They applied the quenching electric field to observed the emissions from $H^*(2s)$ state. The measured emission cross sections include the cascading effects. For example, the 2p state is formed directly by collisions and also by cascading from the 3s and 3d states after the Balmer-α emissions. Considering the life times of these states and their excitation cross sections, Birely and McNeal[4] concluded that the corrections due to the cascading effects are less than 2% for $\sigma_p(2s)$, less than 5% for $\sigma_p(2p)$ and $\sigma_t(2s)$ and less than 15% for $\sigma_t(2p)$. The measured cross sections $\sigma_p(2p)$, $\sigma_t(2s)$ and $\sigma_t(2p)$ decrease sharply with decreasing the collision energy. Thus, the cross sections below a few keV observed by Dunn et al.[1)] and van Zyl et al.[2)] are interpreted to be mainly due to the charge capture into 2p state of projectiles. A shoulder of the cross sections at around 1-2 keV is explained to be due to the coupling between the ground (1s)state and excited state (2p)[2)]. In fact, the cross sections of capture into the ground state of projectiles become largest there. However, further investigations are necessary to understand this shoulder.

References

1. G.H. Dunn, R. Geballe and D. Pretzer, Phys. Rev. 128 (1962) 2200
2. B. van Zyl, D. Jaecks, D. Pretzer and R. Geballe, Phys. Rev. 158 (1967) 29
3. J.E. Bayfield, Phys. Rev. 182 (1969) 115
4. J.H. Birely and R.J. McNeal, Phys. Rev. A 5 (1972) 692

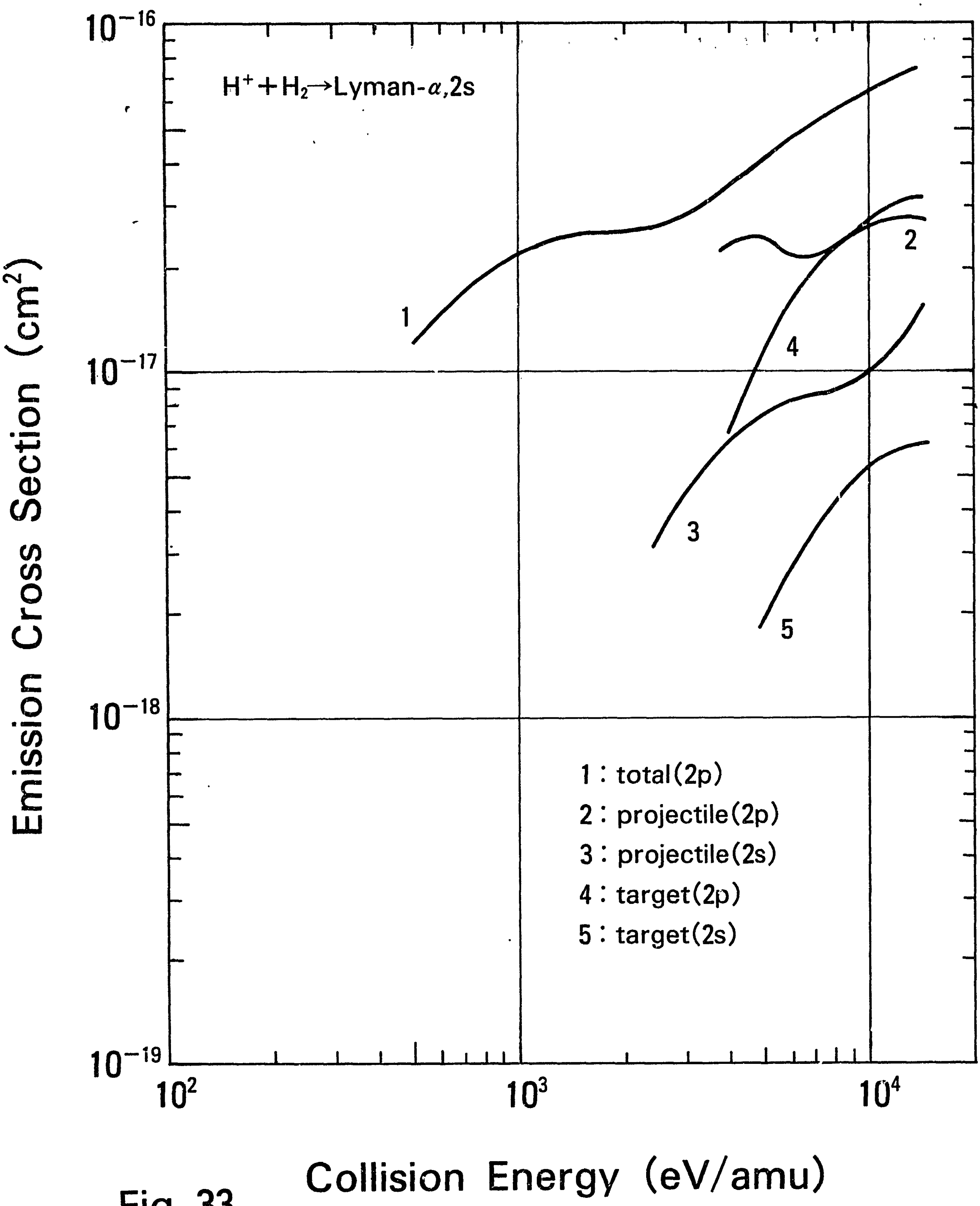

10^{-16}
10^{-17}
10^{-18}
10^{-19}
10^2
10^3
10^4
Emission Cross Section (cm^2)
Collision Energy (eV/amu)
$H^+ + H_2 \rightarrow$ Lyman-α,2s
1
2
3
4
5
1 : total(2p)
2 : projectile(2p)
3 : projectile(2s)
4 : target(2p)
5 : target(2s)

Fig. 33

This page is intentionally left blank

III-3 Lyman - α line emissions in $H + H_2$ collisions

In this collision system, two processes contribute to Lyman - α emissions :

$$\underline{H} + H_2 \rightarrow \underline{H}^*(\,2s,\,2p\,) + H_2 \qquad \sigma_p\text{:projectile excitation} \quad (1)$$

$$\rightarrow \underline{H} + H^*(\,2s,\,2p\,) + H \qquad \sigma_t\text{:dissociative excitation} \quad (2)$$

In their experiment, Birely and McNeal[1)] produced the neutral projectiles by neutralizing protons passing through an Ar-filled chamber and deflected away protons by the condenser plates which also quenched the metastable atoms produced in the chamber. Then, only the ground state hydrogen atoms H(1s) are contained in projectiles (see Fig.34).

Similar technique was used by Morgan et al.[2)] to determine $\sigma_p(2p)$ and $\sigma_t(2p)$. Their data are normalized to those of Birely and McNeal at 15 keV.

References

1. J.H. Birely and R.J. McNeal, Phys. Rev. A 5 (1972) 692
2. T.J. Morgan, J. Geddes and H.B. Gilbody, J. Phys. B 7 (1974) 142

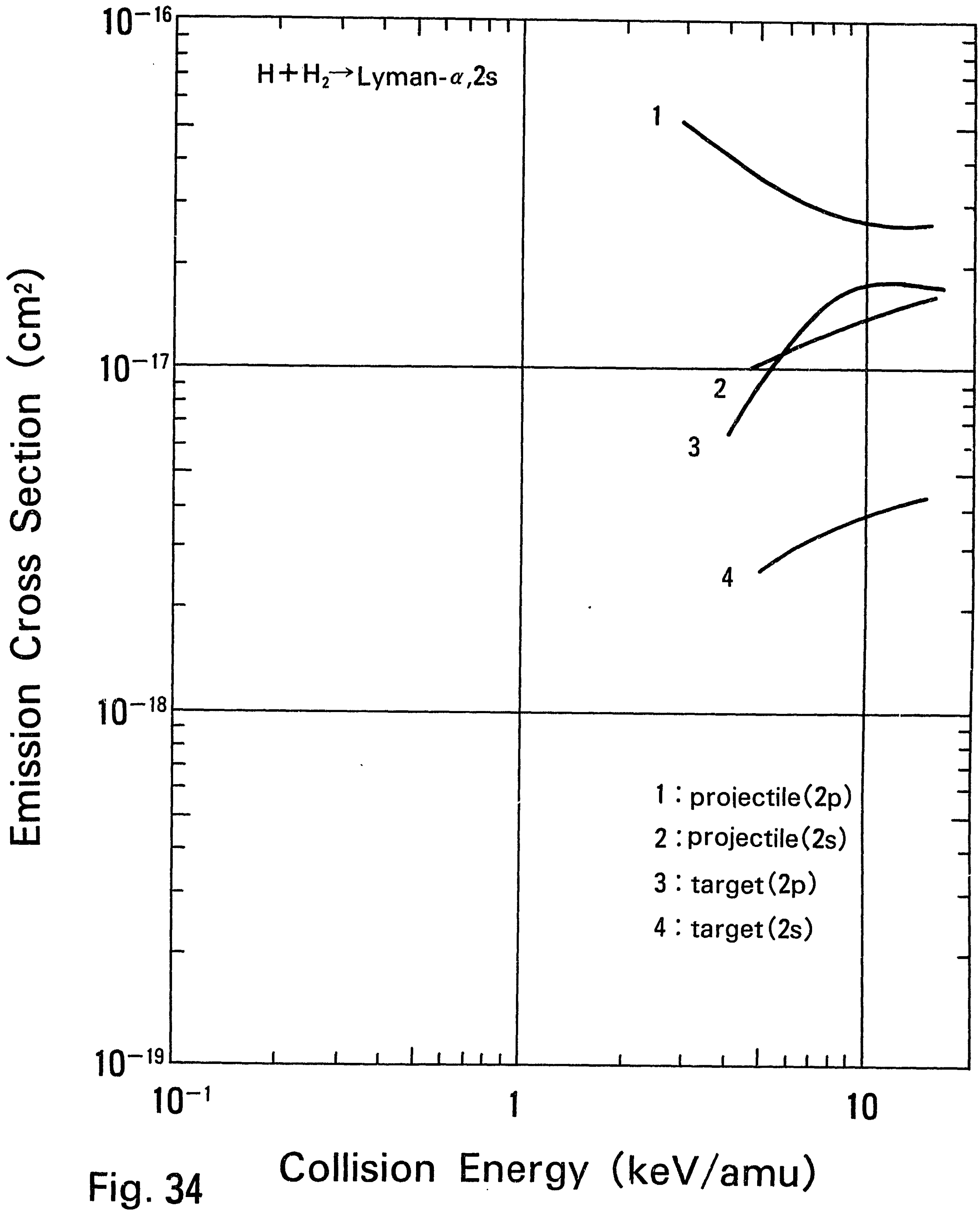

$H + H_2 \rightarrow$ Lyman-α,2s
Emission Cross Section (cm²)
10^{-16}
10^{-17}
10^{-18}
10^{-19}
10^{-1}
1
10
Collision Energy (keV/amu)
1
2
3
4
1 : projectile(2p)
2 : projectile(2s)
3 : target(2p)
4 : target(2s)

Fig. 34

III-4 Lyman-α line emissions in $H_2^+ + H_2$ collisions

A number of processes should be responsible for production of the Lyman-α line in this collision. The following two processes are typical:

$$\underline{H}_2^+ + H_2 \rightarrow \underline{H}^* (2s, 2p) + [\underline{H}] + [\ H_2^+]$$: dissociative charge capture into projectil (1)

$$\rightarrow \underline{H}_2^+ + H^* (2s, 2p) + [H]$$: dissociative excitation of target (2)

At higher energies, these processes are coupled together. The sum of the cross sections leading to production of Lyman-α, $\Sigma\sigma$ (2p), was measured.[1,2] Data by van Zyl et al.[2] are normalized to that by Dunn et al.[1] at 3 keV (see Fig. 35). The errors of the absolute cross sections are ± 55%. It should be noted that, at the same collision energy, these cross sections for production of Lyman-α line in H_2^+ ion impact are about a factor of two larger than those in H^+ ion impact, indicating that two hydrogens in H_2^+ ion behave independently.

References

1. G.H. Dunn. R. Geballe and D. Pretzer, Phys. Rev. 128 (1962) 2200
2. B. van Zyl, D. Jaecks, D.Pretzer and R.Geballe, Phys. Rev. 158 (1967) 29

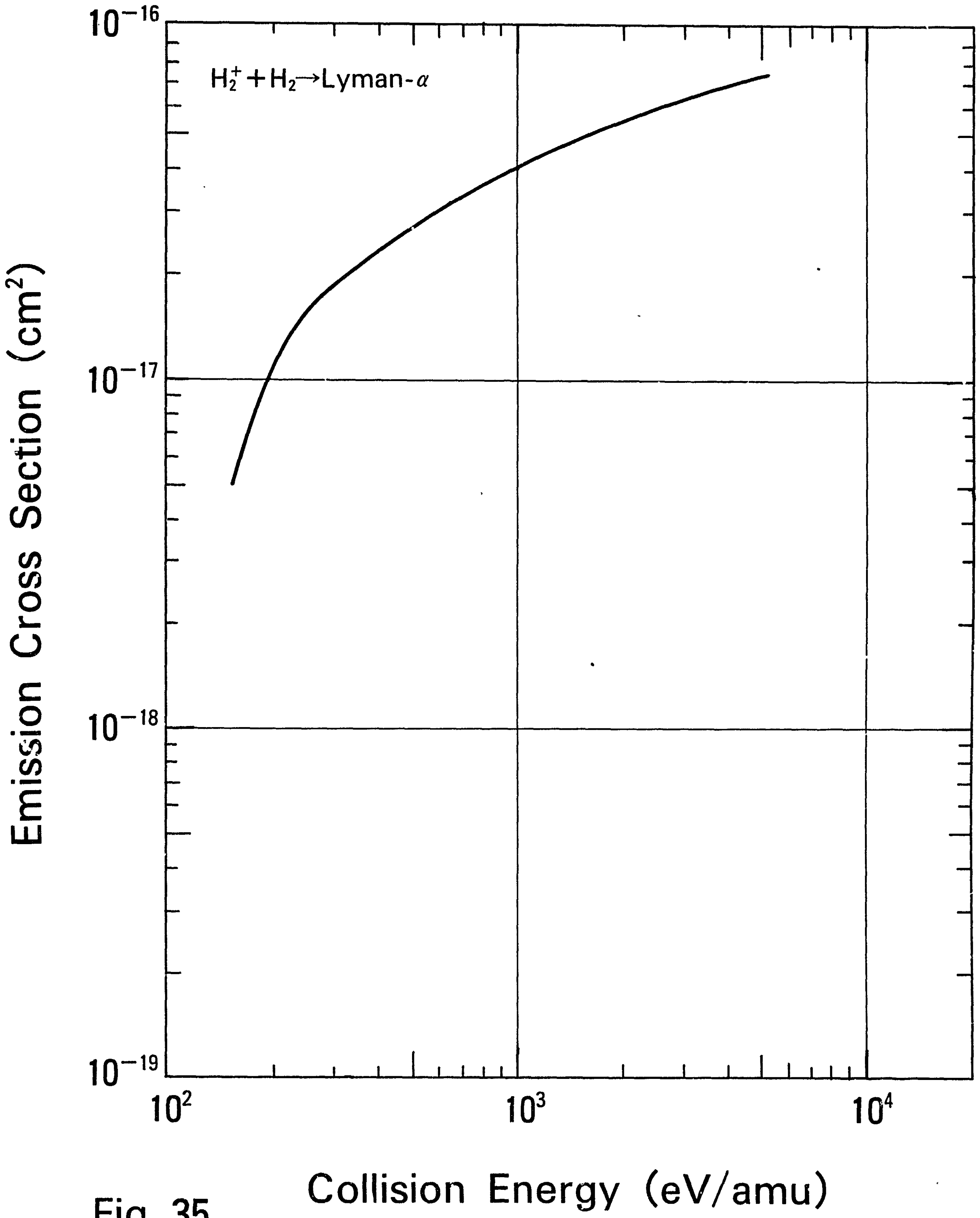

$H_2^+ + H_2 \rightarrow$ Lyman-α
10^{-16}
10^{-17}
10^{-18}
10^{-19}
Emission Cross Section (cm^2)
10^2
10^3
10^4
Collision Energy (eV/amu)

Fig. 35

III-5 Countable UV emissions in $H_3^+ + H_2$ collisions

The cross sections for the countable uv line emissions in this collisions system were measured by Dunn et al.[1] (see Fig. 36). Unfortunnately, no cross sections for the state-specified line emissions are reported.

Reference

1. G.H. Dunn, R. Geballe and D. Pretzer, Phys. Rev. 128 (1962) 2200

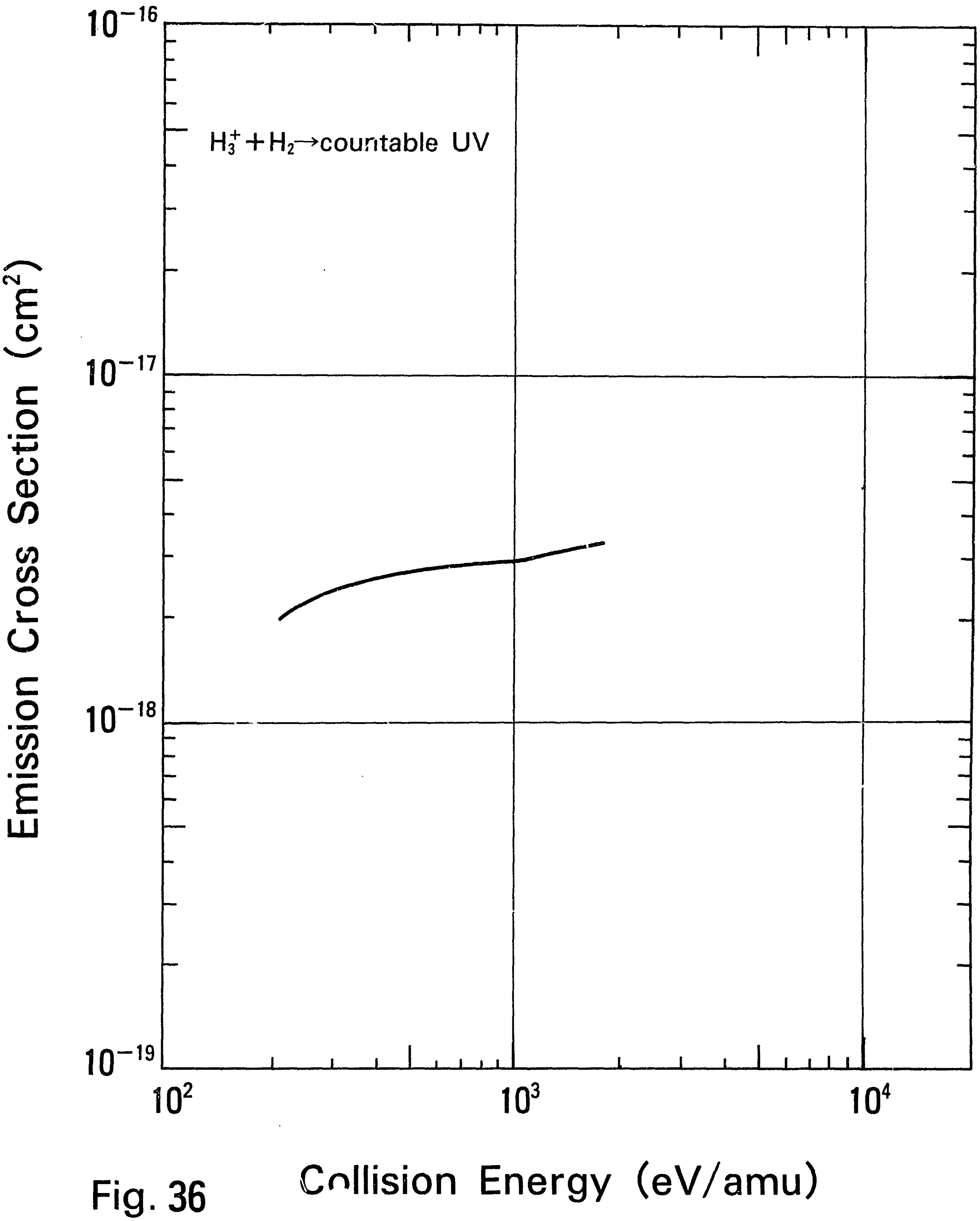
10^{-16}
10^{-17}
10^{-18}
10^{-19}
$H_3^+ + H_2 \rightarrow$ countable UV
Emission Cross Section (cm^2)
10^2
10^3
10^4
Collision Energy (eV/amu)

Fig. 36

III-6 Balmer-α line emissions in $H^+ + H_2$ collisions

The Balmer-α line (n = 3 → 2 transition) and Balmer-β line (n = 4 → 2) are produced either by the charge transfer into projectile protons

$$H^+ + H_2 \rightarrow H^* \,(n = 3,4 \rightarrow 2) + H_2^+ \qquad : \sigma_p \qquad (1)$$

or the dissociative excitation of targets

$$H^+ + H_2 \rightarrow H^+ + H^* \,(n = 3,4 \rightarrow 2) + H. \qquad : \sigma_t \qquad (2)$$

The experimental methods are essentially the same as those used for the Lyman-α measurements : The Doppler shift is used to separate the emissions from projectiles and those from targets. Using the difference in the life-times of those states produced by collisions, the states can be resolved by setting the detectors at different positions from the collision region. The branching ratios in 3s→2p and 3d→2p transitions are both unity[1], meanwhile that in 3p→2s transitions resulting in the Balmer-α line emissions is 0.12. Therefore, the measured cross sections σ(3p + 3d) correspond to the sum of the cross sections for the excitation to the 3d state, σ(3d), and 12% of those to the 3p state, σ(3p). The cascade contribution must be taken into account because the branching ratio for 4f→3d is unity. The estimation of the cascades is done by Williams et al.[2] who show that their contribution is less than 2% for σ_p(3s), less than 9% for σ_p(3p + 3d) and less than 15% for σ_t. The data shown in Fig.37 are based upon mainly those by Williams et al[2]. It is clearly seen that at lower energies the charge capture into 3p and 3d states of projectiles is dominant, meanwhile that into 3s states becomes dominant at higher energies. Data by Loyd and Dawson[3] for σ_p(3s) are in agreement with those shown. On the other hand, data by Dawson and Loyd[4] for σ_p(3p + 3d) are by a factor of about two smaller than those shown. Though the results by Hess for σ_p[5] are by a factor of 30-40 smaller than those by Williams et al., the energy dependence seems to be very similar. Then, data by Hess at 0.5 - 2 keV are shown by normalizing to that by Williams et al. at 1.5 keV.

References

1. E.U. Condon and W. Shortley, The Theory of Atomic Spectra (Cambridge Univ. Press, 1951) p.136
2. I.D. Williams, J. Geddes and H.B. Gilbody, J. Phys. B 15 (1982) 1377
3. D.H. Loyd and H.R. Dawson, Phys. Rev. A 11 (1975) 140
4. H.R. Dawson and D.H. Loyd, Phys. Rev. A 15 (1977) 43
5. W.R. Hess. Phy. Rev. A 9 (1974) 2036

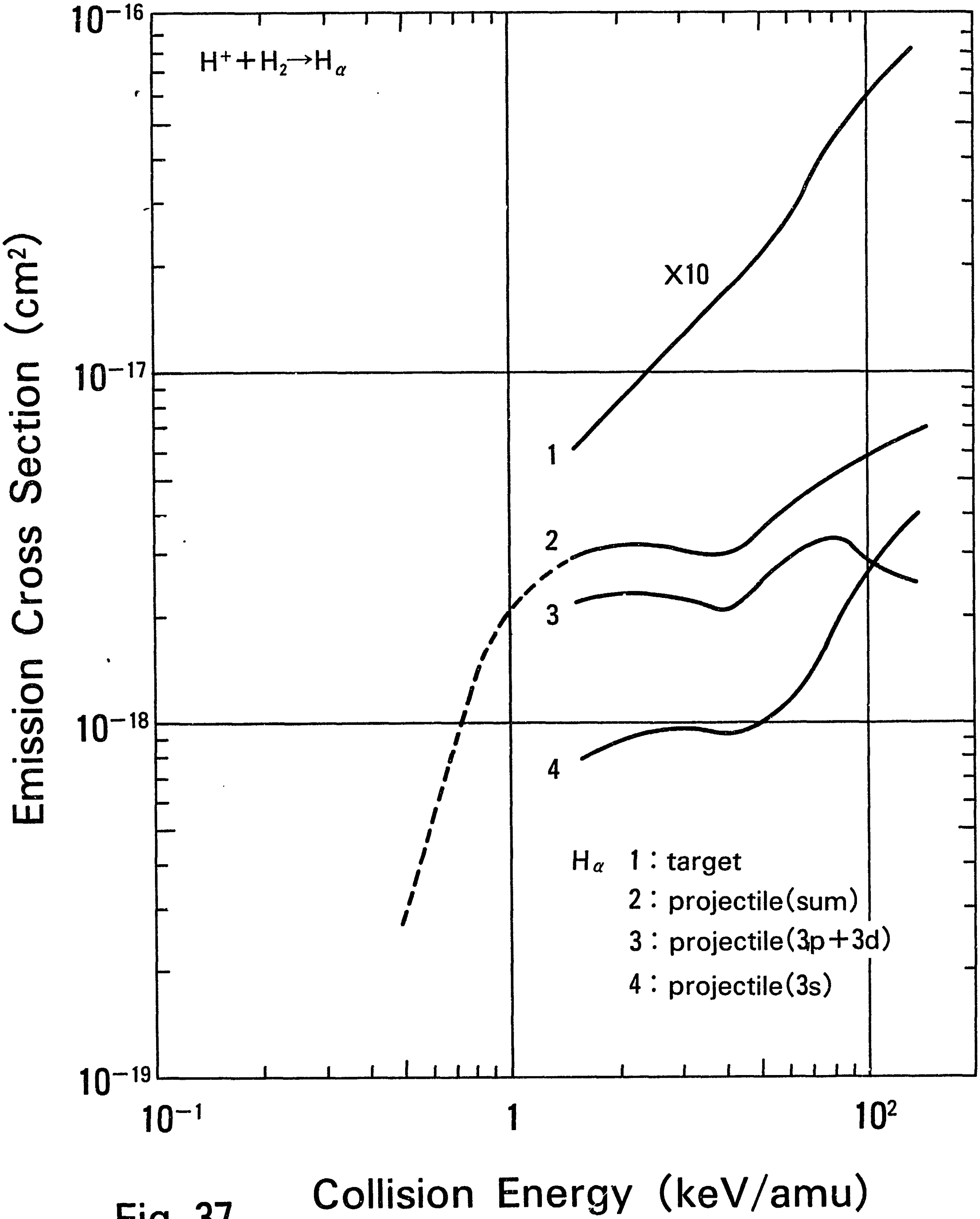

$H^+ + H_2 \rightarrow H_\alpha$
X10
1
2
3
4
H_α 1 : target
2 : projectile(sum)
3 : projectile(3p+3d)
4 : projectile(3s)
10^{-16}
10^{-17}
10^{-18}
10^{-19}
10^{-1}
1
10^2
Emission Cross Section (cm^2)
Collision Energy (keV/amu)

Fig. 37

III-7 Balmer-α and -β line emissions in $H + H_2$ collisions

The Balmer-α and -β lines can be produced through either excitation process of projectiles

$$\underline{H} + H_2 \rightarrow \underline{H}^* (n=3,4 \rightarrow 2) + H_2 : \qquad \sigma_p \qquad (1)$$

or the dissociative excitation process of targets

$$\underline{H} + H_2 \rightarrow \underline{H} + H^* (n=3,4 \rightarrow 2) + H. : \qquad \sigma_t \qquad (2)$$

These neutral ground state hydrogen atom projectiles are provided either by the neutralization + electric quenching technique or by the photo detachment technique from H^- beam. As van Zyl et al.[1] observed the Balmer-α and -β emissions at 90σ only, they could not separate the emission lines from projectiles and those from targets. But they determined the cross sections, $\Sigma\sigma$ (total), $\sigma_p(3s)$ and $\sigma_p(3p + 3d) + \sigma_t$ over the energy range of 0.05 - 2.5 keV. Based upon these observed values, total cross sections for projectiles, σ_p, and for targets, σ_t, can be deduced and are shown in Fig.38. These data are in fairly good agreement with those by Williams et al.[2] (1.5 - 100 keV) at the overlapped energies. Thus, the main contribution to the observed Balmer-β line emissions at low energies comes from the excitation of projectiles into 3p and 3d states. $\sigma_p(3s)$ is less than 20% and σ_t is only a few percent. On the other hand, at higher energies, all the cross sections become comparable.

Similar situations are seen in the Balmer-β line emissions, though no estimation of σ_t' which may be small contribution to total cross sections, can be made. It should be noted that, as the branching ratio for 4s → 2p transition is 0.58, the measured emission cross sections, σ(4s), correspond to 58% of the excitation cross sections, $\sigma_E(4s)$, of projectiles. Similarly,

$\sigma(4p + 4d)$ is equal to $0.12\ \sigma_E(4p) + 0.74\sigma_E\ (4d)$. The cascade contribution to the Balmer-α and -β lines is estimated to be not too large, according to the analysis by van Zyl et al.[1] though the branching ratios for nf→3d and nf→4d transitions are not negligible.

Note that data by Hughes et al.[3] (10-35 keV) seem to be too small because the energetic excited atoms (for example H(3s)) arising from the dissociation of H_2 may emit the Balmer line photons outside the detector-viewing region[2].

References

1. B. van Zyl, M.W. Gealy and H. Neumann, Phys. Rev. A 28(1983) 176
2. I.D. Williams, J. Geddes and H.B. Gilbody, J. Phys. B 15(1982) 1377
3. R.H. Hughes, H.M. Petefish and H. Kisner, Phys. Rev. A 5 (1972) 2103

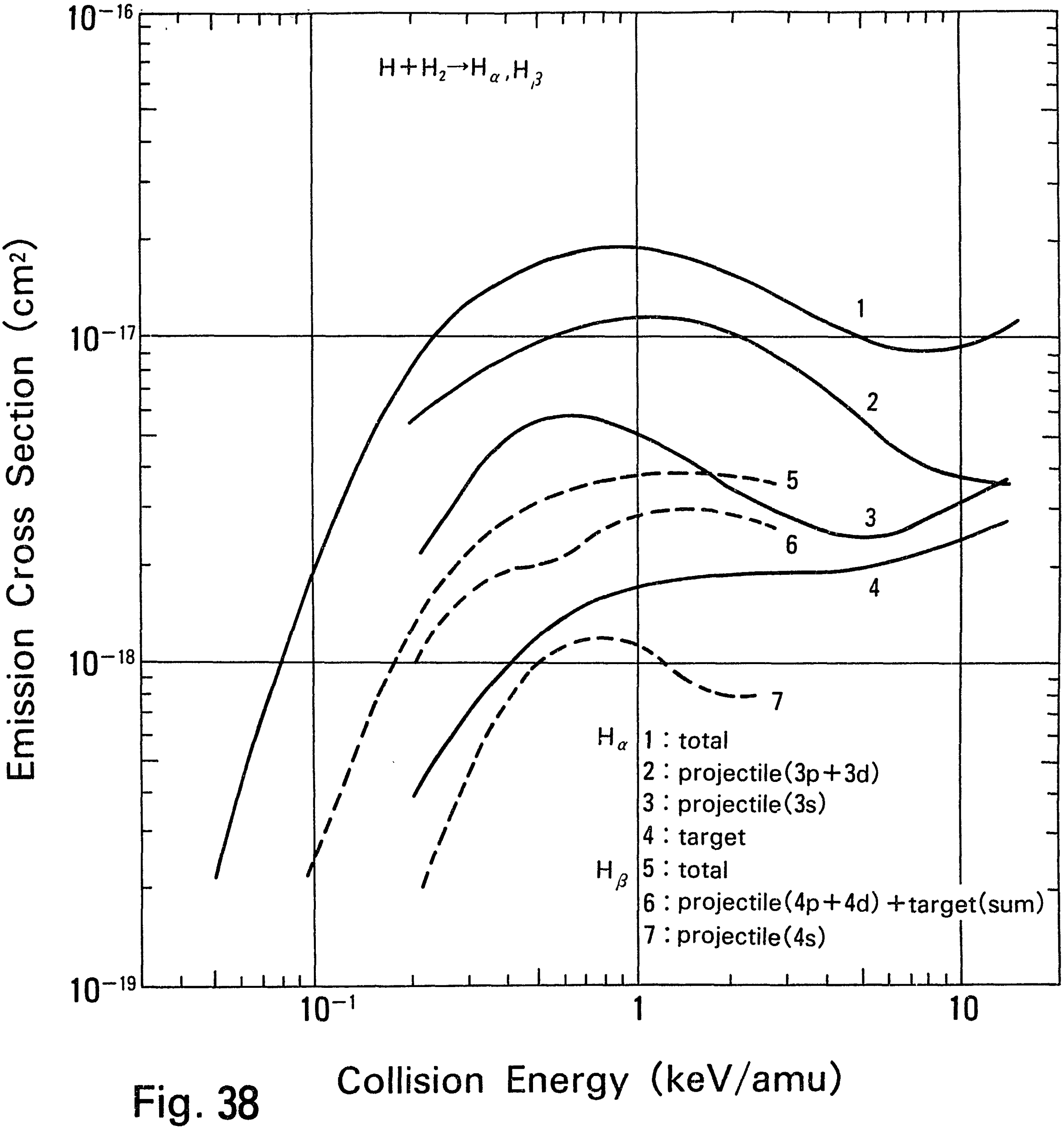
H+H2→Hα,Hβ
10−16
10−17
10−18
10−19
Emission Cross Section (cm2)
10−1
1
10
Collision Energy (keV/amu)
1
2
3
4
5
6
7
Hα 1 : total
2 : projectile(3p+3d)
3 : projectile(3s)
4 : target
Hβ 5 : total
6 : projectile(4p+4d) +target(sum)
7 : projectile(4s)

Fig. 38

III-8 Balmer-α and -β line emissions in $H_2^+ + H_2$ collisions

In these collisions, the following processes are responsible for Balmer line emissions; dissociative charge transfer into projectiles:

$$\underline{H}_2^+ + H_2 \rightarrow \underline{H}^* (n = 3, 4 \rightarrow 2) + \underline{H} + H_2^+ \qquad \sigma_p \qquad (1)$$

dissociative excitation of targets:

$$\underline{H}_2^+ + H_2 \rightarrow \underline{H}_2^+ + H^* (n = 3, 4 \rightarrow 2) + H . \qquad \sigma_t \qquad (2)$$

Williams et al.[1] measured $\sigma_p(3s)$, $\sigma_p(3p + 3d)$ and σ_t over the energy range 2-100 keV. Based upon these data, the cross sections for total cross sections for Balmer-α, $\sigma_p(3s)$, $\sigma_p(3p + 3d)$ and σ_t are shown in Fig.39.

As expected, the dissociative excitation of targets becomes dominant at higher energies. Also this process again becomes dominant at lower energies. In contrast to the Balmer-α line emissions, the ratios of the cross sections for H_2^+ impact to those for H^+ impact are not a factor of two but change with the collision energy.

Similar data for Balmer-α line emissions were reported by Hatfield and Hughes[2] whose values are consistently smaller by a factor of 2 or more and by Hess[3] whose values are a factor of about 30 smaller than the data shown.

The cross sections for Balmer-β line emissions by Hatfield and Hughes are also shown in Fig.39. It should be noted that these values might be too small, as noted in the Balmer-α line emissions. The contribution from the dissociative excitation of targets becomes significant at higher energies, meanwhile the dissociative charge transfer processes into projectiles are far dominant at low energies.

References

1. I.P. Williams, J. Geddes and H.B. Gilbody, J. Phys. B 15 (1982) 1977

2. L.L. Hatfield and R.H. Hughes, Phys. Rev. 131 (1963) 2556

3. W.R. Hess, Phys. Rev. A 9 (1974) 2036

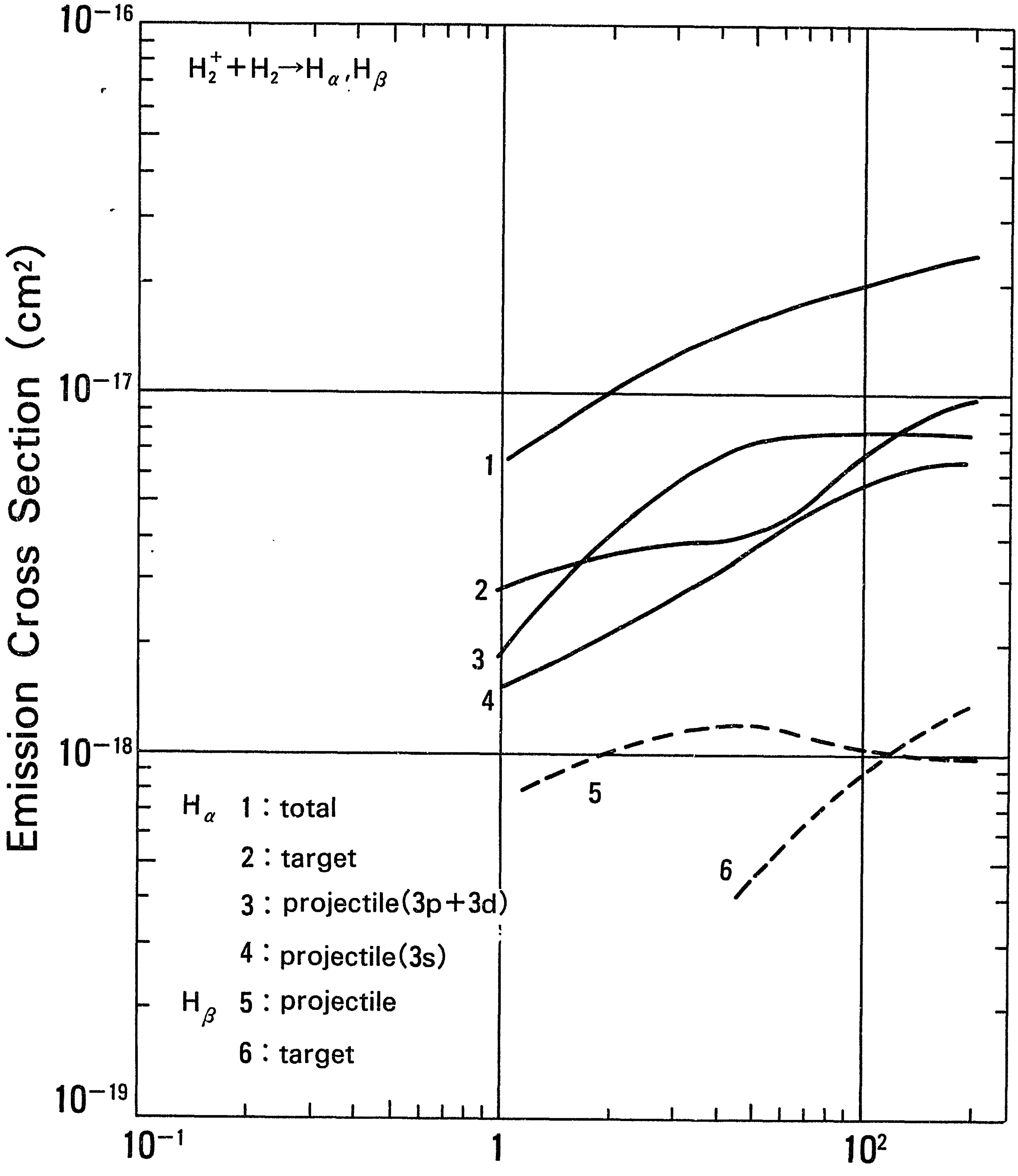

Fig. 39 Collision Energy (keV/amu)

This page is intentionally left blank

III-9 Balmer-α line emissions in $H_3^+ + H_2$ and $H_2 + H_2$ collisions

Similar to other collision processes, the Balmer-α line emissions originate either from projectile (σ_p) or from target (σ_t). The emission cross sections were measured by Williams et al.[1] over the energy range 0.67-3.3 keV/amu. Total σ, $\sigma_p(3s)$, $\sigma_p(3d + 3p)$ and σ_t are shown in Fig.40. Ratio of these values to those by protons and by H_2^+ ions changes in complicated manners. Thus, H_3^+ ions can not be equivalent to three independent protons in these collisions.

Also the Balmer-α line emission cross sections were determined in $H_2 + H_2$ collisions over the energy range 5-50 keV/amu.[2] At 5 keV/amu, σ total = $(7.7 \pm 2.5) \times 10^{-18}$ cm^2, $\sigma_p(3s) = (2.9 \pm 0.8) \times 10^{-18}$ cm^2 and $\sigma_p(3a + 3p) = (4.8 \pm 2.1) \times 10^{-18}$ cm^2, decreasing with decreasing the collision energy.

References

1. I.D. Williams, J. Geddes and H.B. Gilbody, J. Phys. B 15 (1982) 1377
2. I.D. Williams, J. Geddes and H.B. Gilbody, J. Phys. B 16 (1983) L765

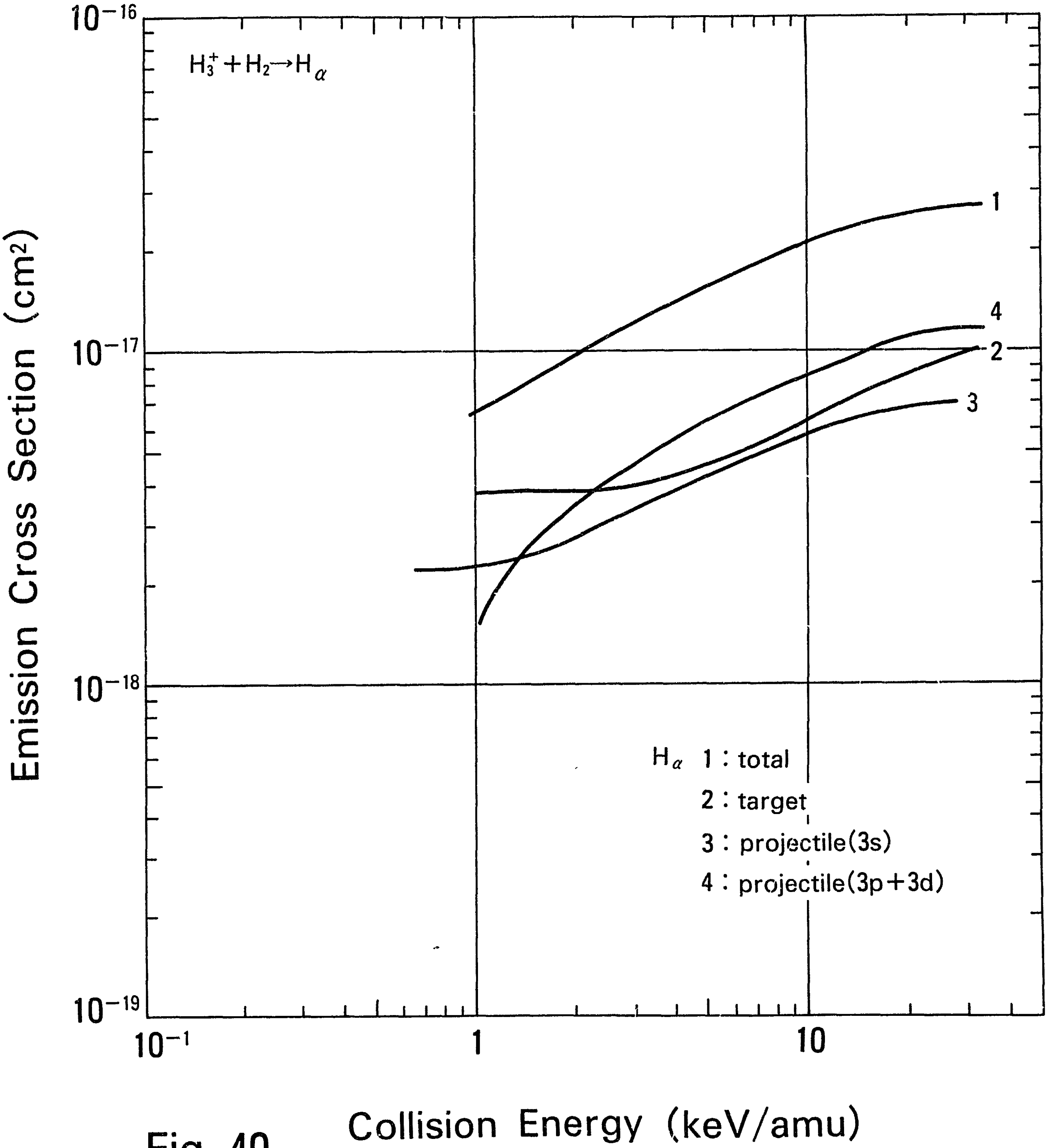
$H_3^+ + H_2 \rightarrow H_\alpha$
H_α 1 : total
2 : target
3 : projectile(3s)
4 : projectile(3p+3d)
1
2
3
4
Emission Cross Section (cm²)
10^{-16}
10^{-17}
10^{-18}
10^{-19}
10^{-1}
1
10
Collision Energy (keV/amu)

Fig. 40

III-10 Charge transfer and stripping of H^+, H^0 and H^- ions in collisions with H_2 molecules

The cross sections for the following processes have been surveyed and compiled[1] (see Fig.41):

$$H^+ + H_2 \rightarrow H^0 + H_2^+ \qquad (1)$$

$$\rightarrow H^- + 2H^+ \qquad (2)$$

$$H^0 + H_2 \rightarrow H^+ + e + H_2 \qquad (3)$$

$$\rightarrow H^- + H_2^+ \qquad (4)$$

$$H^- + H_2 \rightarrow H^0 + e + H_2 \qquad (5)$$

$$\rightarrow H^+ + 2e + H_2. \qquad (6)$$

These cross sections are generally determined tnrough direct observation of the charge-changed projectiles. However, because of difficulties of collecting all these projectiles at very low energies, the cross sections are often estimated by means of the measurement of secondary electrons and/or secondary ions.

Reference

1. H. Tawara, At. Data and Nucl. Data Tables 22 (1978) 491

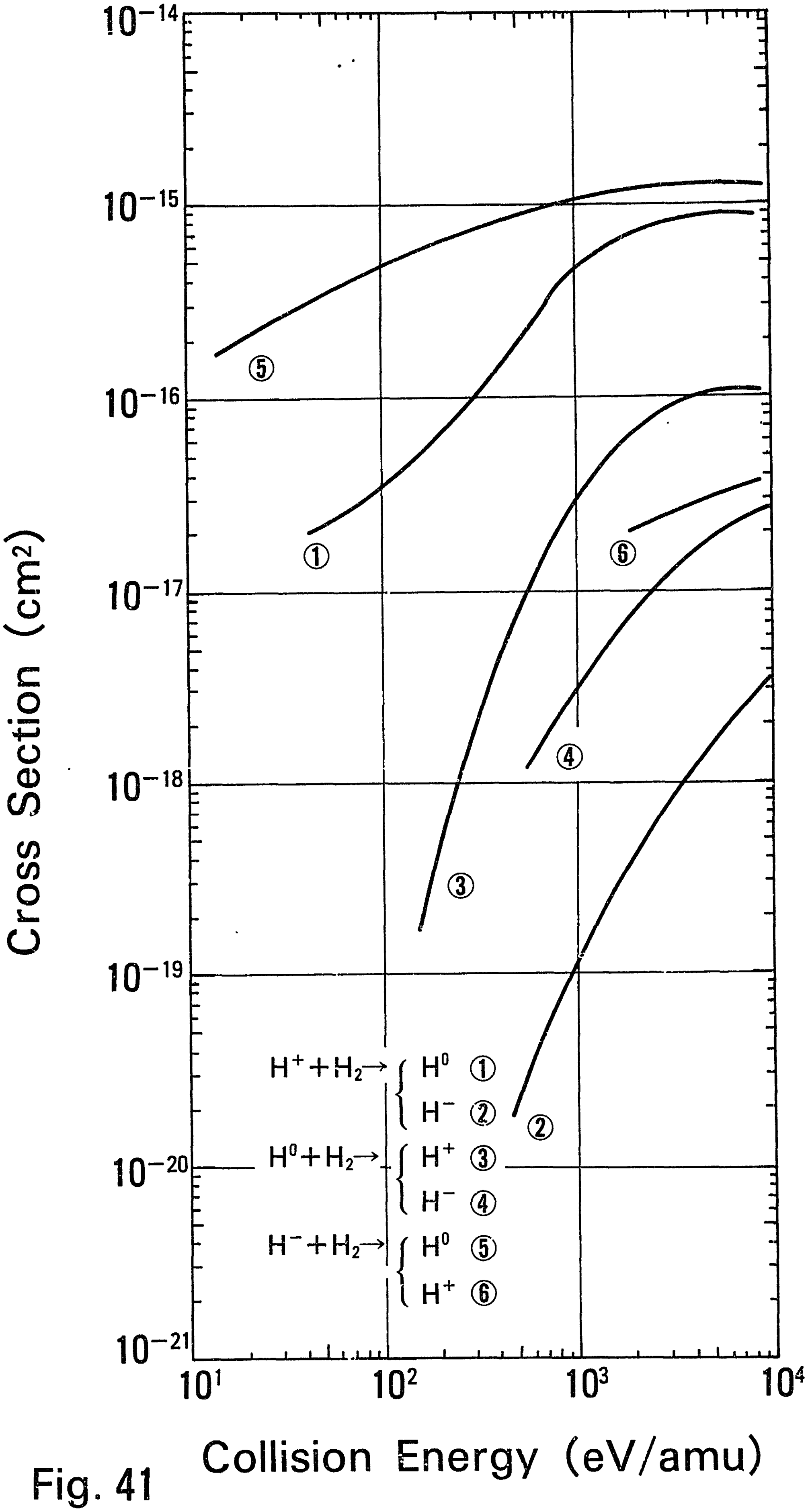

Cross Section (cm²)
10^{-14}
10^{-15}
10^{-16}
10^{-17}
10^{-18}
10^{-19}
10^{-20}
10^{-21}
10^{1}
10^{2}
10^{3}
10^{4}
Collision Energy (eV/amu)
⑤
①
⑥
④
③
②
$H^+ + H_2 \rightarrow$ H^0 ① H^- ②
$H^0 + H_2 \rightarrow$ H^+ ③ H^- ④
$H^- + H_2 \rightarrow$ H^0 ⑤ H^+ ⑥

Fig. 41

III-11 Electron capture by H_2^+ ions from H_2 molecules

$$\underline{H}_2^+(v) + H_2(v=0) \rightarrow \underline{H}_2(v') + H_2^+(v'') \qquad (1)$$

The apparent charge transfer cross sections using H_2^+ ions of the unspecified states were measured by a number of people[1-5] and a recommendation for these cross sections was made by Barnett et al.[6] (see Fig.42). The projectile H_2^+ ions used were mostly produced by electron impact. Therefore, the vibrational states (up to v=18) of projectiles are considered to be populated according to the Franck-Condon principle. These cross sections show the character of the resonant-charge transfer up to about E=500 eV and, then, begin to increase with increasing the collision energy. This increase is interpreted to be due to the opening of the non-resonant charge tranfer at higher energies. On the other hand, a steep decrease of the cross sections below a few eV is due to the opening of the competing ion-molecule rearrangement collisions:

$$H_2^+ + H_2 \rightarrow H_3^+ + H. \qquad (2)$$

The dependence of these cross sections on the vibrational states of H_2^+ ions was also investigated theoretically[7] and experimentally.[4,9,10] In a recent experiment by Liao et al.[10], their vibrationally state-selected H_2^+ ions were created by photoionization and their cross sections were normalized to those of Barnett et al.[6] For normalizaion, they selected the wavelength of photons (688 Å) to produce H_2^+ ions, whose vibrational population was assumed to be the same to that for H_2^+ ions produced by electron impact. Their results show that the cross sections of charge transfer for the lowest vibrational states, v=0 and v=1, over the energy range 8-400 eV have their maximum at around 10-20 eV, meanwhile those for higher excited states, $v \leq 18$, increase with decreasing the energy, similar to the resonant charge transfer. Generally speaking, the vibrational state dependence of the cross sections seems to be not too large.

The final vibrational states(v") of the product H_2^+ ions were also investigated, with the result that about 90% of the product H_2^+ ions at their energy range are in the ground state.

References

1. W.H. Cramer, J. Chem. Phys. 35 (1961) 836
2. D.W. Vance and T.L. Bailey, J.Chem. Phys. 44 (1966) 486
3. D.W. Koopman, Phys. Rev. 154 (1967) 79
4. H.C. Hayden and R.C. Amme, Phys. Rev. 172 (1968) 104
5. H.L. Rothwell, B. van Zyl and R.C. Amme, J. Chem. Phys. 61 (1974) 3851
6. C.F. Barnett, J.A. Ray, E. Ricci, M.T. Wilker, E.W. McDaniel, E. W. Thomas and H. B. Gilbody, ORNL-5206 (1977)
7. T.F. Moran and J.R. Roberts, J. Chem. Phys. 49 (1968) 3411
8. R.N. Stocker and H. Neumann, J. Chem. Phys. 61 (1974) 3852
9. F.M. Campbell, R.Browning and C.J. Latimer, J.Phys. B 14 (1981) 3491
10. C.L. Liao, C.X. Liao and C.Y. Ng, J.Chem. Phys. 81 (1984) 5672

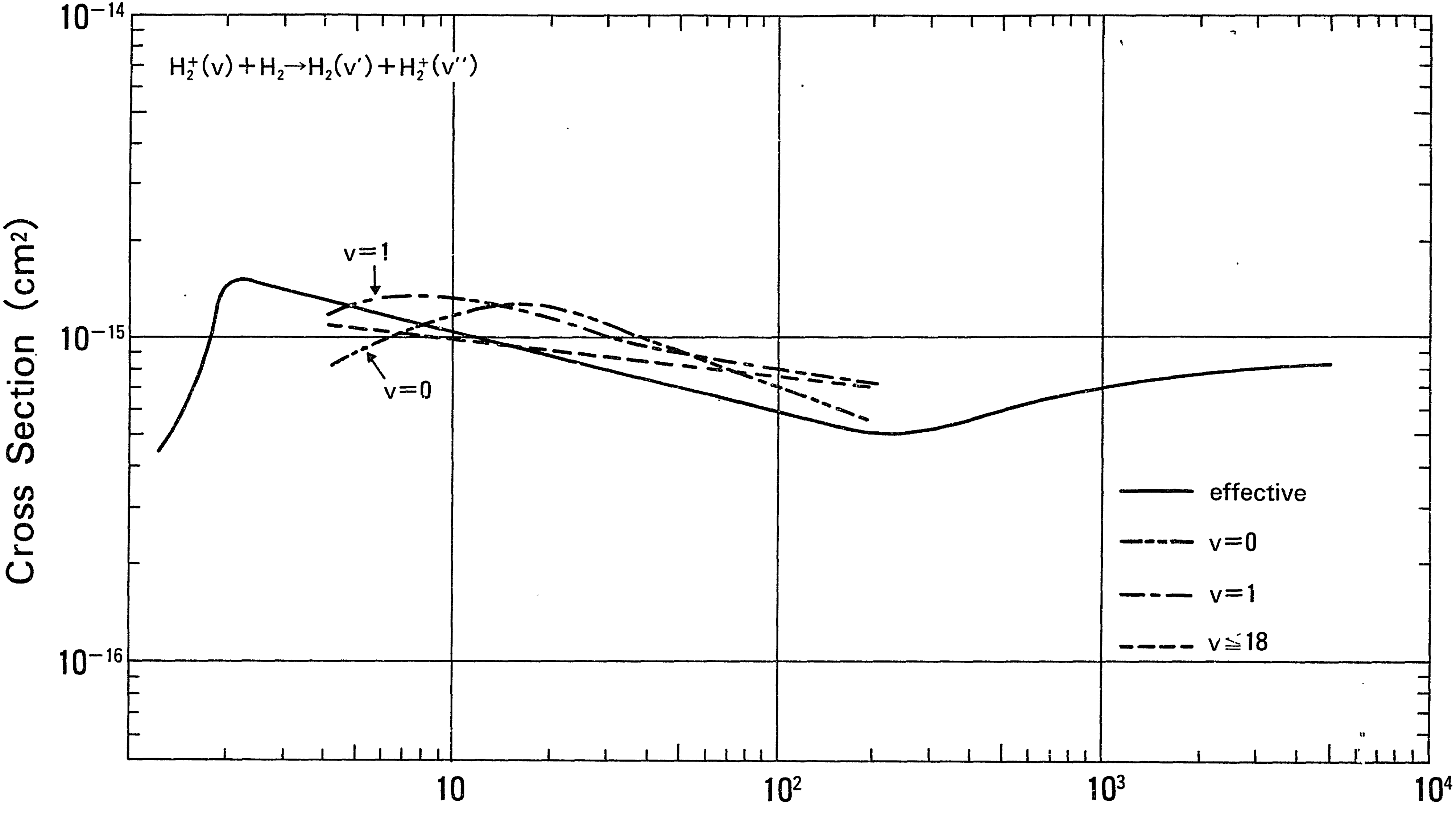

H₂⁺(v) + H₂ → H₂(v') + H₂⁺(v'')
Cross Section (cm²)
10⁻¹⁴
10⁻¹⁵
10⁻¹⁶
10
10²
10³
10⁴
v=1
v=0
effective
v=0
v=1
v≦18
Collision Energy (eV/amu)

Fig. 42

This page is intentionally left blank

III-12 Charge transfer, excitation and ionization in $H^+ + H$ collisions

$$H^+ + H \rightarrow H + H^+ \quad (1)$$
$$\rightarrow H^*(2p) + H^+ \quad (2)$$
$$\rightarrow H^*(2s) + H^+ \quad (3)$$
$$\rightarrow H^+ + H^*(2p) \quad (4)$$
$$\rightarrow H^+ + H^*(2s) \quad (5)$$
$$\rightarrow H^+ + H^*(n=2) \quad (6)$$
$$\rightarrow H^+ + H^*(n=3) \quad (7)$$
$$\rightarrow H^+ + H^+ + e \quad (8)$$

All the cross sections for these processes have been compiled[1)] (see Fig.43). Clearly at lower energies the symmetric charge transfer process (1) is far dominant over other processes.

Reference

1. H. Tawara, T. Kato and Y. Nakai, IPPJ-AM-30 (1983)

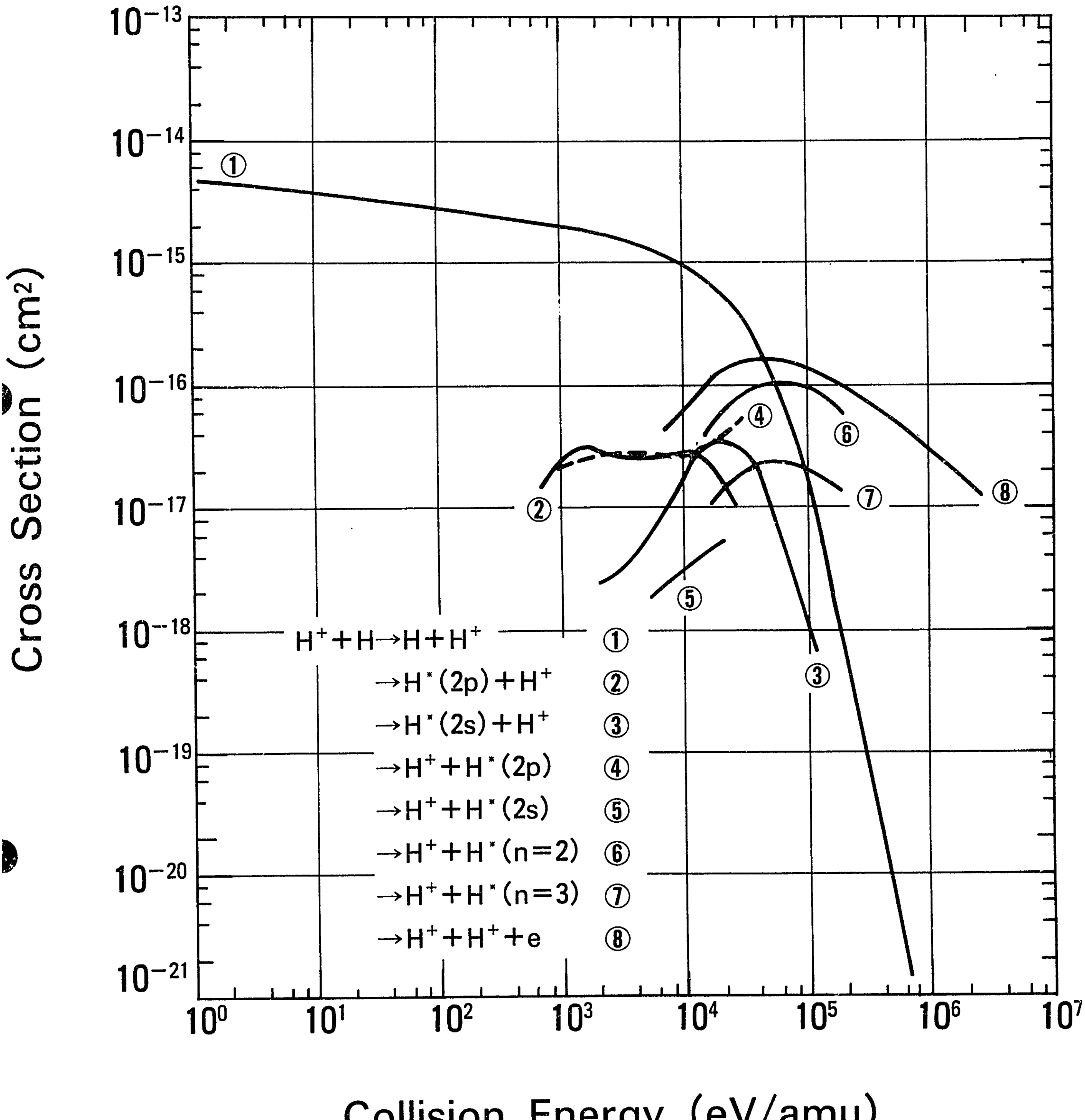
Cross Section (cm²)
10⁻¹³
10⁻¹⁴
10⁻¹⁵
10⁻¹⁶
10⁻¹⁷
10⁻¹⁸
10⁻¹⁹
10⁻²⁰
10⁻²¹
H⁺+H→H+H⁺ ①
→H*(2p)+H⁺ ②
→H*(2s)+H⁺ ③
→H⁺+H*(2p) ④
→H⁺+H*(2s) ⑤
→H⁺+H*(n=2) ⑥
→H⁺+H*(n=3) ⑦
→H⁺+H⁺+e ⑧
10⁰
10¹
10²
10³
10⁴
10⁵
10⁶
10⁷
Collision Energy (eV/amu)

Fig. 43

III-13 Stripping, excitation and charge transfer between neutral hydrogens

All the cross sections for the following processes have been compiled[1] (see Fig.44):

$$H + H \rightarrow H^+ \quad (1)$$

$$\rightarrow H^*(2s) \quad (2)$$

$$\rightarrow H^*(2p) \quad (3)$$

$$\rightarrow H^- + H^+ \quad (4)$$

Reference

1. H. Tawara, T. Kato and Y. Nakai, IPPJ-AM-30(1983)

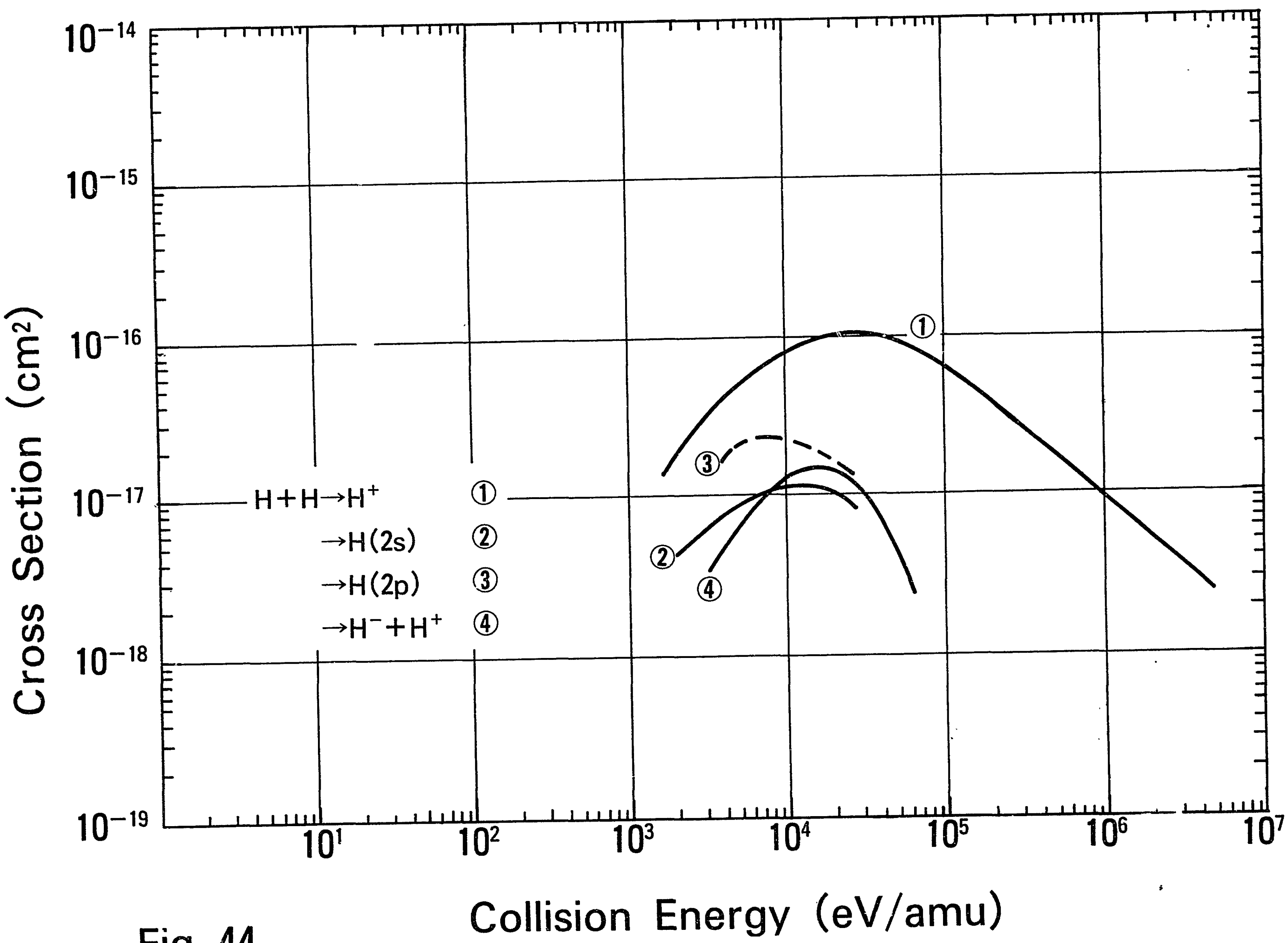

Cross Section (cm²)
10⁻¹⁴
10⁻¹⁵
10⁻¹⁶
10⁻¹⁷
10⁻¹⁸
10⁻¹⁹
10¹
10²
10³
10⁴
10⁵
10⁶
10⁷
H+H→H⁺ ①
→H(2s) ②
→H(2p) ③
→H⁻+H⁺ ④
Collision Energy (eV/amu)

Fig. 44

III-14 Stripping of H^- ions

The cross sections for H^- ions in collisions with H targets have been already compiled in our previous compilation[1] (see Fig.45):

$$\underline{H}^- + H \rightarrow \underline{H} + H + e \qquad (1)$$

$$\rightarrow \underline{H} + H^+ + 2e \qquad (2)$$

$$\rightarrow \underline{H}^+ . \qquad (3)$$

At low energies, pure single electron stripping process (1) is dominant, meanwhile single electron stripping + target ionization process (2) becomes dominant at high energies. Further it is noted that at higher energies double electron stripping process (3) overcome pure single electron stripping process.

Reference

1. H. Tawara, T. Kato and Y. Nakai, IPPJ-AM-30 (1983)

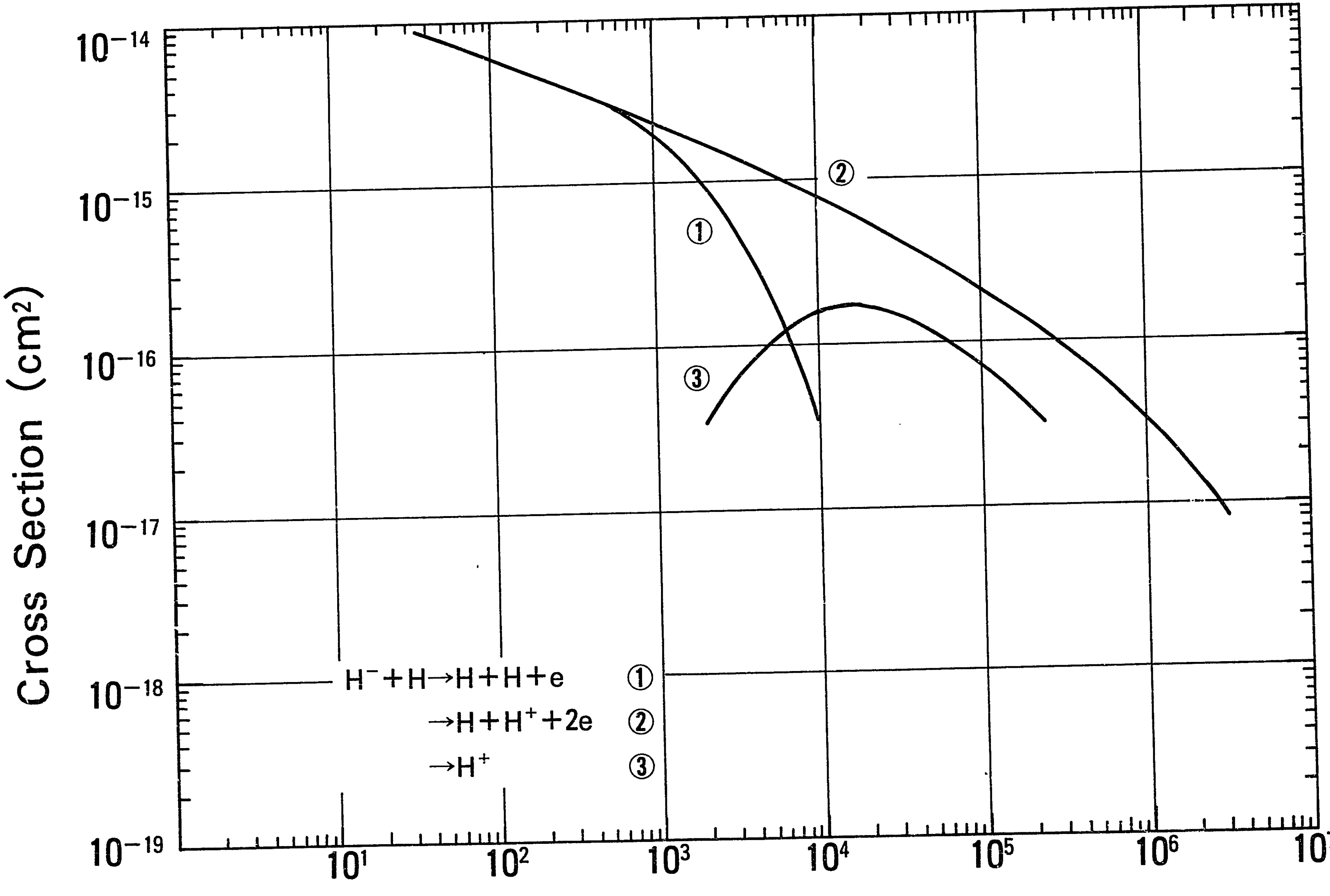
10−14
10−15
10−16
10−17
10−18
10−19
Cross Section (cm²)
10¹
10²
10³
10⁴
10⁵
10⁶
10⁷
Energy (eV/amu)
①
②
③
H⁻+H→H+H+e ①
→H+H⁺+2e ②
→H⁺ ③

Fig. 45

III-15 Ionization of H_2 molecules by H^+, H_2^+ and H_3^+ ions

$$H^+ + H_2 \rightarrow H^+ + H_2^+ + e \qquad (1)$$

$$H_2^+ + H_2 \rightarrow H_2^+ + H_2^+ + e \qquad (2)$$

$$H_3^+ + H_2 \rightarrow H_3^+ + H_2^+ + e \qquad (3)$$

The cross sections of pure ionization of H_2 molecules by ion impact are determined through measuring the secondary electrons.[1)] So the ionization through charge transfer into projectiles is excluded. At lower energies the ratios of the cross sections for H_2^+ and H_3^+ ions to those for H^+ ions are more than 2 and 3, respectively, and tend to become small at high energies (see Fig.46).

Reference

1. M. Sataka, T. Shirai, A. Kikuchi and Y. Nakai, JAERI-M-9310 (1981)

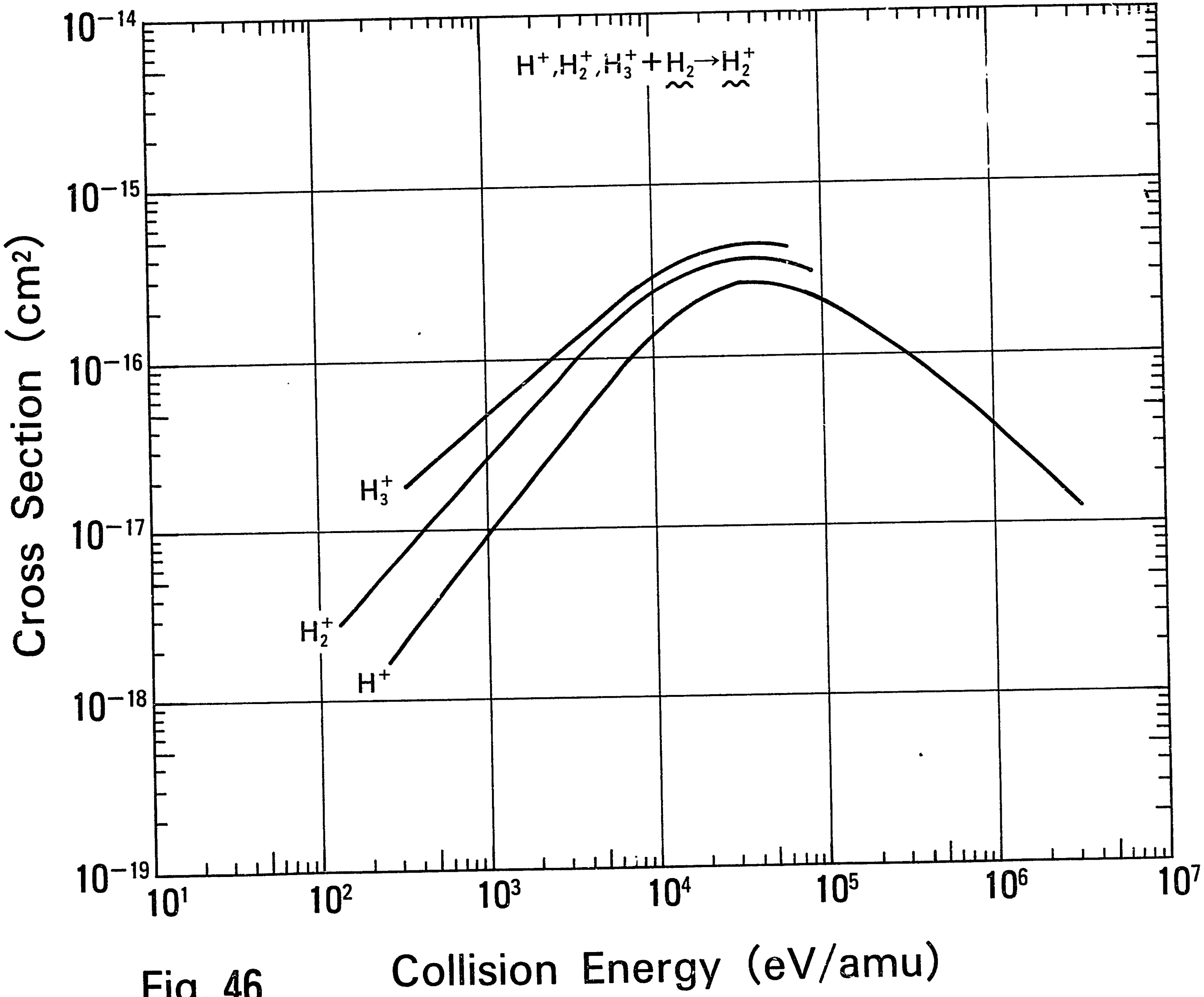

$H^+, H_2^+, H_3^+ + H_2 \rightarrow H_2^+$
H_3^+
H_2^+
H^+
10^{-14}
10^{-15}
10^{-16}
10^{-17}
10^{-18}
10^{-19}
Cross Section (cm²)
10^1
10^2
10^3
10^4
10^5
10^6
10^7
Collision Energy (eV/amu)

Fig. 46

III-16 H_3^+ ion production

$$H_2^+(v) + H_2 \rightarrow H_3^+ + H \qquad (1)$$

This process is important in formation of H_3^+ ions. THe following two processes contribute to H_3^+ ion production:

$$\underline{H}_2^+ + H_2 \rightarrow \underline{H}_2^+ H + H \qquad \text{(atom transfer)} \qquad (2)$$

$$\underline{H}_2^+ + H_2 \rightarrow \underline{H} + \underline{H}^+ H_2 \qquad \text{(proton transfer).} \qquad (3)$$

The H_3^+ ion formation cross sections were measured using various experimental methods: tandem-mass spectrometer[1], merging beams technique,[2,3] threshold electron-secondary ion coincidence method[4], radio-frequency beam-guide technique.[5] The measured cross sections are found to follow the theoretically expected $E^{-1/2}$ dependence below 1 eV(see Fig. 47). The steep decrease of the cross sections above a few eV is due to the competing charge transfer process :

$$H_2^+ + H_2 \rightarrow H_2 + H_2^+. \qquad (4)$$

The cross sections are found to be dependent upon the internal states of H_2^+ ions. For example, only the first four vibrationally excited states are expected to play a role, the contribution of the ground state of H_2^+ ions being dominant.[6] In fact, the observed dependence of the cross sections on the initial vibrational states[4,5] in atom transfer process(2) seems to follow this expectation. This also seems to be true in proton transfer process(3) at low energies. However, the situation for proton transfer at higher energies is reversed. The reasons for this difference are not well understood. It should be noticed that the cross sections shown in Fig.47 were obtained using the merging-beams technique[2] where the vibrational state distributions in neutral molecules are fairly broad, because they are prepared using the charge-transfer reaction, $H_2^+(v) + H_2 \rightarrow H_2^0(v') + H_2^+$.

Data of Giese and Maier seem to be fairly large, particularly at low energies. Douglass et al.[3] estimated the vibrational state distribution in their neutral beam by convoluting the Franck-Condon distribution for the ionization $H_2(0) \rightarrow H_2^+(v)$ by electrons and again with the Franck-Concon distribution for the charge-transfer process, $H_2^+(v) \rightarrow H_2(v')$. The average vibrational energy is estimated to be 2.5 eV. To distinguish two processes (2) and (3) from each other, the isotope ions are often used. The results of Douglass et al.[3] can be fitted to the following form over the energy range of 0.01 to 8 eV (shown in Fig.47 with solid lines):

$$\log_{10}\sigma = (B_1 + B_2 \log_{10} E_i) F(-y) + (B_3 + B_4 \log_{10} E_i) F(y),$$

where

$$y = (\log_{10} E_i - B_5) B_6^2$$

and

$$F(y) = e^y / (1+e^y).$$

The adjustable parameters B_n corresponding to the center-of-mass energies E_i in eV 2 are given in the following table for the measured processes.

initial	$HD^+ + D_2 \rightarrow$		$D_2^+ + HD \rightarrow$	
final	$HD_2^+ + D$	$D_3^+ + H$	$HD_2^+ + D$	$D_3^+ + H$
B_1	1.2438	0.7703	1.0719	0.6294
B_2	-0.4146	-0.5242	-0.4249	-0.5232
B_3	-1.6950	-0.2259	1.0529	-0.0260
B_4	-8.1470	-2.8924	-6.1341	-2.1136
B_5	1.4972	0.8912	1.1622	0.5060
B_6	1.5638	1.6516	1.4880	1.7555

References

1. C.F. Giese and W.B. Maier II, J.Chem. Phys. 39 (1963) 739

2. P.H. Neynaber and S.M. Trujillo, Phys. Rev. 167 (1908) 63

3. .H. Douglass, D.J. McClure and W.R. Gentry, J.Chem. Phys. 67 (1977) 4931

4. I. Koyano and K. Tanaka, J. Chem. Phys. 72 (1980) 4858

5. S.L. Anderson, F.A. Houle, D. Gerlich and Y.T. Lee, J. Chem. Phys. 75 (1981) 2153

6. A. Weingartshofer and E.M. Clarbe, Phys. Rev. Letters 12 (1964) 591

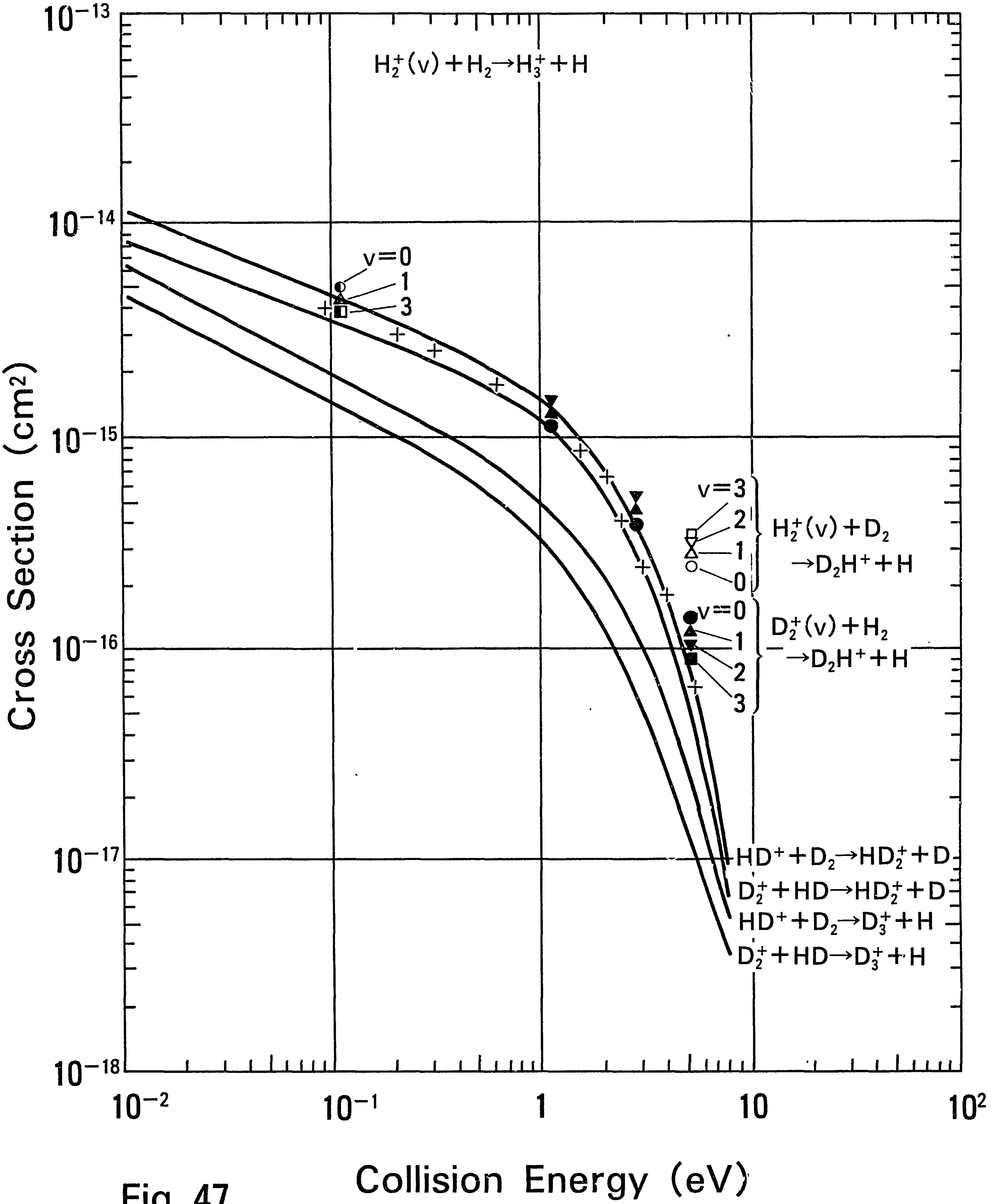

$H_2^+(v) + H_2 \to H_3^+ + H$
v=0
1
3
v=3
2
1
0
$H_2^+(v) + D_2 \to D_2H^+ + H$
v=0
1
2
3
$D_2^+(v) + H_2 \to D_2H^+ + H$
$HD^+ + D_2 \to HD_2^+ + D$
$D_2^+ + HD \to HD_2^+ + D$
$HD^+ + D_2 \to D_3^+ + H$
$D_2^+ + HD \to D_3^+ + H$
Cross Section (cm²)
10^{-13}
10^{-14}
10^{-15}
10^{-16}
10^{-17}
10^{-18}
10^{-2}
10^{-1}
1
10
10^2
Collision Energy (eV)

Fig. 47

III-17 Destruction of H_3^+ ions

H_3^+ ions can be destructed through a number of processes. Only the cross sections for the following processes have been determined(see Fig.48):

$$H_3^+ + H_2 \rightarrow H^+ + 2H_2 \qquad (1)$$
$$\rightarrow H_2^+ + H_2 + H \qquad (2)$$
$$\rightarrow H_3^{\circ} + H_2^+ \qquad (3)$$
$$\rightarrow \text{total destruction.} \qquad (4)$$

The measurements at low energies were reported by Lange et al.[1] and Huber et al.[2] who noticed that the isotope effect between H_3^+ and D_3^+ becomes clear at energies lower than 100 eV/amu because of the difference in the internal energy (at 30 eV/amu, the cross section for D_3^+ ions are about a half those for H_3^+ ions.)

On the other hand, total destruction cross sections of H_3^+ ions at higher energies have been determined by Williams et al.[3] who found that the cross sections can be varied with the ion source condition.

References

1. G. Lange, B.A. Huber and K. Wiesemann, Z. Phys. A281 (1977) 21
2. B.A. Huber, U. Schulz and K. Wiesemann, Phys. Letters 79A (1980) 58
3. J.D. Williams, J. Geddes and H.B. Gilbody, J. Phys. B 17 (1984) 811

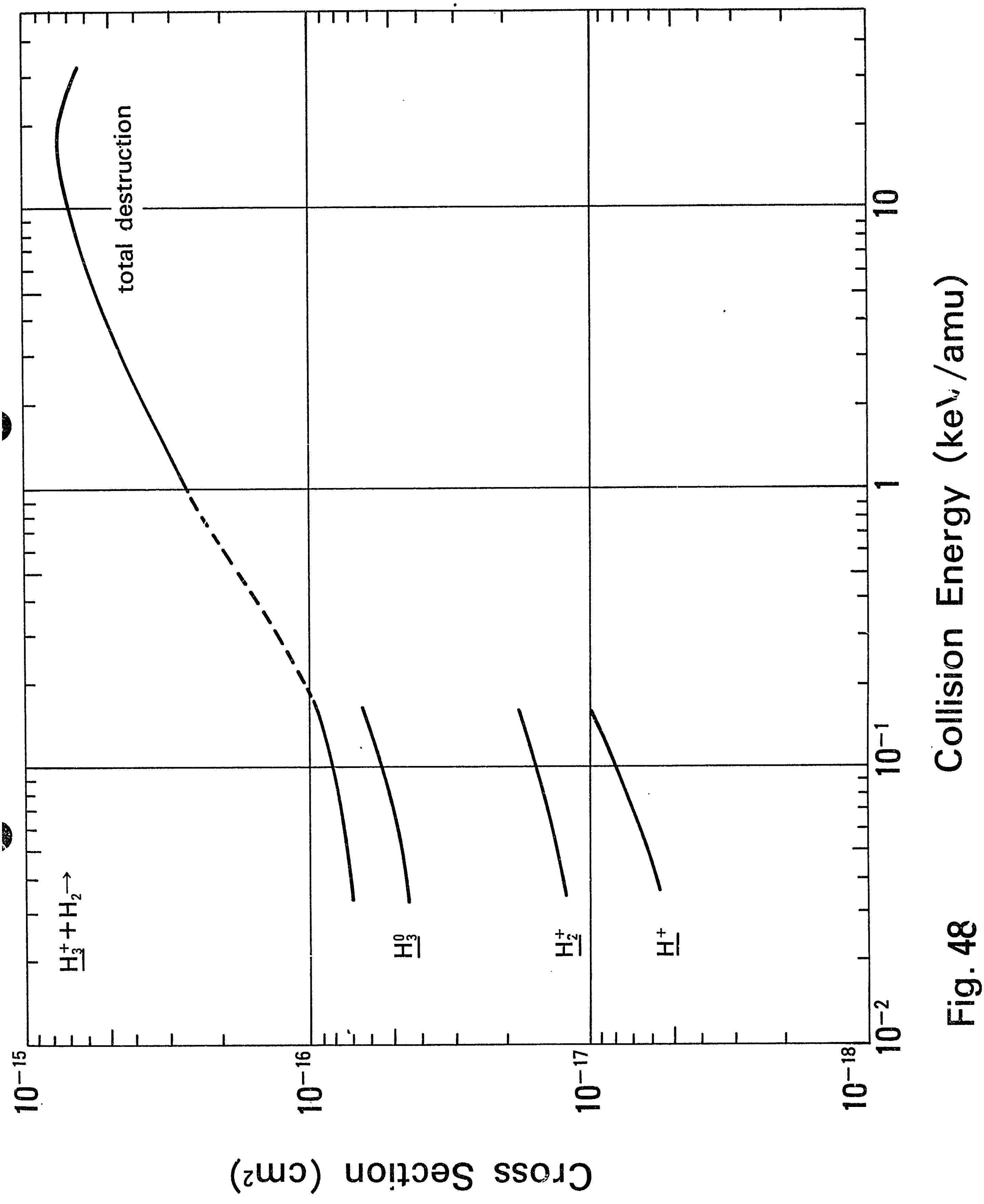

$H_3^+ + H_2 \rightarrow$
total destruction
H_3^0
H_2^+
H^+
10^{-15}
10^{-16}
10^{-17}
10^{-18}
10^{-2}
10^{-1}
1
10
Collision Energy (keV/amu)
Cross Section (cm²)

Fig. 48

III-18 $H_2^+ + H_2^+$ and $H_3^+ + H_3^+$ collisions

The following processes are possible in $H_2^+ + H_2^+$ collisions:

$$H_2^+ + H_2^+ \rightarrow H + H^+ + H_2^+ \qquad : \sigma_1 \qquad (1)$$

$$\rightarrow H + H^+ + H + H^+. \qquad : \sigma_2 \qquad (2)$$

According to the calculation based upon the sudden approximation[1], these cross sections are given as follows over the energy range 10 - 100 eV (with the uncertainties of ± 50%):

$$\sigma_1 = 1.2 \times 10^{-16} \; E^{-1/2} \qquad (cm^2)$$

$$\sigma_2 = 6.9 \times 10^{-16} \; E^{-1/2} \qquad (cm^2),$$

where the collision energy, E, is given in eV. Thus, in this collision system, i) the simultaneous dissociation process (2) of both particles is most likely to occur, ii) as σ is inversely proportional to the square root of the dissociation energy of molecular ions, these cross sections for the vibrationally excited states become larger than those for the ground state, and iii), as the Coulomb repulsion between ions become significant at low energies (< 20 eV), the cross sections are reduced.

A preliminary experimental result for $H_2^+ + H_2^+$ collisions shows the cross sections for proton formation to be $(0.87 \pm 0.51) \times 10^{-16}$ cm^2, at 7.3 eV which is compared with theoretical values of 3.4×10^{-16} cm^2.
Similarly in $H_3^+ + H_3^+$ collisions, the followings are probable:

$$H_3^+ + H_3^+ \rightarrow H_3^+ + H_2 + H^+ \quad : \sigma_3 \qquad (3)$$
$$\rightarrow H_2 + H^+ + H_2 + H^+ \quad : \sigma_4 \qquad (4)$$

The above calculations result in the cross sections for each process:

$$\sigma_3 = 3.3 \times 10^{-17} \quad E^{-1/2} \qquad (cm^2)$$

$$\sigma_4 = 4.8 \times 10^{-16} \quad E^{-1/2} \qquad (cm^2)$$

over the energy range 20-100 eV. Similar to $H_2^+ + H_2^+$ collisions, the simultaneous dissociation process (4) is likely to occur.

Reference

1. V.A. Belyaev, M.M. Dubrovin, L.I. Menshikov and A.N. Khlopkin, IAEA Report INDC(CCP) -224/GA (1984)

III-19 Collisions between ions

$$H^+ + H^- \rightarrow H(n\ell) + H(n\ell) \quad (1)$$

$$\rightarrow H^+ + H + e \quad (2)$$

$$\rightarrow H^- + H^+ \quad (3)$$

$$\rightarrow H_2^+ + e \quad (4)$$

The cross sections for single electron transfer (1) between positive and negative ions (mutual neutralization) have been investigated over a wide range of the collision energy. Data shown are in Fig.49 based upon recent experimental[1-3] and theoretical results.[4,5] They are found to follow their $E^{1/2}$-dependence at very low energies where electron is transferred dominantly to n=3 state.[5]

Previously observed structures at the energy of a few tens of eV to 200 eV have not been confirmed.[6,7] Data by Gaily and Harrison and by Rundel et al. are fairly larger than those shown.[8,9] The recent calculation by Shingal et al.[10] using two-center atomic expansion method with travelling atomic orbitals show more rapid decrease of the cross sections at higher energies (above 10 keV), compared with data shown in Fig.49.

The cross sections for process (2), electron detachment from H^- ions, have been determined by subtracting the mutual neutralization cross section from total cross sections for formation of neutral atoms from H^- ions[1] and are found to be in agreement with recent calculation[11]. The experimental cross sections for double electron transfer process(3) show some structures or oscillations at the energy of around 100 eV.[12,13]

The cross sections for the associative ionization process (4) were measured by Poulaert et al.[14] and examined theoretically by Urbain et al.[15] over the energy range of 10^{-3} - 5 eV. The agreement between experiment and calculation is found to be good, particularly at low energies where cross sections decrease roughly with E^{-1}.

References

1. B. Peart, R. Grey and K.T. Dolder, J. Phys. B 9 (1976) 3047
2. S. Szucs, M. Karemera, M. Terao and F. Brouillard, J. Phys. B 17 (1984) 1613
3. B. Peart, M.A. Bennett and K.Dolder, J.Phys. B 18 (1985) L439
4. V. Sidis, C. Kubach and D. Fussen, Phys. Rev, A 27 (1983) 2431
5. D. Fussen and C. Kubach, J. Phys. B 19 (1986) L31
6. J. Moseley, W. Aberth and J.R. Peterson, Phys.Rev. Letters 24 (1970) 435
7. B. Peart, R. Grey and K.T. Dolder, J. Phys. B 9 (1976) L369
8. T.D. Gaily and M.F.A. Harrison, J. Phys. B 3 (1970) L25
9. R.D.Rundel, K.L. Aitken and M.F.A. Harrison, J. Phys.B 2 (1969) 954
10. R. Shingal, B.H.Bransden and D.R.Flower, J. Phys. B 18 (1985) 2485
11. D. Fussen and W. Claeys, J. Phys. B 17 (1984) L89
12. B. Peart and R.A. Forrest, J. Phys. 12 (1979) L23
13. F. Brouillard, W.Claeys, G. Poulaert, G. Rahmat and G. van Wassenhove, J. Phys. B12 (1979) 1253
14. G. Poulaert, F. Brouillard, W. Claeys, J.W. McGowan and G. van Wassenhove, J. Phys. B 11 (1978) L671
15. X. Urbain, A. Giusti-Suzor, D.Fuseen and C. Kubach, J.Phys. B 19 (1986) L273

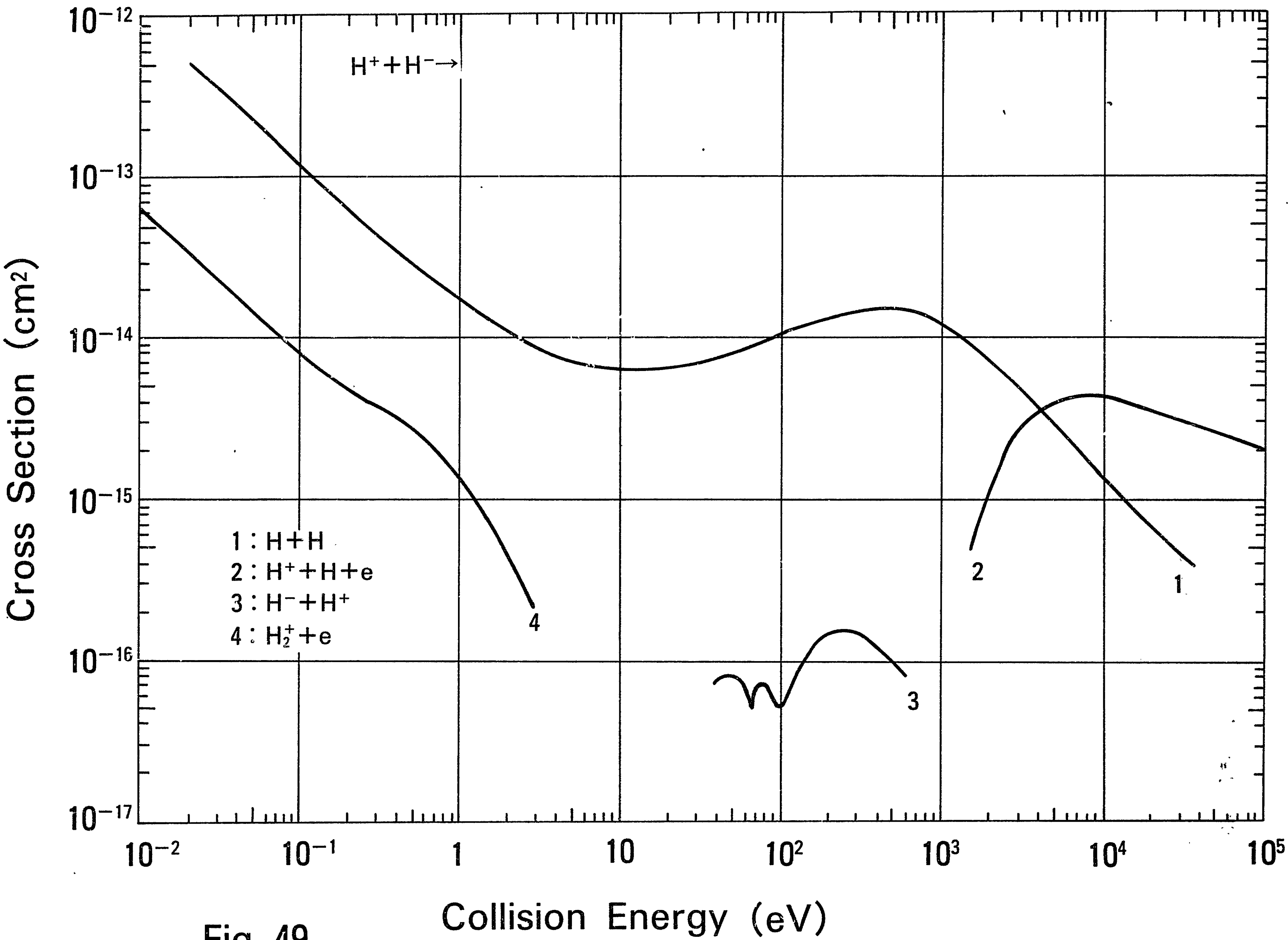

H⁺+H⁻→
1 : H+H
2 : H⁺+H+e
3 : H⁻+H⁺
4 : H₂⁺+e
1
2
3
4
Cross Section (cm²)
10⁻¹²
10⁻¹³
10⁻¹⁴
10⁻¹⁵
10⁻¹⁶
10⁻¹⁷
10⁻²
10⁻¹
1
10
10²
10³
10⁴
10⁵
Collision Energy (eV)

Fig. 49

This page is intentionally left blank

III-20 Molecular formation through three-body collisions

$$H + H + M \rightarrow H_2 + M \quad (M=H,H_2) \qquad (1)$$

$$D + D + M \rightarrow D_2 + M \quad (M=D,D_2) \qquad (2)$$

The rate coefficients for these processes were usually determined with shock-wave tube technique. Data shown in Fig.50 are taken from other compilations[1] which are mainly based on experimental data[2]. Those for $M=H_2$ and D_2 seem to roughly follow the $T^{-0.67}$ dependence if data over the temperature range 77-300 K are used.[2] (It should, however, be noted that, because of difficulties in data analysis, discrepancies among experimental data are often large. The rate coefficients for M=H and D seem to be fairly larger (by a factor of 10) than those for $M=H_2$ and D_2 shown in Fig.50. Theoretical calculations are still few and not well established yet.[3]

References

1. J. Troe, Ann. Rev. Phys. Chem. 29 (1978) 223 : V.N. Kondoratiev, Rate Constants of Gas Phase Reactions (transl. by L.J. Holtschlag and ed. by R.M.Fristrom, Office of Standard Reference Data, NBS,1972).
2. D.W.Trainor, D. Ham and F. Kaufman, J. Chem. Phys. 58 (1973) 4599
3. V.H. Shui and J.P. Appleton, J. Chem. Phys. 55 (1971) 3126, V. H. Shui, J. Chem. Phys. 58 (1973) ; R.T.V. Kung and J.B. Anderson, T. Chem. Phys. 60 (1974) 3731

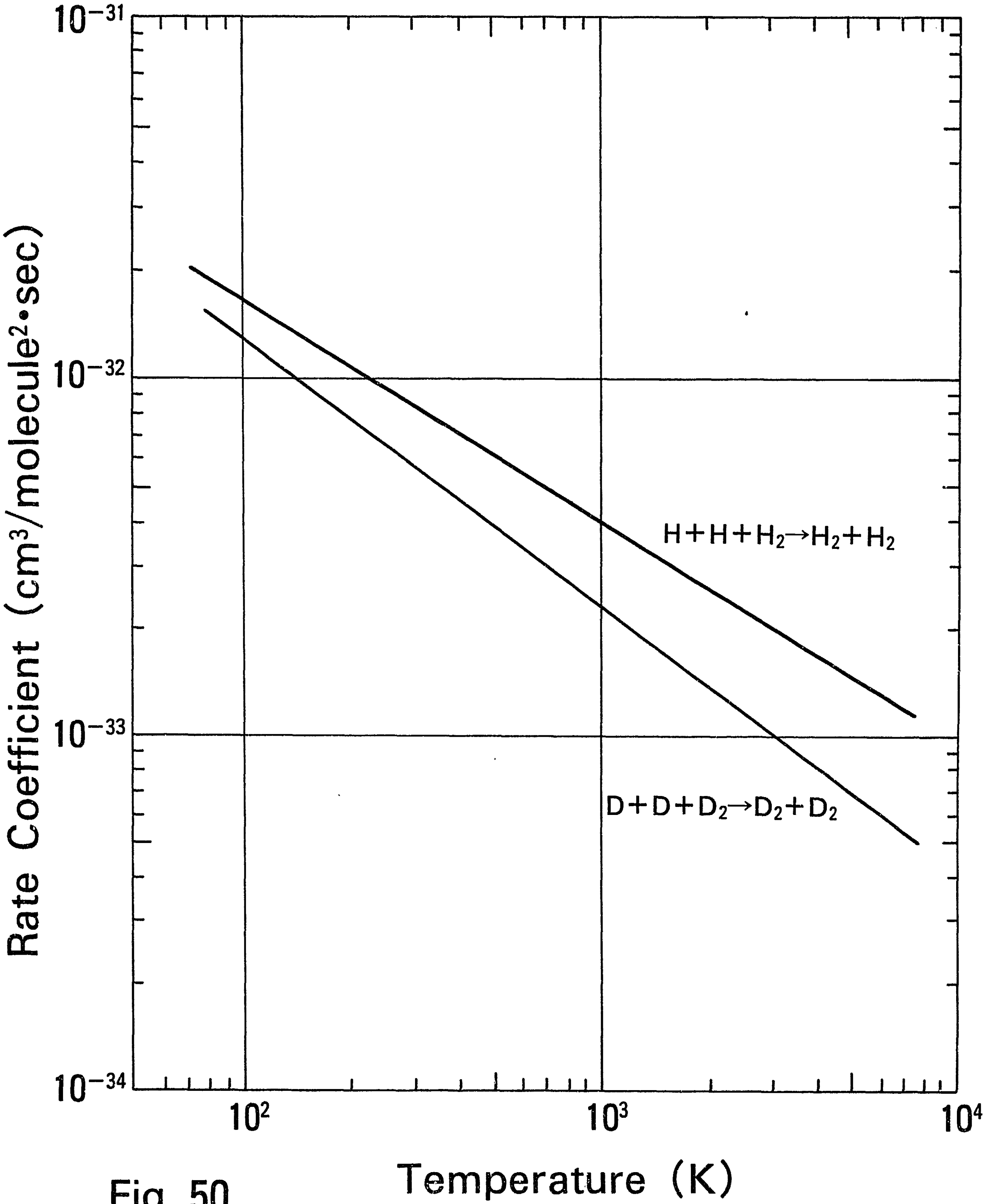

10^−31
10^−32
10^−33
10^−34
Rate Coefficient (cm³/molecule²•sec)
H+H+H₂→H₂+H₂
D+D+D₂→D₂+D₂
10²
10³
10⁴
Temperature (K)

Fig. 50

III-21 Thermal dissociation of H_2

The thermal dissociation process

$$M + H_2 \rightarrow M + H + H$$

has been investigated through shock wave tube experiment. The rate coefficients measured by Breshears and Bird[1] are shown in Fig.51 (solid lines) and the following analytic formulas can be used to express these data in (cm^3/mol.s) over the temperature range of 3500-8000 K:

$$M=H_2 : 5.48 \times 10^{-9} \exp(-53013/T)$$

$$M=H : 3.52 \times 10^{-9} \exp(-43900/T).$$

For comparison, the compiled data by Kondratiev[2] are expressed by the followings:

$$M=H_2 : 4.90 \times 10^{-7} T^{-1/2} \ 1-\exp(-6000/T) \exp(-51980/T)$$

(for 300-3500 K)

$$2.99 \times 10^{-4} T^{-3/2} \exp(-51980/T)$$

(for 3000-4500 K)

$$M=H : 2.00 \times 10^{-6} T^{-1/2} \exp(-51980/T)$$

(for 3000-4500 K)

and also shown in Fig.51 (dashed lines).

References

1) W.D. Breshears and P.F. Bird, 14th International Symp. on Combustion (Pittsburgh: Combustion Inst., 1973) p.211

2) V.N. Kondratiev (translated by L.J.Holtschlag and ed. by R.M. Fristrom) Rate Constants of Gas Phase Reactions - Reference Book (Office of Standard Reference Data, NBS, 1972)

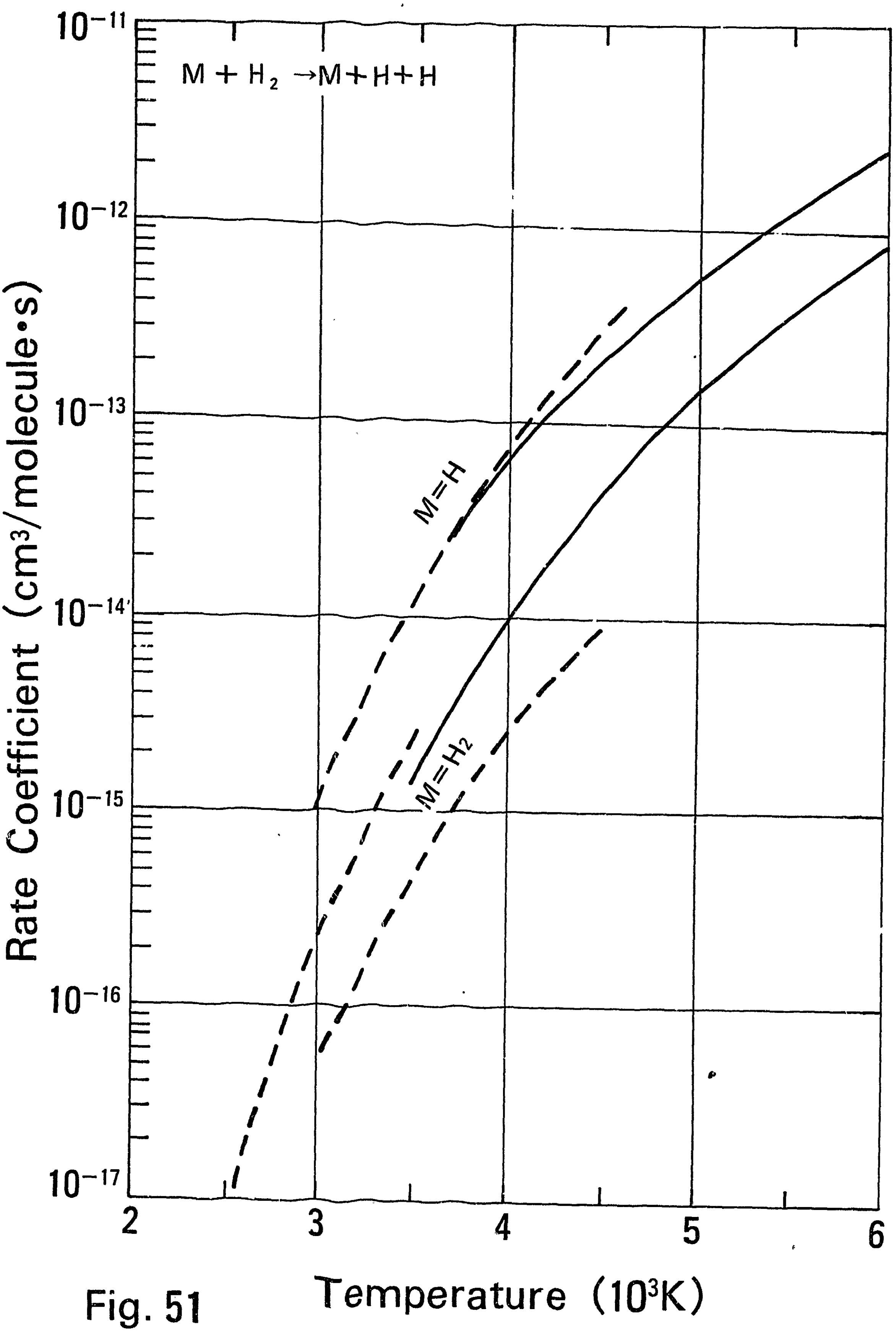

M + H2 →M+H+H
M=H
M=H2
Rate Coefficient (cm3/molecule•s)
10−11
10−12
10−13
10−14
10−15
10−16
10−17
2
3
4
5
6
Temperature (10³K)

Fig. 51

LIST OF IPPJ-AM REPORTS

IPPJ-AM-1* "Cross Sections for Charge Transfer of Hydrogen Beams in Gases and Vapors in the Energy Range 10 eV–10 keV"
H. Tawara (1977) [Published in Atomic Data and Nuclear Data Tables 22, 491 (1978)]

IPPJ-AM-2* "Ionization and Excitation of Ions by Electron Impact –Review of Empirical Formulae–"
T. Kato (1977)

IPPJ-AM-3 "Grotrian Diagrams of Highly Ionized Iron FeVIII-FeXXVI"
K. Mori, M. Otsuka and T. Kato (1977) [Published in Atomic Data and Nuclear Data Tables 23, 196 (1979)]

IPPJ-AM-4 "Atomic Processes in Hot Plasmas and X-Ray Emission"
T. Kato (1978)

IPPJ-AM-5* "Charge Transfer between a Proton and a Heavy Metal Atom"
S. Hiraide, Y. Kigoshi and M. Matsuzawa (1978)

IPPJ-AM-6* "Free-Free Transition in a Plasma –Review of Cross Sections and Spectra–"
T. Kato and H. Narumi (1978)

IPPJ-AM-7* "Bibliography on Electron Collisions with Atomic Positive Ions: 1940 Through 1977"
K. Takayanagi and T. Iwai (1978)

IPPJ-AM-8 "Semi-Empirical Cross Sections and Rate Coefficients for Excitation and Ionization by Electron Collision and Photoionization of Helium"
T. Fujimoto (1978)

IPPJ-AM-9 "Charge Changing Cross Sections for Heavy-Particle Collisions in the Energy Range from 0.1 eV to 10 MeV I. Incidence of He, Li, Be, B and Their Ions"
Kazuhiko Okuno (1978)

IPPJ-AM-10 "Charge Changing Cross Sections for Heavy-Particle Collisions in the Energy Range from 0.1 eV to 10 MeV II. Incidence of C, N, O and Their Ions"
Kazuhiko Okuno (1978)

IPPJ-AM-11 "Charge Changing Cross Sections for Heavy-Particle Collisions in the Energy Range from 0.1 eV to 10 MeV III. Incidence of F, Ne, Na and Their Ions"
Kazuhiko Okuno (1978)

IPPJ-AM-12* "Electron Impact Excitation of Positive Ions Calculated in the Coulomb-Born Approximation –A Data List and Comparative Survey–"
S. Nakazaki and T. Hashino (1979)

IPPJ-AM-13 "Atomic Processes in Fusion Plasmas -- Proceedings of the Nagoya Seminar on Atomic Processes in Fusion Plasmas Sept. 5-7, 1979"
Ed. by Y. Itikawa and T. Kato (1979)

IPPJ-AM-14 "Energy Dependence of Sputtering Yields of Monatomic Solids"
N. Matsunami, Y. Yamamura, Y. Itikawa, N. Itoh, Y. Kazumata, S. Miyagawa, K. Morita and R. Shimizu (1980)

IPPJ-AM-15 "Cross Sections for Charge Transfer Collisions Involving Hydrogen Atoms"
Y. Kaneko, T. Arikawa, Y. Itikawa, T. Iwai, T. Kato, M. Matsuzawa, Y. Nakai, K. Okubo, H. Ryufuku, H. Tawara and T. Watanabe (1980)

IPPJ-AM-16 "Two-Centre Coulomb Phaseshifts and Radial Functions"
H. Nakamura and H. Takagi (1980)

IPPJ-AM-17 "Empirical Formulas for Ionization Cross Section of Atomic Ions for Electron Collisions –Critical Review with Compilation of Experimental Data–"
Y. Itikawa and T. Kato (1981)

IPPJ-AM-18 "Data on the Backscattering Coefficients of Light Ions from Solids"
T. Tabata, R. Ito, Y. Itikawa, N. Itoh and K. Morita (1981) [Published in Atomic Data and Nuclear Data Tables 28, 493 (1983)]

IPPJ-AM-19 "Recommended Values of Transport Cross Sections for Elastic Collision and Total Collision Cross Section for Electrons in Atomic and Molecular Gases"
M. Hayashi (1981)

IPPJ-AM-20 "Electron Capture and Loss Cross Sections for Collisions between Heavy Ions and Hydrogen Molecules"
Y. Kaneko, Y. Itikawa, T. Iwai, T. Kato, Y. Nakai, K. Okuno and H. Tawara (1981)

IPPJ-AM-21 "Surface Data for Fusion Devices – Proceedings of the U.S–Japan Workshop on Surface Data Review Dec. 14-18, 1981"
Ed. by N. Itoh and E.W. Thomas (1982)

IPPJ-AM-22 "Desorption and Related Phenomena Relevant to Fusion Devices"
Ed. by A. Koma (1982)

IPPJ-AM-23 "Dielectronic Recombination of Hydrogenic Ions"
T. Fujimoto, T. Kato and Y. Nakamura (1982)

IPPJ-AM-24 "Bibliography on Electron Collisions with Atomic Positive Ions: 1978 Through 1982 (Supplement to IPPJ-AM-7)"
Y. Itikawa (1982) [Published in Atomic Data and Nuclear Data Tables 31, 215 (1984)]

IPPJ-AM-25 "Bibliography on Ionization and Charge Transfer Processes in Ion-Ion Collision"
H. Tawara (1983)

IPPJ-AM-26 "Angular Dependence of Sputtering Yields of Monatomic Solids"
Y. Yamamura, Y. Itikawa and N. Itoh (1983)

IPPJ-AM-27 "Recommended Data on Excitation of Carbon and Oxygen Ions by Electron Collisions"
Y. Itikawa, S. Hara, T. Kato, S. Nakazaki, M.S. Pindzola and D.H. Crandall (1983) [Published in Atomic Data and Nuclear Data Tables 33, 149 (1985)]

IPPJ-AM-28 "Electron Capture and Loss Cross Sections for Collisions Between Heavy Ions and Hydrogen Molecules (Up-dated version of IPPJ-AM-20)
H. Tawara, T. Kato and Y. Nakai (1983) [Published in Atomic Data and Nuclear Data Tables 32, 235 (1985)]

IPPJ-AM-29 "Bibliography on Atomic Processes in Hot Dense Plasmas"
T. Kato, J. Hama, T. Kagawa, S. Karashima, N. Miyanaga, H. Tawara, N. Yamaguchi, K. Yamamoto and K. Yonei (1983)

IPPJ-AM-30 "Cross Sections for Charge Transfers of Highly Ionized Ions in Hydrogen Atoms (Up-dated version of IPPJ-AM-15)"
H. Tawara, T. Kato and Y. Nakai (1983) [Published in Atomic Data and Nuclear Data Tables 32, 235 (1985)]

IPPJ-AM-31 "Atomic Processes in Hot Dense Plasmas"
T. Kagawa, T. Kato, T. Watanabe and S. Karashima (1983)

IPPJ-AM-32 "Energy Dependence of the Yields of Ion-Induced Sputtering of Monatomic Solids"
N. Matsunami, Y. Yamamura, Y. Itikawa, N. Itoh, Y. Kazumata, S. Miyagawa, K. Morita, R. Shimizu and H. Tawara (1983) [Published in Atomic Data and Nuclear Data Tables 31, 1 (1984)]

IPPJ-AM-33 "Proceedings on Symposium on Atomic Collision Data for Diagnostics and Modelling of Fusion Plasmas, Aug. 29 – 30, 1983"
Ed. by H. Tawara (1983)

IPPJ-AM-34 "Dependence of the Backscattering Coefficients of Light Ions upon Angle of Incidence"
T. Tabata, R. Ito, Y. Itikawa, N. Itoh, K. Morita and H. Tawara (1984)

IPPJ-AM-35 "Proceedings of Workshop on Synergistic Effects in Surface Phenomena Related to Plasma-Wall Interactions, May 21 – 23, 1984"
Ed. by N. Itoh, K. Kamada and H. Tawara (1984) [Published in Radiation Effects 89, 1 (1985)]

IPPJ-AM-36 "Equilibrium Charge State Distributions of Ions ($Z_1 \geqq 4$) after Passage through Foils – Compilation of Data after 1972"
K. Shima, T. Mikumo and H. Tawara (1985) [Published in Atomic Data and Nuclear Data Tables 34, 357 (1986)]

IPPJ-AM-37 "Ionization Cross Sections of Atoms and Ions by Electron Impact"
H. Tawara, T. Kato and M. Ohnishi (1985)

IPPJ-AM-38 "Rate Coefficients for the Electron-Impact Excitations of C-like Ions"
Y. Itikawa (1985)

IPPJ-AM-39 "Proceedings of the Japan-U.S. Workshop on Impurity and Particle Control, Theory and Modeling, Mar. 12 – 16, 1984"
Ed. by T. Kawamura (1985)

IPPJ-AM-40 "Low-Energy Sputterings with the Monte Carlo Program ACAT"
Y. Yamamura and Y. Mizuno (1985)

IPPJ-AM-41 "Data on the Backscattering Coefficients of Light Ions from Solids (a Revision)"
R. Ito, T. Tabata, N. Itoh, K. Morita, T. Kato and H. Tawara (1985)

IPPJ-AM-42 "Stopping Power Theories for Charged Particles in Inertial Confinement Fusion Plasmas (Emphasis on Hot and Dense Matters)"
S. Karashima, T. Watanabe, T. Kato and H. Tawara (1985)

IPPJ-AM-43 "The Collected Papers of Nice Project/IPP, Nagoya"
Ed. by H. Tawara (1985)

IPPJ-AM-44 "Tokamak Plasma Modelling and Atomic Processes"
Ed. by T. Kawamura (1986)

IPPJ-AM-45 Bibliography of Electron Transfer in Ion-Atom Collisions
H. Tawara, N. Shimakura, N. Toshima and T. Watanabe (1986)

IPPJ-AM-46 "Atomic Data Involving Hydrogens Relevant to Edge Plasmas"
H. Tawara, Y. Itikawa, Y. Itoh, T. Kato, H. Nishimura, S. Ohtani, H. Takagi, K. Takayanagi and M. Yoshino (1986)

Available upon request to Research Information Center, Institute of Plasma Physics, Nagoya University, Nagoya 464, Japan, except for the reports noted with*.